AN INVESTIGATION OF NUCLEAR LIPID DROPLET PROTEINS AND NUCLEAR LIPID DROPLET PROTEIN DYNAMICS

by

Jason Roger Foster

Submitted in partial fulfilment of the requirements

for the degree of Master of Science

at

Dalhousie University

Halifax, Nova Scotia

June 2022

DEDICATION PAGE

Is there any greater honor in one's life than making the dedication page of your son's master's thesis? Some questions not even science can answer. But maybe it doesn't need to. I would like to dedicate my thesis first and foremost to my parents, Roger and Darlene. It is a testament to the time and effort you put into raising me that someone who has had no one on either side of their family attend university (let alone graduate university) will (hopefully) graduate with a master's degree. For all that you have done for me over the years and shall continue to do, a simple dedication page in my thesis seems woefully inadequate. But it's a start.

Second, I dedicate my thesis to Ryan. You are my brother. And you are like a brother to me. For many, those two things are not mutually inclusive. I am fortunate that they are.

And finally, I would like to dedicate this thesis to my future self. If you ever need an example of what you can do through sheer determination and hard work, look back to this page. Then look ahead. You got this.

TABLE OF CONTENTS

LIST OF FIGURES

Abstract

Aberrant lipid storage is a hallmark of many pathologies, including non-alcoholic fatty liver disease (NAFLD). NAFLD is characterized by an accumulation of lipids stored in lipid droplets (LDs) in the cytoplasm. A subpopulation of nuclear LDs (nLDs) has been reported to form in response to excess fatty acids in hepatocytes and other cells. nLDs associate with nuclear proteins, including the nuclear body-forming promyelocytic leukemia (PML) proteins to form lipid-associated PML structures (LAPS), along with the lipid metabolic enzymes LIPIN1 and CTP:phosphocholine cytidylyltransferase α (CCTα). My research aimed to characterize protein association with nLDs over time, investigating the mechanisms regulating CCTα and LIPIN1 translocation to nLDs and determining whether apolipoprotein L6 (APOL6) associates with LAPS. PML recruitment to nLDs and thus LAPS formation was found to precede CCTα and LIPIN1 recruitment. The ability for CCTα to associate with nLDs was found to be inhibited by the degree of phosphorylation in its C-terminal phosphorylation domain. Interferon (IFN) γ was found to stimulate LAPS formation and APOL6 expression. Furthermore, the combination of IFNγ and fatty acids were found to stimulate greater LAPS formation and APOL6 expression and recruitment to LAPS under conditions which simulate NAFLD. These results demonstrate that nLDs are a heterogenous population of nuclear structures that dynamically recruit PML, CCT, LIPIN1 and APOL6 in response to fatty acids and IFNγ stimulus, possibly to quell the lipotoxic effects of fatty acid overload. Additionally, the establishment of connections between IFNγ, APOL6 and LAPS creates a paradigm in which NASH may be stimulated in hepatic tissue by fatty acids and inflammatory signalling driving the expression of pro-apoptotic APOL6.

LIST OF ABBREVIATIONS USED

ACSL	Long-chain fatty-acyl coenzyme A ligase
AGPAT	Acylglycerophosphate acyltransferase
AI	Autoinhibitory
AMP	Adenosine 5'-monophosphate
ApoB100	Apolipoprotein B100
ApoL	Apolipoprotein L
ATGL	Adipose triglyceride lipase
ATP	Adenosine 5'-triphosphate
BSA	Bovine serum albumin
CCT	CTP:phosphocholine cytidylyltransferase
CDP	Cytidine 5'-diphosphosphate
CE	Cholesterol ester
CEPT	Choline/choline-ethanolamine phosphotransferase
CHOK1	Chinese hamster ovary K1
cLD	Cytoplasmic lipid droplet
CMA	Chaperone-mediated autophagy
CoA	Coenzyme A
CTDNEP	C-terminal domain nuclear envelope phosphatase
DAG	Diacylglycerol
DAXX	Death domain-associated protein 6
DGAT	Diacylglycerol acyltransferase
DMEM	Dulbecco's modified Eagle's medium
EDTA	Ethylenediamine tetraacetic acid
eLD	Endoplasmic reticulum luminal lipid droplet
ER	Endoplasmic reticulum
FA	Fatty acid
FSP	Fat specific protein
G3P	Glycerol-3-phosphate
GPAT	Glycerol-3-phosphate acyltransferase
HEK	Human embryonic kidney
HNF	Hepatic nuclear factor
HSL	Hormone-sensitive lipase
IFNγ	Interferon γ
INM	Inner nuclear membrane
LAPS	Lipid-associated PML structure
LD	Lipid droplet
LF	Lipofectamine
LPCAT	Lyso-phosphatidylcholine acyltransferase
LPS	Lipopolysaccharide
LXR	Liver X receptor
MAG	Monoacylglycerol
MLX	Max-like protein X
mRNA	Messenger ribonucleic acid

mTOR	Mechanistic target of rapamycin
NAFLD	Non-alcoholic fatty liver disease
NASH	Non-alcoholic steatohepatitis
NE	Nuclear envelope
nLD	Nuclear lipid droplet
NLS	Nuclear-localization signal
NR	Nucleoplasmic reticulum
NT	Non-targetting
OA	Oleate
OMM	Outer mitochondrial membrane
PA	Phosphatidic acid
PBS	Phosphate-buffered saline
PC	Phosphatidylcholine
PCR	Polymerase chain reaction
PE	Phosphatidylethanolamine
PEI	Polyethylenimine
PEMT	Phosphatidylethanolamine N-methyltransferase
PGC	Peroxisome proliferator-activated receptor gamma coactivator
PL	Phospholipid
PLIN	Perilipin
PML	Promyelocytic leukemia
PML-KO	Promyelocytic leukemia knockout
PML NB	Promyelocytic leukemia nuclear body
PPAR	Peroxisome proliferator-activated receptor
RA	Retinoic acid
RAR	Retinoic acid receptor
RXR	Retinoid X receptor
SA	Serine to alanine
SD	Serine to aspartate
SDS	Sodium dodecyl sulfate
SE	Serine to glutamate
SREBP	Sterol regulatory element-binding protein
STAT	Signal transducer and activator of transcription
TBS	Tris-buffered saline
TBS-T	Tris-buffered saline-Tween 20
TG	Triacylglycerol
VLDL	Very low-density lipoprotein

ACKNOWLEDGEMENTS

There are many folks whom I feel the utmost gratitude to for helping me throughout my course of study. I would like to thank my committee members Jamie Kramer and Petra Kienesberger for their valuable feedback and suggestions. I would like to thank my co-supervisor Graham Dellaire, who identified APOL6 as a potential LAPS protein. I would like to thank Brianne Lindsay for microscopy assistance and Rob Douglas for his cell culture expertise. I would also like to thank Debbie Hayes and Brenda O'Brien for their administrative work, allowing me to focus my time and energy towards science and not packing slips and backorders. My funding came from CIHR and scholarships from Research NS and the JD Shatford Memorial Trust fund.

I would like to acknowledge my labmates, both past and current. Senior lab members Kexin Zhao, Mark Charman and Kyle Lee provided technical assistance that helped me immensely. I would like to Michael McPhee for both technical expertise, as an excellent person to bounce ideas off of and overall just being a great guy. I would also like to acknowledge my labmates Gabriel Dorighello, Katie Halliday and former roommate Jordan Thompson for making my experience in the Ridgway lab excellent.

Finally, I would like to give my sincere gratitude to my supervisor, Neale Ridgway. His stoic patience in the face of my countless setbacks, encouragement to pursue my project independently and personability made my experience in his lab a great one. On the occasions I have talked to former lab members who have gone off to other labs, they have without fail acknowledged his aptitude at handling people in addition to his ability as a scientist. I can personally attest this praise is every bit deserved.

Chapter 1: Introduction

1.1 Research objectives

The research presented in this thesis focuses on interactions between nuclear lipid droplets (nLDs) and nLD-associated proteins. The three primary objectives of this research were to 1) quantify when key nLD proteins associate with nLDs; 2) determine the mechanism regulating interactions between nLDs and CTP:phosphocholine cytidylytransferase α (CCTα), the rate-limiting enzyme in the Kennedy pathway of phosphatidylcholine (PC) synthesis; and 3) to characterize the novel nLD-associated protein apolipoprotein L6 (APOL6).

This research will be contextualized with a review of relevant literature. I will begin with a brief overview of lipids and lipid storage, focusing on lipid synthesis as it relates to lipid storage in LDs, followed by an in-depth review of nLDs, their functions and how they differ from cytoplasmic LDs (cLDs). Along the way, I will discuss relevant nLD-associated proteins, with a focus on CCTα, LIPIN1, promyelocytic leukemia proteins (PML) and APOL6 and their roles in nLD structure and function.

1.1 Lipid droplets: An introduction to lipid storage

1.2.1 Lipid droplets exist: A biophysical explanation

Energy is required for everything from intercellular transport to nucleotide synthesis and thus a constant supply is vital. Energy and its storage pose an existential conundrum for cells: while its demand is continuous, its supply is not. Energy is most readily consumed in the form of nucleotide triphosphates, predominantly adenosine 5'-triphosphate (ATP). However, ATP has a half-life on a timeframe of seconds and thus

more enduring forms of energy storage are required for its on-demand synthesis. Cells have evolved to convert a variety of molecules into ATP, including carbohydrates, amino acids, ketones and fatty acids (FAs). Oxidation of these molecules is required to generate ATP and thus the amount of energy generated per molecule is proportional to how many times the molecule can be oxidized. FAs, as the most reduced energy molecules, provide the most opportunities for oxidation and therefore are the most efficient way to transport and store energy for later use. However, FAs are inadequate as storage molecules due to their cytotoxic effects on cells (Lee et al., 1994). The toxicity of FAs is quelled by esterifying them to a glycerol backbone to produce triacylglycerols (TG; **Figure 1.1A**). TG is more hydrophobic than FAs and thus poses difficulty for storage in the aqueous environment of cells. As a result, cells have evolved specialized organelles that store and mobilize lipids contained in LDs.

The effectiveness of LDs at storing lipids is due to their morphology, which minimizes thermodynamically unfavorable interactions between hydrophobic and aqueous phases. LD structure (**Figure 1.1B**) consists of a monolayer of amphipathic phospholipids (PLs; **Figure 1.1C**) surrounding a core of hydrophobic sterol esters and TG. Additionally, proteins can interact with the LD surface electrostatically or insert into the phospholipid monolayer.

The LD profile varies by quantity, size, and function within different tissues. LDs are present in virtually all mammalian tissues. LDs are most abundant in adipose but are also common in liver, skeletal muscle, cardiomyoctes, intestinal epithelium, and steroidogenic cells. LDs are also connected to the pathology of many diseases prevalent in Western societies, such as obesity, atherosclerosis, heart disease, type 2 diabetes

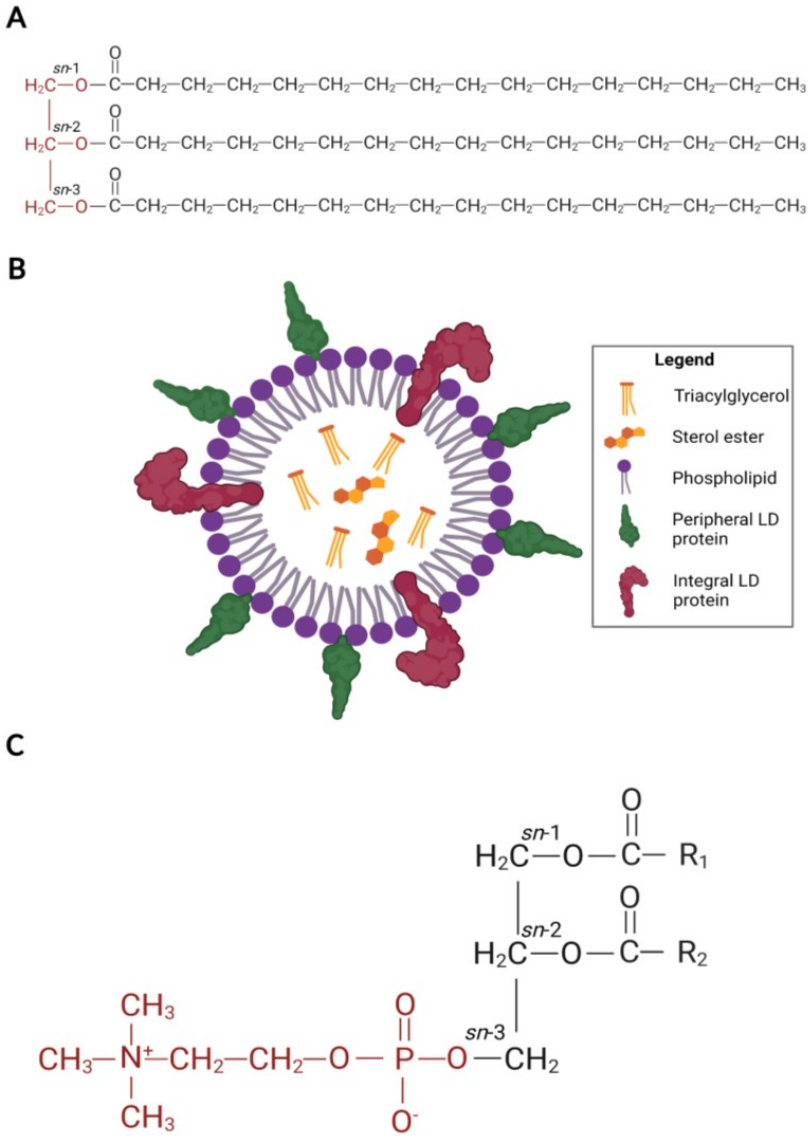

Figure 1.1. Structure of TG, PC and LDs. (A) Structure of a triacylglycerol with three palmitatic acids esterified to a glycerol backbone (red). The long acyl chains and lack of polar groups make TAG hydrophobic. **(B)** Lipid droplet structure. A core of hydrophobic triacylglycerols and sterol esters is surrounded by a layer of amphipathic phospholipids. Associated proteins interact peripherally through electrostatic interactions or integrate into the phospholipid monolayer via hydrophobic domains. **(C)** Generic structure of a phosphatidylcholine molecule. R1 and R2 represent fatty acid acyl chains which make PC amphipathic. Image made using BioRender.

mellitus and non-alcoholic fatty liver disease (NAFLD) (Gluchowski et al., 2017). Most research surrounding LDs has been conducted in adipocytes as white adipose serves as the primary lipid storage tissue. White adipocytes act as a sink for FAs derived from TG-rich lipoproteins during times of energy abundance and mobilize TG reserves during starvation. Excess TG storage is a hallmark of obesity and has myriad of harmful consequences including reduced insulin sensitivity, perturbed endocrine functions and inappropriate accumulation of TG in other tissues (Vázquez-Vela et al., 2008). Unlike other cells, white adipocytes tend to have a single, large LD rather than several smaller LDs. Adipocyte LDs also have a unique complement of LD-associated proteins that enhance the storage or mobilization of FAs and TG such as fat-specific protein (FSP) 27 and perilipin 1 (Greenberg et al., 1991; Puri et al., 2007). A large body of research surrounding LDs in hepatocytes also exists due to the liver's role as hub of lipid metabolism. LDs also have pathological relevance in hepatocytes as they are connected with hepatic steatosis and NAFLD, an inappropriate accumulation of liver fat that can progress to non-alcoholic hepatic steatohepatitis (NASH) when coupled with excess liver inflammation or other insult (Gluchowski et al., 2017). NASH can lead to cell death, eventually leading to irreversible hepatic scaring called liver cirrhosis and organ failure. In addition to NAFLD, excess LDs in skeletal muscle and cardiomyocytes is often a pathological indicator of certain conditions such as type 2 diabetes mellitus. The link between LDs and disease runs deep and thus an understanding of modernity's most pressing pathologies is built upon fundamental understanding of lipids and LDs.

Lipidomic analysis has illuminated our understanding of the variety of lipid species in LDs in both the PL monolayer and neutral lipid core. The mammalian LD

monolayer possesses a diverse array of PLs, with PC constituting a majority of the total PL content (Chitraju et al., 2012; Tauchi-Sato et al., 2002). Significant quantities of phosphatidylethanolamine (PE) are also present along with minor amounts of other PLs such as phosphatidylinositides and sphingomyelin (Bartz et al., 2007; Chitraju et al., 2012; McIntosh et al., 2010). PC has been demonstrated to be crucial for LD stability and inhibition of LD coalescence (Krahmer et al., 2011). It has been suggested that the biophysical properties of PC contribute to this unique phenotype. PC has a cylindrical shape with a head group roughly equivalent in diameter to its PL tails, whereas other PLs such as PE have a headgroup smaller than its base that promotes negative curvature. The importance of PC as a regulator of LD size is demonstrated by studies that have shown enlarged LDs after knockout of the nuclear rate-limiting enzyme in the Kennedy pathway of PC synthesis, CCT (Aitchison et al., 2015; Krahmer et al., 2011; Liu et al., 2021). LD membranes are also enriched in lyso-PLs, particularly lyso-PC, compared to other membranes (Bartz et al., 2007). Lyso-PLs have only one esterified fatty acid and thus a headgroup with a larger diameter than its base that promotes positive curvature, allowing the LD monolayer to adopt a confirmation with much more curvature than the planar ER membrane from which it is derived (M'barek et al., 2017).

The hydrophobic core of LDs is primarily composed of TG and cholesterol esters (CEs). TG is the far more abundant component of the core, although subpopulations of LDs enriched in CEs have been noted (Hsieh et al., 2012; Layerenza et al., 2013). It is unknown whether these sterol-rich LD populations have a different complement of monolayer PLs. The LD core also contains small amounts of other hydrophobic lipids,

including vitamin D, retinyl esters and monoalkyl diacylglycerols (Chitraju et al., 2012; Malmberg et al., 2014).

LD lipids are primarily acquired from one of two methods: membrane contact sites with the endoplasmic reticulum (ER) or *de novo* synthesis directly on LDs. PLs are mostly derived from ER contact sites as LDs lack most PL synthetic machinery, although the presence of lyso-PC acyl transferases (LPCATs 1 and 2) on the LD surface enable the conversion of lyso-PC to PC, allowing some PC synthesis (Moessinger et al., 2011). TG, on the contrary, can be effectively acquired through ER contact or *de novo* synthesis. Regardless of how the lipids are obtained, understanding both PC and TG synthesis are important for understanding LD formation.

1.2.2 Lipid droplet building blocks: Triacylglycerol and phosphatidylcholine synthesis

LD formation occurs at the ER and is dependent on having the right lipids available at the right time and place. Most lipid synthesis occurs at the smooth ER membrane, which contains a myriad of lipid synthetic enzymes and regulatory machinery while also maintaining contact sites with other organelles (Henne et al., 2020). Concentrating lipid synthesis at the ER facilitates lipid transport to key organelles while also streamlining lipid synthesis in a manner responsive to cellular lipid levels (Brown & Goldstein, 1997; Fagone & Jackowski, 2009). This streamlining of lipid synthesis is important for LD formation. The ultimate steps of TG and PC synthesis, the most abundant components of the LD core and monolayer respectively, are catalyzed in the ER. I will thus outline the metabolic pathways that produce PC and TG followed by links between the two pathways.

1.2.3 Triacylglycerol synthesis

TG synthesis acts as a storage mechanism for cells exposed to excess fatty acids while simultaneously preventing the cytotoxic effects of fatty acid accumulation. TG synthesis can also be stimulated by signalling pathways independent of cellular FA concentrations. For example, the antiviral inflammatory cytokine interferon (IFN) γ stimulates TG synthesis and storage in pancreatic cells, as IFNγ stimulation decreased TG storage at 6 h but caused an increase by 24 h. Interestingly, IFNγ-induced TG synthesis was also found to enhance upregulation of IFNγ-upregulated genes (Truong et al., 2019).

The *de novo* pathway of TG synthesis is the *sn*-glycerol-3-phosphate (G3P) pathway (**Figure 1.2**; also known as the Kennedy pathway (Weiss et al., 1960)). This pathway initially produces phosphatidic acid (PA) (Lee & Ridgway, 2020). PA is a branch point in lipid metabolism: it can be incorporated into membranes, cytidylated to form CDP-diacylglycerol (DAG) for phosphatidylglycerol and cardiolipin synthesis or dephosphorylated to form DAG for PC or PE synthesis, or subsequently fatty acylated to form TG.

The glycerol backbone of TG is derived from G3P. The most significant sources of G3P are glycolysis and gluconeogenesis, which is a glucose-independent source that is activated when glucose levels are insufficient (Reshef et al., 2003). G3P can also be obtained by phosphorylation of glycerol by glycerol kinase (Bartley & Ward, 1985). Regardless of the source, G3P is acylated to form lyso-PA by G3P acyltransferases (GPATs) using a fatty acyl-coenzyme A (CoA) produced by fatty acyl-CoA synthase

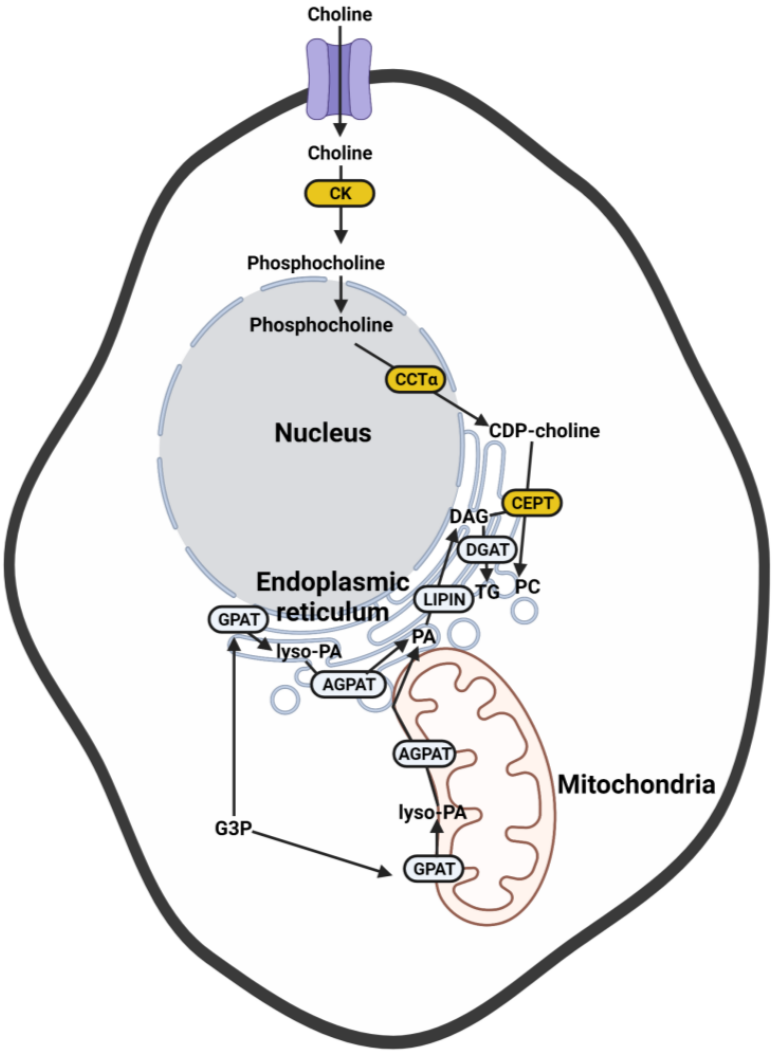

Figure 1.2. The CDP-choline and glycerol-3-phosphate pathways. The glycerol-3-phosphate (G3P) pathway begins with the acylation of G3P by GPAT on the ER or outer mitochondrial membrane to make lyso-phosphatidic acid (lyso-PA). Lyso-PA is acylated by AGPAT to form PA in the ER or mitochondria. PA in the ER is dephosphorylated by LIPIN1 to form diacylglycerol, which can then be acylated to form TG. The CDP-choline pathway begins with exogenous choline uptake. Choline kinase (CK) phosphorylates choline to produce phosphocholine. Phosphocholine is cytidylated to make CDP-choline on the inner nuclear membrane by CCTα. CDP-choline is combined with DAG to form PC on the ER membrane. Image made using BioRender.

(Lee & Ridgway, 2020). GPAT1, the most significant GPAT isoform for TG synthesis, and GPAT2 are located in the outer mitochondrial membrane (OMM) whereas GPATs 3 and 4 are found in the ER (Cao et al., 2006; Lewin et al., 2004; Nagle et al., 2008; Vancura & Haldar, 1994). Lyso-PA is then converted to PA by an additional acylation by acylglycerophosphate acyltransferase (AGPAT). Both the ER and OMM have AGPAT activity and thus this step can occur in either organelle (Prasad et al., 2011). Subsequent TG synthesis enzymes are ER-associated and thus PA in the OMM destined for TG synthesis must be transferred to the ER, possibly by membrane contact sites of lateral diffusion (Flis & Daum, 2013). Isoforms of the PA phosphatase LIPIN catalyze PA dephosphorylation to form DAG, which is then fatty acylated to produce TG by diacylglycerol acyltransferase (DGAT). TG made in the ER can then be used to form nascent LDs, stored in existing LDs via ER-LD contacts or packaged into lipoproteins and secreted by hepatic and intestinal epithelial tissue provided sufficient PLs are present (Lee & Ridgway, 2018; Yao & Vance, 1988). Alternatively, LDs also have GPAT4, AGPAT3, LIPIN1 and DGAT2 associated with their surface, allowing them to directly synthesize and store TG without ER-contact (Wilfling et al., 2013).

1.2.4 Phosphatidylcholine synthesis

PC is the predominant component of the LD monolayer and is essential for the formation of LDs, while also being necessary to package TG in lipoproteins in hepatocytes and intestinal epithelium (Lee & Ridgway, 2018; Penno et al., 2013; Yao & Vance, 1988). Mammalian PC synthesis occurs via three distinct pathways: the CDP-choline pathway (also known as the Kennedy pathway of PC synthesis), methylation of PE and the acylation of lyso-PC by the Lands cycle LPCATs.

The CDP-choline pathway (**Figure 1.2**) is the primary *de novo* pathway for PC synthesis (Li & Vance, 2008). The pathway begins with the uptake of exogenous choline as mammals are unable to produce choline *de novo* and must acquire it from the diet. Choline, as a charged molecule, requires the use of transporter proteins to cross the lipid membrane of the cell. Choline uptake for PC synthesis is primarily through the ubiquitously expressed choline transporter-like proteins, although choline is also taken up by organic cation transporters (Hedtke & Bakovic, 2019; Sinclair et al., 2000). Once in the cell, choline is phosphorylated in an ATP-dependent manner by cytoplasmic choline kinases α and β to produce phosphocholine. Phosphocholine is then cytidylated by the rate-limiting enzyme of PC synthesis CCT. CCT has two isoforms: a ubiquitous nuclear α and a tissue-restricted cytoplasmic β isoform. This step can thus occur in either the cytoplasm or nucleus, although CCTα is the far more significant contributor to PC synthesis (Lykidis et al., 1998). Finally, CDP-choline is bonded to DAG to produce PC. This reaction is primarily catalyzed by choline-ethanolamine phosphotransferase (CEPT) in the ER, with choline phosphotransferase serving as a secondary source of catalysis in the Golgi apparatus. Both enzymes are transmembrane proteins that allow newly synthesized PC to be directly incorporated into membranes. Unlike TG synthesis, some intermediates in PC synthesis are polar molecules that allow easy movement throughout the cell and thus early steps in PC synthesis is not concentrated in the ER.

Regulation of the CDP-choline pathway is primarily at the step catalyzed by CCT. The α and β isoforms of CCT are encoded by separate genes: *PCYT1A* and *PCYT1B*, respectively, with β isoform having three splice variants (Karim et al., 2003; Lykidis et al., 1999; Lykidis et al., 1998). The most significant functional difference between α and

β is the presence of a nuclear localization signal (NLS) on the former that results in its nuclear localization (Lykidis et al., 1998). CCTα is also the more abundant and metabolically significant isoform (Lykidis et al., 1999). CCTα exists as a homodimer in both a soluble and membrane-bound form with its activity regulated by its ability to associate with membranes, most significantly the nuclear envelope (NE). CCTα consists of the following domains: an NLS, a catalytic domain, a membrane binding (M-) domain enriched in basic residues and a phosphorylation (P-) domain containing 16 serine residues that can be phosphorylated (**Figure 1.3**). The NLS is enriched in basic residues and is responsible for the nuclear import of CCTα while also contributing to the increased membrane affinity of CCTα relative to the β isoforms (Dennis et al., 2011). The catalytic domain is highly conserved among species compared to the rest of the protein, indicating its functional significance (Cornell & Ridgway, 2015). The active site contains several loops and alpha helices containing positively-charged amino acids that help stabilize the negatively-charged phosphates of CTP and phosphocholine (Cornell & Ridgway, 2015). The most significant catalytic residue is lysine 122, whose mutation to either arginine or alanine results in a catalytically-dead enzyme (Helmink et al., 2003). Residues essential for CCTα dimerization are also present in the catalytic domain (Cornell, 1989; Lee et al., 2009). The catalytic domain is subject to inhibition from an autoinhibitory (AI) helix from the neighboring M-domain. This helix is enriched with hydrophobic residues and is immediately followed by a tight turn (Lee et al., 2014). When CCTα is inactive, the AI helix associates with active site helices impairing CCTα catalytic activity by restricting both substrate and K122 from the active site (Cornell & Ridgway, 2015). The M-domain is a semi-ordered region when CCTα is inactive and is itself an inducible amphipathic

Human CCTα P-domain

314-ISPKQSPSSSPTHERSPSPSFRWPFSGKTSPPCSPANLSRCKAAAYDISEDEED-**367**

Rat CCTα P-domain

314-ISPKQSPSSSPTHERSPSPSFRWPFSGKTSPSSSPASLSRCKAVTCDISEDEED-**367**

Figure 1.3. CCTα P-domain phosphosites. The domains of CCTα (from left to right) include a nuclear localization signal (NLS), a catalytic domain, a membrane-binding (M-) domain and a phosphorylation (P-) domain containing 13 (human) and 16 (rat) serine residues that can be phosphorylated. The sequence of the P-domain is shown for human and rat CCTα, with serine phosphosites in red.

α-helix enriched in basic residues that inserts into lipid bilayers when CCTα is active. When CCTα is inactive the M-domain is mostly disordered, excluding the AI helix. When activated, the amphipathic M-domain helix assumes a structure with a face enriched in positively-charged lysine residues opposing a face enriched in glutamate residues. These lysine residues are integral for NE association, as their mutation reduces NE association (Gehrig et al., 2008; Johnson et al., 2003). M-domain insertion into the NE is activated by the presence of lipid activators in the membrane, including anionic PLs, FAs, DAG, farnesol and oxysterols (Arnold & Cornell, 1996; Gehrig et al., 2009; Lagace et al., 2002). These lipids enhance M-domain insertion by instilling membranes with one of two properties: increased concentration of negative charge or membrane packing defects (Cornell, 2016). Anionic lipids promote M-domain insertion by altering the domain's charge balance. The glutamate residues are protonated in proximity to anionic membranes, whose enrichment in negatively-charged PLs results in a more acidic local pH (Dunne et al., 1996; Johnson et al., 2003). Packing defects generated by conical or reverse-conical lipids expose the hydrophobic fatty acid tails of PLs to water molecules; insertion of the M-domain mitigates these energetically unfavorable interactions. M-domain interactions are modulated by the CCTα P-domain, a disordered region containing a multitude of serine, threonine and tyrosine residues that can be phosphorylated. Phosphorylation introduces negative charges on the P-domain that impair membrane association (Chong et al., 2014; Wang & Kent, 1995), although dephosphorylation is not necessary for membrane binding (Houweling et al., 1994). How P-domain phosphosites antagonize membrane association is unknown. One explanation is that P-domain phosphates can form charge-based interactions with the lysine residues of

the M-domain, inhibiting the M-domain from inserting into membranes. The P-domain undergoes large scale dephosphorylation when stimulated with oleate (Wang et al., 1993), although not all residues are affected; S319 becomes dephosphorylated in response to oleate stimulation, whereas C-terminal residues Y359 and S362 remain phosphorylated (Yue et al., 2020). CCTα phosphorylation appears to involve a multitude of kinases, although the identity of these kinases remains enigmatic. Glycogen synthase kinase 3 and cyclin dependent kinase 1 phosphorylate a few unknown serine-proline sites *in vitro* while casein kinase 2A phosphorylates S362 at the C-terminus (Cornell et al., 1995). Interestingly, abatement of S362 phosphorylation reduced total CCTα phosphorylation by 20%, suggesting that phosphorylation at other sites is dependent on the phosphorylation status of S362 in a form of hierarchal phosphorylation. Other kinases identified through *in vitro* screens include cell division control kinase 2 and protein kinase C α and βII isoforms. Even less is known about CCTα phosphatases as only one phosphatase has been identified *in vitro*: protein phosphatase 1 (Arnold et al., 1997). Protein phosphatase 1 treatment only produced a 2 kDa band shift on SDS-PAGE gels, suggesting that it only acts on a subset of phosphosites. One possible candidate phosphatase is C-terminal domain nuclear envelope protein (CTDNEP1; also known as Dullard). CTDNEP1 as the name suggests is a NE phosphatase that dephosphorylates C-terminal phosphoserines sites on LIPIN1, an enzyme that also has membrane association negatively-regulated by phosphorylation (Kim et al., 2007). CTDNEP1 is thus a promising CCTα phosphatase candidate given that some CCTα dephosphorylation occurs on the NE. Better understanding of CCTα phosphoregulation is essential to understanding how PC synthesis is regulated and is a major component of my research.

A secondary mechanism of PC synthesis is the methylation of the PE ethanolamine headgroup. This requires three successive methylations using S-adenosyl methionine, all of which are catalyzed at the ER by phosphatidylethanolamine N-methyltransferase (PEMT). This secondary pathway occurs primarily in the liver and constitutes 30% of hepatic synthesis (DeLong et al., 1999), although differentiated adipocytes also express PEMT (Cole & Vance, 2010). PEMT has been noted on LDs in hepatocytes (Lehner et al., 1999) and adipocytes, with adipocyte PEMT being important for LD stability (Hörl et al., 2011).

The Lands cycle acts as a third pathway of PC synthesis. Unlike the CDP-choline or PEMT pathways, the Lands cycle does not produce *de novo* PC but acts as a remodelling and salvage mechanism between PC and lyso-PC. Phospholipase A2 removes the FA at the *sn*-2 position of PC to generate lyso-PC, which is then converted back to PC by LPCATs (Lands, 1958). LPCATs are primarily localized to the ER (Moessinger et al., 2014), although LPCATs 1 and 2 have been identified on LDs and are capable of converting lyso-PC to PC (Moessinger et al., 2011). PC generated from the Lands cycle is important for TG storage as LPCAT1/2 knockdown resulted in enlarged LDs (Moessinger et al., 2014).

The relative importance of each of these PC biosynthesis pathways for LD biogenesis is unknown. Studies reducing PC synthesis by disrupting any of the PC synthetic pathways consistently show enlarged LDs due to reduced LD surface to volume ratio (Aitchison et al., 2015; Moessinger et al., 2014). A study comparing disruption of PC synthesis between the CDP-choline pathway and the Lands cycle found that disruption of both pathways yielded larger LDs through two different mechanisms (Moessinger et al.,

2014). Disruption of the CDP-choline pathway resulted in increased TG synthesis with less PC to package it while disruption of the Lands cycle changed LD packing dynamics due to the inability to convert the reverse conical lyso-PC to cylindrical PC. Disruption of the CDP-choline pathway also led to a larger increase in LD size. Considering that the CDP-choline pathway produces the majority of PC in the ER, it is likely the most important contributor to LD PC. PEMT methylation and the Lands cycle likely provide more nuanced curation of PC species since PEMT methylation preferentially generates PC species with polyunsaturated fats at the *sn*-2 position (DeLong et al., 1999), while the Lands cycle allows the remodeling of PC species at that same position.

1.2.5 Connections between phosphatidylcholine and triacylglycerol synthesis

Both TG and PC synthesis are essential for lipid storage in LDs and share DAG as an intermediate, suggesting some level of interplay between the two pathways. PC can be converted to TG precursors DAG and PA by phospholipases C and D, respectively, while TG can be hydrolyzed to DAG that can be incorporated into PC. These interconversions are important *in vivo*, as a significant component of lipoprotein-derived PC is converted to TG in hepatocytes (Minahk et al., 2008; Van Der Veen et al., 2012). PC synthetic capacity also affects TG synthetic flux. Inhibition of the CDP-choline pathway increased TG synthesis, likely due to the diversion of DAG from PC synthesis (Caviglia et al., 2004; Lee & Ridgway, 2018; Moessinger et al., 2014). Finally, PC synthesis can elevate the secretion of TG via lipoproteins. Intestinal epithelial cells preferentially secreted TG-rich lipoproteins when supplemented with PC, while impairing PC synthesis reduced TG secretion and led to greater LD TG accumulation (Lee & Ridgway, 2018; Mathur et al., 1996). A similar reduction in TG secretion was observed with very low-density

lipoprotein (VLDL) in hepatocytes with impaired PC synthesis (Yao & Vance, 1988). Given the importance of PC for proper cell handling of TG coordination between the two synthetic pathways is of paramount importance. This coordination likely occurs at the substrate level, as the increased formation of DAG would drive the formation of TG while also elevating PC synthesis by increasing translocation of CCTα to membranes (Pelech & Vance, 1984).

1.2.6 Lipid droplet formation

LD formation occurs via budding from the ER, the most significant site of lipid synthesis. TG and CE synthesized in the ER accumulate between the leaflets of the ER membrane, forming a lens-like structure (**Figure 1.4**). Increased lipid accumulation induces greater membrane curvature that promotes LD budding into the cytoplasm due to greater cytoplasmic leaflet coverage of the neutral lipid core versus the ER luminal leaflet (Chorlay et al., 2019). LD formation can be characterized by three steps: nucleation, ripening and budding, with further LD expansion occurring after budding (**Figure 1.4**) (Wilfling et al., 2014).

LD formation begins with nucleation, the coalescing of neutral lipids into a lens-like structure between the cytosolic and luminal leaflets of the ER membrane. Nucleation is thermodynamically-driven as it becomes more energetically-favorable for hydrophobic neutral lipids between the leaflets to coalesce into a lens that minimizes contact with aqueous surroundings (Thiam & Ikonen, 2021). Nucleation occurs instantaneously after the concentration of neutral lipids reaches a specific threshold.

Expansion of neutral lipid lenses occurs spontaneously via Ostwald ripening, which is the energetically-favorable transfer of neutral lipids from smaller lenses to larger

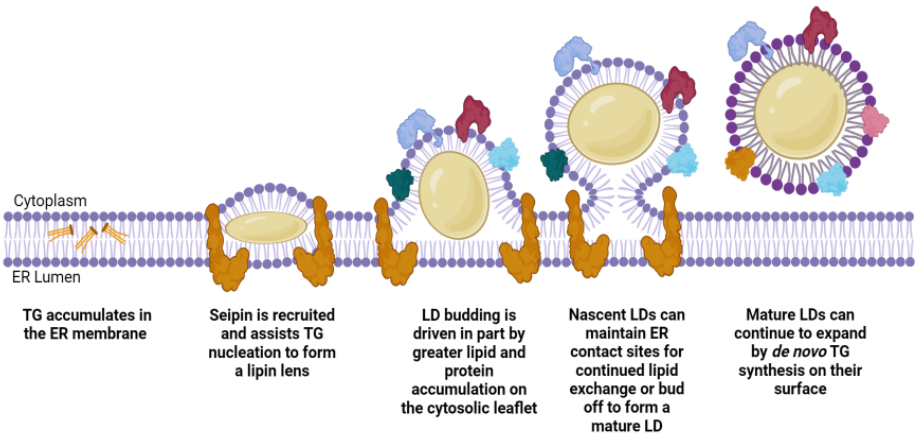

Figure 1.4. Cytoplasmic LD formation. LDs form when TG accumulates in the ER membrane. Once TG reaches a threshold it spontaneously nucleates into a lipid lens in a process facilitated by seipin. LD budding towards the cytoplasm is driven by greater protein and lipid concentration on the cytoplasmic leaflet, which reduces surface tension by minimizing TG exposure to aqueous interactions. Nascent LDs can maintain ER contacts and undergo further growth or pinch off from the ER to form a mature LD. Mature LDs can undergo further expansion via *de novo* TG synthesis on their surface. Image made using BioRender.

ones in order to minimize the surface area of lipid exposed to water. Expansion of LD lenses is also assisted by seipin. Seipin is an integral ER membrane protein that forms oligomeric rings around the edges of ripening LDs, preventing the loss of neutral lipids (Salo et al., 2019). However, seipin is not required for LD formation, although its knockdown is characterized by LD heterogeneity, with many small, immature LDs and few very large ones (Wang et al., 2016). Seipin thus ensures that larger LDs do not continually expand at the expense of smaller LDs, moderating LD size distribution. Seipin further enhances LD ripening by concentrating TG synthesis at sites of LD formation.

The process of LD ripening occurs concurrently with LD budding. As a neutral lipid lens expands, the LD protrusion is pushed further out into the cytosol and can pinch off from the ER membrane or retain ER contact. LD budding is driven by a number of biophysical properties bestowed by lipid composition. Lipid compositional asymmetry between the phospholipid-rich cytosolic and luminal leaflets of the ER helps drive LD budding towards the cytosol due to disparities in coverage. LDs preferentially emerge from whichever leaflet of the ER minimizes surface tension between the aqueous and lipid phase (Chorlay & Thiam, 2018). Emergence from the lipid-rich cytosolic leaflet has greater coverage and lower surface tension and thus is thermodynamically favorable (Chorlay et al., 2019). This directionality is primarily driven by PL concentration since PLs make up the bulk of the ER membrane. The importance of coordinating PC synthesis with TG synthesis is thus apparent, as PC is directly synthesized on the cytosolic leaflet and contributes to the PL asymmetry necessary for LD budding. In particular, impaired PC synthesis in *Drosophila* cells led to larger LDs with reduced budding. Lipid

composition further affects LD budding by inducing membrane curvature. Conical lipids that induce positive curvature (such as lyso-PC) promote membrane protrusion in addition to minimizing surface tension and thus enhance LD budding (Chorlay & Thiam, 2018; Choudhary et al., 2018; Zanghellini et al., 2010). Proteins with hairpin confirmations, such as pex30, seipin and lipid droplet assembly factor 1, can also assist LD formation by inducing positive curvature (Chung et al., 2019; Santinho et al., 2020; Wang et al., 2018).

Once budded from the ER, LDs can undergo further expansion through mechanisms involving LD fusion or *de novo* synthesis of lipids. LDs can grow via fusion where multiple smaller LDs in close proximity merge to form a larger one. LDs in close proximity are drawn together by the dissipation of the aqueous phase between them in a process driven by thermodynamic, electrostatic and Van der Waals forces (Thiam et al., 2013). Pore formation in the surface monolayer occurs when the distance between LDs is only a few nanometers. However, pore formation is not sufficient for LD fusion and pores may exist only transiently if unstable. Pore formation requires membranes to bend with negative curvature and is thus stabilized by inverted conical lipids such as DG, FAs or PE while lipids with positive curvature, such as lyso-PC, oppose pore stability (Leikin et al., 1996; Thiam et al., 2013). LD-LD contact sites are further facilitated by proteins and often share machinery with other forms of fusion, as LD fusion is also dependent on the microtubule network and utilizes SNAP receptor proteins to facilitate fusion (Boström et al., 2007; Boström et al., 2005). Proteins also influence LD fusion as regulators. The complex of FSP27, Rab8a-GDP and the GTPase-activating protein AS160 form at LD-LD contact sites and promote LD fusion (Wu et al., 2014). Fusion is

antagonized by the Rab8a chaperone MSS4, which sequesters nucleotide-free Rab8a, preventing its association at LD-LD contact sites (Wu et al., 2014).

LDs can also expand through *in situ* TG synthesis (Wilfling et al., 2013). A subpopulation of LDs harbor enzymes required for TG synthesis, including the rate limiting enzyme GPAT4, AGPAT3, LIPIN1 and acyl-CoA synthetases 1 and 3. These enzymes are primarily obtained during LD budding or through ER contacts, although some LDs can acquire them after ER separation. Growth of the neutral lipid core requires the monolayer to also expand. Unlike TG, PC cannot be synthesized *de novo* on the LD surface as LDs lack the terminal PC synthesis enzyme choline ethanolamine phosphotransferase (CEPT). However, CEPT is found on the ER membrane, allowing for easy transfer to neighbouring LDs. Alternatively, lyso-PC can be converted to PC by LPCAT1 and 2, both of which are present on the LD surface (Moessinger et al., 2011).

1.2.7 Lipid droplet degradation

LDs primarily store fatty acids and sterols as neutral lipid esters which cannot freely cross membranes or cells and thus require hydrolysis into their components. Thus hydrolysis of TG and CE is required to mobilize and distribute fatty acids and cholesterol for production of energy, membranes and signalling factors. LD lipid mobilization has been primarily studied in adipocytes given their central role in lipid storage. LD lipids can be degraded through two pathways: hydrolysis by LD-associated lipases or lipophagy.

Lipase-mediated TG lipolysis is sequentially catalyzed by three lipases. Adipose triglyceride lipase (ATGL) hydrolyzes TG into DAG and a free fatty acid, preferentially targeting the *sn*-2 site although the *sn*-1 site can be hydrolyzed in the presence of the

coactivator CGI-58 (Eichmann et al., 2012). Next, hormone-sensitive lipase (HSL) hydrolyzes DAG into monoacylglycerol (MAG) and a free fatty acid. Finally, monoacylglycerol lipase hydrolyzes MAG into glycerol and a free fatty acid. Sterol esters are primarily hydrolyzed by HSL, although carboxylesterases (CES) 1 and 3 have also been implicated (Dolinsky et al., 2001; Zhao et al., 2007). It is possible that the different enzymes catalyzing sterol ester hydrolysis are tissue-dependant, as HSL has lower expression in-non adipocytes. Lipolysis is enhanced by the degradation of LD coat proteins perilipin (PLIN) 2 and 3 by increasing lipase access to substrate (Kaushik & Cuervo, 2015).

Lipophagy is a second form of LD lipolysis that uses autophagic machinery (Singh et al., 2009). Autophagy acts as a mechanism to degrade damaged proteins and organelles and is elevated during periods of nutrient deficiency. Autophagy is initiated by the formation of autophagosome, consisting of an autophagic membrane that surrounds the material destined for degradation (Mizushima et al., 2008). The autophagosome then fuses with the lysosome, exposing the contents of the autophagosome to a more acidic pH along with a host of lipases, proteases and other catabolic enzymes. The resulting breakdown products are then exported. Autophagy is less selective than other forms of degradation such as lipolysis or ubiquitin-targeting to proteasomes, although chaperone-mediated autophagy (CMA) acts a more targeted method of autophagy.

Lipophagy was first noted in hepatocytes when inhibition of autophagy led to increased TG storage and LD size (Singh et al., 2009). Lipophagy primarily occurs under conditions of starvation, although it also stimulated by cold exposure and occurs during oleate challenge as a means to moderate LD size by promoting the degradation of large

LDs (Martinez-Lopez et al., 2016; Singh et al., 2009). Later studies noted that lipophagy was enhanced by CMA degradation of PLINs 2 and 3 (Kaushik & Cuervo, 2015). Furthermore, PLIN2/3 dissociation from LDs and subsequent autophagic degradation is promoted by phosphorylation by choline kinase α2 during glucose deprivation in an AMP kinase-dependent cascade (Kaushik & Cuervo, 2016; Liu et al., 2021). While most lipophagy research has been hepatic-centric, lipophagy has also been noted in foam cells, brown adipose and hypothalamic neurons suggesting that it could be a generic mechanism (Kaushik et al., 2011; Martinez-Lopez et al., 2016; Ouimet et al., 2011).

The relative importance of these two methods of lipolysis remains unknown but there appears to be a synergistic relationship between the two mechanisms. Lipophagy in foam cells is dependent on lipase activity, as knockout of ATGL and HSL inhibited lipophagy without otherwise impairing autophagy (Goeritzer et al., 2015). Additionally, hepatic ATGL was necessary for the induction of autophagy and lipophagy in a sirtuin 1-dependent mechanism (Sathyanarayan et al., 2017). However, the autophagy-lipolysis relationship also works in reverse as autophagy is required for lipolysis (Sathyanarayan et al., 2017). Both mechanisms require the clearance of PLINs from the LD surface and thus the dependence of lipolysis on autophagy could be due to the CMA degradation of PLINs 2 and 3. Lipases ATGL and HSL are further dependent on interactions with the autophagic protein LC3, with mutation of LC3 interaction motifs preventing lipase recruitment of LDs (Martinez-Lopez et al., 2016). The lipolysis-lipophagy relationship is not strictly intracellular either, as cold-induced autophagy in hypothalamic neurons promoted lipophagy in brown adipose and liver (Martinez-Lopez et al., 2016).

1.2.8 Lipid droplet function: an organelle of many talents

While LDs were initially thought to simply serve as storage depots for neutral lipids, it is now appreciated that LDs are deeply intertwined with metabolism. The presence of LDs in prokaryotes and nearly all eukaryotes demonstrates the ubiquitous nature of the problem of lipid storage and the effectiveness of LDs as a storage solution. The role of LDs in cells includes a host of metabolic and non-metabolic functions.

The most immediately obvious function of LDs is lipid storage. LDs can store vitamins and other hydrophobic nutrients along with precursors for membrane synthesis, but they are most well known for buffering energy supply. LDs store TG during times of excess energy and release FAs during energy starvation. These functions are connected to overall cell and organismal energy balance through cell signalling pathways. TG synthesis and storage is promoted by insulin signalling, while TG hydrolysis is promoted by catecholamines and glucagon. Insulin signalling promotes TG synthesis and thus LD formation through a number of mechanisms, including upregulating TG synthetic genes, increasing activity of the rate limiting step of TG synthesis catalyzed by GPATs and inhibiting lipolysis (Bronnikov et al., 2008; Chakrabarti & Kandror, 2009; Meegalla et al., 2002). In contrast, hepatic TG synthesis and storage is primarily responsive to circulating and intracellular free FA levels rather than insulin signalling (Vatner et al., 2015). The differential TG metabolic responses to insulin between adipocytes and hepatocytes creates a dangerous combination during insulin resistance. Adipocytes unresponsive to insulin continually hydrolyze TG and release free FAs that the liver takes up and stores. This catastrophic combination results in high incidences of NAFLD in insulin resistant and diabetic populations. Meanwhile, glucagon and catecholamines

promote LD catabolism by upregulating β-oxidation genes and increasing lipolysis (Galsgaard et al., 2019; Jocken & Blaak, 2008; Perea et al., 1995). Intracellular signalling thus serves as an important mechanism for coupling the energy buffering capacity of LDs located in adipose and hepatocytes to energy levels of the organism as a whole.

In addition to buffering energy supply, TG storage in LDs serves a second important function: as a mitigator of lipotoxic stress induced by free FAs (Listenberger et al., 2003). Excess FAs can have deleterious consequences on cell function and lead to cell death by perturbing ER membrane properties, increasing synthesis of lipids that are toxic in large quantities such as ceramide and increasing formation of reactive oxygen species leading to mitochondrial dysfunction (Nguyen et al., 2017; Shimabukuro et al., 1998; Velázquez et al., 2016). LDs protective function against lipotoxicity is especially important in the context of pancreatic islet β-cells during metabolic syndrome, where excess free FAs can perturb insulin secretion and induce lipotoxic cell death further exacerbating insulin resistance and type 2 diabetes (Shimabukuro et al., 1998; Zhou & Grill, 1995).

LDs also influence cell metabolism through cell signalling that results in changes to gene expression. LDs store sterol esters, such as retinyl and cholesteryl esters, that are precursors to signalling molecules. Retinyl esters are primarily stored in hepatic stellate cells and can be converted to the nuclear receptor ligand retinoic acid (RA). Target receptors of RA include retinoic acid receptors (RAR) and retinoid X receptors (RXR), which dimerize with other transcription factors to modulate expression of target genes. Examples of transcription factors that interact with RARs and RXRs to modulate lipid

homeostasis include peroxisomal proliferator-activated receptor (PPAR) γ which promotes lipid uptake and liver X receptors (LXRs) that enhance cholesterol efflux (Chandra et al., 2008; Janowski et al., 1996). RA-dependent signalling pathways have been implicated in directly altering the expression of more than 25 genes and indirectly altering hundreds more, including genes essential for lipid metabolism such as long-chain fatty-acyl-CoA ligase (ACSL) 1 and long-chain fatty acid transport protein (Balmer & Blomhoff, 2002). Cholesteryl esters serve as another example of signal transduction ligand precursors stored in LDs. Cholesteryl esters can be converted to free cholesterol, which can be modified to produce oxysterols and steroid hormones, potent regulators of intra- and extra-cellular gene transcription respectively. Steroidogenic cell LDs are cholesteryl-ester rich and steroid synthetic enzymes have been copurified with LDs suggesting that LDs could also serve as platforms of steroid synthesis (Yamaguchi et al., 2015). Finally, more direct examples of LDs in cell signalling and transcription regulation also exist. For example, the adipocyte protein FSP27 can sequester the transcription factor nuclear factor of activated T cells 5, suppressing synthesis of inflammatory and osmoprotective genes (Ueno et al., 2013). Additionally, catecholamine signalling in Leydig cells can induce PLIN5 to dissociate from the LD monolayer and translocate to the nucleus (Gallardo-Montejano et al., 2016). Once in the nucleus, PLIN5 promotes PPARγ coactivator1 (PGC1) transcriptional activity, leading to increased mitochondrial biogenesis and β-oxidation. Another example of LD-regulated transcription factors is the max-like protein X (MLX) transcription factor that regulates glucose metabolism. Under conditions of LD accumulation, an MLX C-terminal amphipathic helix binds to LDs, causing MLX exclusion from the nucleus and thus

downregulating the expression of MLX target genes (Mejhert et al., 2020). This effectively couples lipid storage to the expression of glucose metabolic gene expression.

LDs can also serve as protein storage units. The most well-characterized example of LD protein storage is histones which are essential for chromatin structure and regulation of gene expression. *Drosophila* embryo LDs can sequester histones, delaying histone entry into the nucleus and thus modulating early embryonic development (Li et al., 2014). *Drosophila* LD histones also have anti-bacterial properties (Anand et al., 2012). Histones are also on the surface of LDs in *C.elegans*, rat sebocytes, and mouse oocytes, embryos and hepatocytes (Anand et al., 2012; Welte & Gould, 2017). Hepatic LDs can also store excess apolipoprotein B100 (apoB100) and appear to act as focal points for apoB100 degradation (Ohsaki et al., 2006). This accumulation of apoB100 has been speculated to act as a mechanism to stabilize and prevent aggregation of hydrophobic apoB100. Finally, yeast LDs have been shown to act as reservoirs for the nuclear pore complex proteins nucleoporins (Kumanski et al., 2021).

The functional significance of LDs has continued to expand and novel functions of LDs are continually being discovered. Speculation into LD function has further been expanded by recent reports of a population of LDs present in the nucleus that form primarily under conditions of excess FAs and cellular stress. These nLDs have been a growing area of research over the past decade given the plentiful connections between LDs and lipid metabolism, stress mitigation, cell signalling and gene expression, and histone buffering.

1.3 Nuclear lipid droplets

1.3.1 Nuclear lipid droplets: An introduction

A subpopulation of nLDs were observed as early as 1959 (Leduc & Wilson, 1959) using confocal microscopy and their existence was confirmed later using electron microscopy (Karasaki, 1969, 1973). These early studies revealed two important features of nLDs: their relative abundance in hepatocytes and their formation in cells undergoing stress. However, these observations were not further pursued until the 2010's. nLDs have primarily been observed in oleate-treated lipoprotein-secreting cells such as hepatocytes and intestinal epithelial cells, although they are also present in oleate-treated U2OS osteosarcoma cells, *C.elegans* germ cells and *S.cerevisiae* (Lee et al., 2020; Mosquera et al., 2021; Romanauska & Köhler, 2018). Under basal conditions small quantities also exist in hepatocytes. Interestingly, nLDs have not been reported in adipocytes, the cells with the most significant amount of lipid storage. Why only a fraction of cell types have nLDs is unknown. The existence of two distinct mechanisms of nLD formation (described below) suggests that they may not be a monolithic phenomenon but rather their function may depend on cell type.

Analysis of nLD lipid composition is limited to one study on lipid class content (Layerenza et al., 2013). nLDs isolated from liver tissue of standard diet-fed rats were found to contain relatively more PLs, CEs, cholesterol and proteins while having less TG versus cLDs. The relatively high levels of protein and non-TG lipids is likely a consequence of the smaller size of nLDs relative to cLDs. Additionally, nLD formation is strongly stimulated by excess FAs which could result in greater TG content in nLDs isolated from high fat diet-fed rats compared to rats fed a standard diet.

1.3.2 Nuclear lipid droplet formation

Two mechanisms have been noted so far for nLD synthesis: diffusion of ER luminal LDs (eLDs) through invaginations of the inner nuclear membrane (INM) known as type 1 nucleoplasmic reticulum (NR) and *in situ* synthesis of TG at the INM followed by budding into the nucleoplasm (**Figure 1.5**). The former mechanism is unique to certain lipoprotein-secreting cells such as hepatocytes, while the latter is similar to cLD formation and has been observed in U2OS cells, *S.cerevisiae* and *C.elegans*.

The first reported mechanism of nLD formation occurs in hepatocytes and presumably in other lipoprotein-secreting cells that harbor nLDs, such as intestinal epithelial cells. This mechanism of nLD formation is tightly linked with VLDL secretion, as both are derived from ER luminal LDs precursors (Sołtysik et al., 2019). ER luminal TG is packaged into eLDs by microsomal triglyceride transfer protein (MTP). Under basal conditions, these eLDs will fuse with nascent VLDL containing apoB100 and be secreted as VLDL. However, conditions that lead to excess formation of eLDs or apoB100 degradation such as ER stress result in an accumulation of eLDs that diffuse from the ER lumen to invaginations in the NE inner leaflet called type 1 nucleoplasmic reticulum (NR) (**Figure 1.5**). NR formation was found to be correlated with nLD formation, although it was not required. eLDs can then break through type 1 NR regions that are depleted of lamin A, lamin B receptor and SUN proteins and enter the nucleoplasm in a PML II-dependent process (Ohsaki et al., 2016).

The second mechanism of nLD formation has only been observed in mammals in U2OS osteosarcoma cells, although a similar mechanism has also been noted in *S.cervisiae* and *C.elegans* (Mosquera et al., 2021; Romanauska & Köhler, 2018). Unlike

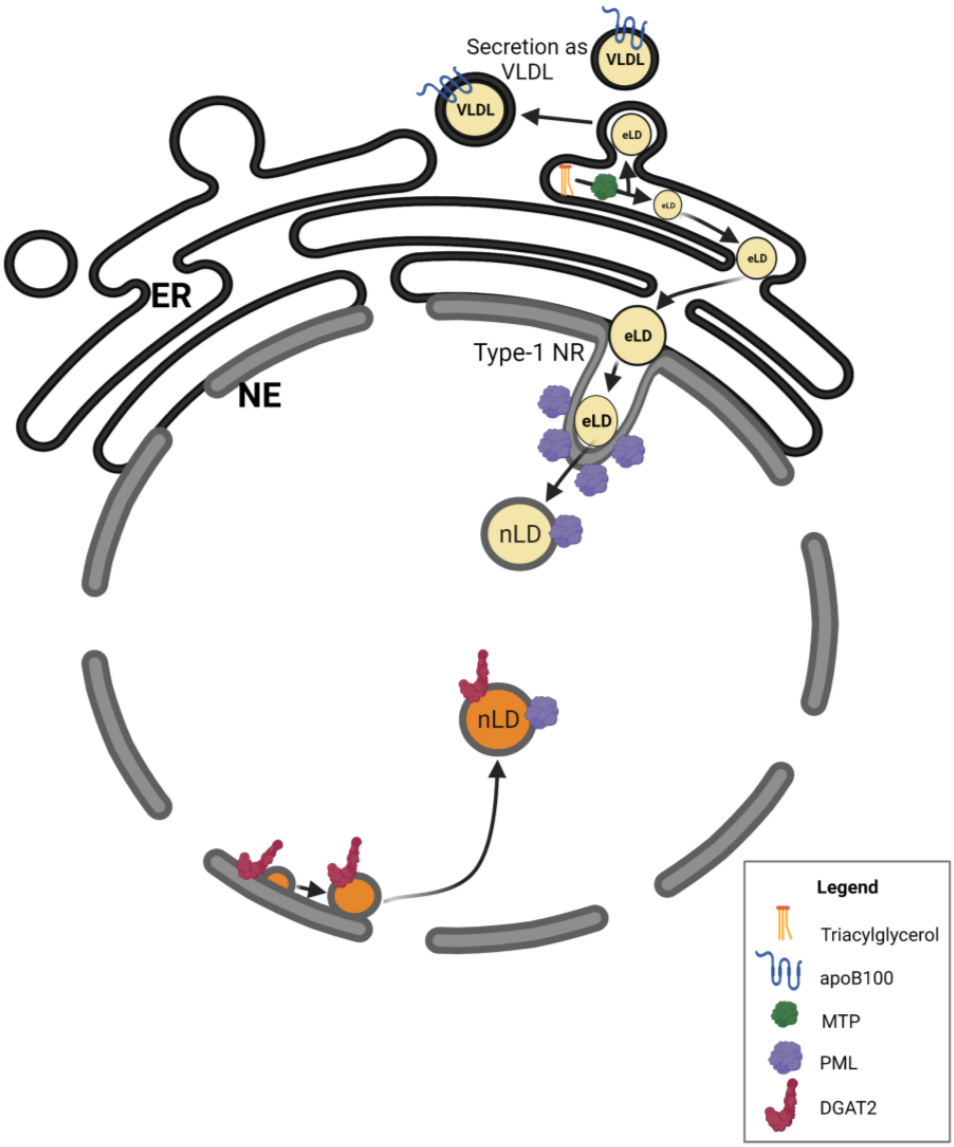

Figure 1.5. Mechanisms of nLD formation. nLDs are formed from two distinct mechanisms. The first mechanism, observed in hepatocytes and shown in yellow, originates with ER-luminal LDs (eLDs) that serve as VLDL precursors. Under conditions of excess FAs, eLDs can defect from the ER lumen to type-1 nucleoplasmic reticulum (NR) invaginations in the inner nuclear membrane (INM) in a PML-dependent manner. The second mechanism, observed in U2OS cells, yeast and *C.elegans* and shown in orange, involves *in situ* TG synthesis on the INM. The INM possess the full complement of TG synthetic enzymes and nLDs bud from the INM in a manner similar to cLDs. Budded nLDs formed through this mechanism retain TG synthetic enzymes and can recruit other nLD protein such as PML.

hepatocytes, nLD formation in U2OS cells is not induced by ER stress or dependent on MTP or PML-II. nLD formation also was not correlated with type 1 NR development. Instead nLDs emerge from the INM in a manner similar to cLD formation from the ER (**Figure 1.5**). The INM of U2OS cells possesses sufficient enzymes for the complete synthesis of TG, including LIPIN1, AGPAT2, DGAT1/2, GPAT3/4 and long-chain FA-CoA ligase (Sołtysik et al., 2021). It was noted that nuclear localization of the LIPIN1 α and β isoforms led to increased nLD formation in a mechanism antagonized by mTOR activity, with LIPIN1β having a more significant effect. Seipin was not directly implicated in nLD formation, as it was absent from the NE. However, seipin indirectly affects nLD formation, protein interactions and lipid content. Seipin knockdown led to increased LIPIN1β expression, nLD formation and PA on nLDs whereas seipin overexpression reduced nLDs but did not alter nLD PA. Seipin indirectly affecting nLD formation was also noted in *C.elegans*, where a mutational screen found that mutation of seipin homologue SEIP1 led to formation of more and larger nLDs (Mosquera et al., 2021). However, this contrasts with yeast nLDs, which also formed TG *in situ* and emerged from the NE but were dependent on seipin (Romanauska & Köhler, 2018). nLDs formed from the INM retained TG synthetic enzymes along with LPCATs, suggesting that TG and PC synthesis can occur on LDs and thus LD expansion is possible post-budding.

1.3.3 Nuclear lipid droplet degradation

In contrast to nLD formation, almost nothing is known about nLD degradation. nLDs decrease in size in the absence of oleate (Lagrutta et al., 2017), however it is unknown whether these lipids are catabolized. Additionally, only one catabolic enzyme

has been identified on nLDs making their mechanism of degradation even more enigmatic. CES1d has been identified as an nLD protein through proteomic screens and could be involved with the degradation of CEs, the most abundant lipid in nLDs under basal conditions (Lagrutta et al., 2021). One potential clearance mechanism is loss of nLDs during mitosis. nLDs are almost completely removed after anaphase of mitosis but completely regenerate within 6 h after mitosis, provided sufficient fatty acid stimulation (Sołtysik et al., 2019). It is unknown if this is the only mechanism of nLD clearance or whether nLDs are degraded by lipolysis or lipophagy. Future research identifying more nLD catabolic enzymes will be essential for determining how nLDs are cleared from cells.

1.3.4 Nuclear lipid droplet proteome

The limited studies of mammalian nLDs have revealed a diverse proteome that includes LD coat proteins, lipid metabolic enzymes and PML nuclear bodies (PML NBs). Most have been identified through cell biology techniques and a single proteomic study has also been reported. This proteomic study (Lagrutta et al., 2021) identified a diverse selection of nLD-associated proteins from liver homogenates isolated from standard-diet fed rats. Cytoskeletal proteins such as actin and keratin were noted, along with histones H2A, H2B, H3.3 and H4 and proteins related to transcription, translation and protein modification such as heat shock protein 7C and elongation factor 1α. However, the study failed to identify any nLD proteins identified by microscopy techniques and the proteins identified (besides CES1d) have not been confirmed to be present on nLDs using immunofluorescence or western blotting. One potential explanation for the failure to identify canonical nLD proteins is that the rats were fed a standard diet whereas most

studies use FAs to stimulate nLD formation. The changes in nLD size, quantity and composition along with broader changes in cell signalling and metabolism stimulated by FAs likely contribute to the absence of many canonical nLD proteins. Alternatively, the isolation methods used could have stripped these proteins from the nLD monolayer

Lipid metabolic enzymes such as CCTα have been reported on hepatic nLDs while a larger cadre of enzymes, particularly TG synthesis enzymes such as GPAT4 and LIPIN1, along with LPCATs have been noted in U2OS cells (Lee et al., 2020; Sołtysik et al., 2019; Sołtysik et al., 2021). PLIN3 was also found on nLDs and promoted the exclusion of CCTα from nLDs. Additionally, nLDs derived from eLD precursors have ER apolipoproteins C3 and E on their surface; whether they maintain any functional significance is unknown (Sołtysik et al., 2019).

One surprising protein found on nLDs and not on cLDs was PML given that PML has not been reported on cLDs. The human *PML* gene encodes at least 7 isoforms generated by alternative splicing that share an N-terminal RBCC/TRIM motif but possess different C-terminal compositions (Jensen et al., 2001). The RBCC/TRIM motif is essential for the formation of nuclear substructures termed PML NBs that are formed collectively from the various PML isoforms. These substructures dynamically associate with a diverse array of nuclear proteins, serving as hubs for post-translational modification and gene regulation (Dellaire & Bazett-Jones, 2004; Salsman et al., 2017). The profile of proteins associated with PML NBs can change in response to stimuli, resulting in PML NBs to have alternative names when possessing certain proteins and/or lacking others. For example, mitotic accumulations of PML proteins are referred to as MAPPS while interactions between PML-II and the lamin or type 1 NR are referred to as

PML patches (Dellaire et al., 2006; Ohsaki et al., 2016; Wang et al., 2020). Thus nLDs associated with PML proteins have been termed lipid-associated PML structures (LAPS) to differentiate them from other PML substructures (Lee et al., 2020) and henceforth, nLDs with PML will be referred to as LAPS, while nLDs will refer to both LAPS and PML-free nLDs.

LAPS have protein profiles that make them distinct from both PML NBs and PML-free nLDs (Lee et al., 2020). LAPS mostly lack canonical PML NB proteins death domain-associated protein 6 (DAXX), SUMO and SP100, although about a quarter of LAPS still retain these proteins. It is unknown whether LAPS containing these proteins constitute a distinct subpopulation or are simply PML NBs transitioning into LAPS that have not yet shed DAXX, SUMO and SP100. Meanwhile, the presence of PML gives LAPs different characteristics than PML-free nLDs. Knockout of all 7 PML isoforms in U2OS cells resulted in decreased CCTα and LIPIN1 recruitment to nLDs, PC and TG synthesis and DAG presence on nLDs, suggesting that PML is essential for CCTα and LIPIN recruitment to and lipid metabolism on LAPS. Interestingly, PML and CCTα localize to distinct locations on LAPS (Lee et al., 2020). The importance of PML on LAPS does not just apply to recruitment of proteins but also nLD formation. In hepatocytes, nLDs form at PML patches on the NE and NR that are depleted in lamins and PML-II knockdown resulted in reduced nLD formation (Ohsaki et al., 2016). Additionally, knockout of all PML isoforms in U2OS reduced nLD formation (Lee et al., 2020). The unique C-terminus of PML-II assists in nLD formation through an unknown mechanism and given the close relationship between PML patches and nLD defection through those patches it is possible that nascent nLDs associate with PML upon nuclear

entry. However, PML is not absolutely necessary for nLD formation as complete knockout of all isoforms still permitted some nLD formation and nLDs form in *C.elegans* and *S.cerevisiae* despite lacking a PML ortholog (Mcphee et al., 2022).

The presence of PML on LAPS expands the potential nLD proteome considerably given the immense number of proteins demonstrated to interact with PML structures. One potential candidate identified is APOL6. Cross-referencing a list of genes identified as possibly PML NB-regulated by chromatin immunoprecipitation and immune-TRAP (Wang et al., 2020) against RNA sequencing data from PML-knockdown U2OS cells (Salsman et al., 2017) by our collaborator Graham Dellaire suggested that APOL6 could be a LAPS-associated protein. One aspect of my project is to determine whether APOL6 is indeed associated with LAPS.

The apoL protein family consists of six members (L1-L6) that are clustered on human chromosome 22 (Page et al., 2001). ApoL1, the first member of the family reported, was found on high-density lipoprotein, resulting in it being named as an apolipoprotein (Duchateau et al., 1997). ApoL1 genetic variants have been implicated in immune defense against trypanosomes by promoting their lysis by inserting and forming a pH-dependent ion channel in the trypanosome membrane (Pérez-Morga et al., 2005; Vanhamme et al., 2003). The remaining apoL family members are strictly intracellular and much more poorly characterized, although apoL3 has been demonstrated to be involved in bacterial lysis in response to IFNγ signalling (Gaudet et al., 2021). Evolutionary analyses have noted that APOL6 is the most ancient of the apoL family members and possesses the most distinct sequence and properties (Pant et al., 2021). Like other apoLs, APOL6 possesses an amphipathic helix nears its N-terminus that could

potentially bind membranes. *In vitro* experiments showed that APOL6 insertion into membranes led to membrane disruption and the formation of large pores whereas other apoLs inserted into membranes and formed ion channels (Pant et al., 2021). This unique property is likely due to an APOL6-only C-terminal transmembrane domain rich in cysteines. APOL6 expression is regulated by RNAs: micro-RNA miR-10b-5p binds to the 3'-untranslated region of APOL6 mRNA in adipocytes and inhibits its expression, whereas super enhancer RNA seRNA1 binds to heterogenous ribonucleoprotein L and upregulates expression in differentiated myotubes (Tan et al. 2019; Zhao et al. 2019). While little is known about APOL6 function, it has been implicated in apoptosis. It possesses a pro-apoptotic BH3 domain and APOL6 overexpression increased apoptosis by binding and inhibiting the pro-survival protein B-cell lymphoma extra large, thus activating mitochondrial-dependent apoptosis and cleavage activation of caspases 3, 8 and 9 (Liu et al., 2005; Zhaorigetu et al., 2011). Additionally, APOL6 overexpression inhibits beclin1-dependent autophagy (Zhaorigetu et al., 2011).

Studies of nLD proteins to date have focused on whether specific proteins are associated with nLDs but have not investigated the temporal dynamics of protein-nLD interactions. Another component of my research aims to understand how nLD-protein association develops over time, helping better understand the functional significance of nLDs and their protein interactions in response to fatty acid overload.

1.3.5 Function of nLDs

Unlike their cytoplasmic counterparts, which have well-characterized functions as reservoirs for energy and cell signalling factors, protein storage and mitigation of ER stress (Welte & Gould, 2017), the functions of nLDs are more speculative. The unique

composition and localization of nLDs suggests that they serve different functions from their cytoplasmic counterparts. Lipid storage for energy metabolism is likely less important as nLDs in mouse liver consist of 37% lipid and 63% protein, whereas cLDs consist of 78% lipid and only 22% protein (Layerenza et al., 2013). Additionally, nLDs contain significantly less TG, the main energy storage lipid; only 19% of lipids in nLDs vs 91% in cLDs. The value of nLDs as energy storage reservoirs is further limited given that nLDs lack proximity or contact sites with the mitochondria and ER, the primary loci of lipid oxidation and synthesis, respectively (Schuldiner & Bohnert, 2017). Potential functions of nLDs are even more expansive due to the existence of LAPS, whose PML connection suggests involvement in post-translational modification and gene regulatory activities. Mammalian nLDs have primarily been observed upon fatty acid stimulation in tissues that handle sudden influxes of lipids, such as hepatocytes and intestinal epithelial cells, and thus it is speculated that nLD biogenesis is a mechanism to preserve lipid homeostasis possibly by coordinating lipid metabolism, gene expression and cell signalling in the nucleus (Mcphee et al., 2022).

A primary function of nLDs could be resolution of ER stress (Sołtysik et al., 2019). In hepatocytes, VLDL is assembled in the ER lumen by fusion of LDs with primordial apoB100-containing droplets. However, ER stress induces apoB100 degradation, ER luminal LD accumulation and release of ER luminal LDs into the nucleoplasm through type 1 NR. The resulting nLDs recruit CCTα, the rate limiting enzyme in the CDP-choline pathway, leading to increased PC synthesis. CCTα recruitment to nLDs is inhibited by PLIN3, which competes with CCTα for binding to nLDs, limiting CCTα access to substrate and PC synthesis. Increased PC synthesis helps

mitigate ER stress, possibly by expanding the ER membrane with an influx of PLs and restoring VLDL secretion by providing PC for packaging luminal LDs into VLDL. Notably, nLDs were not induced by the ER stressor tunicamycin alone, implying that nLDs are specifically produced in response to stress in the presence of excess fatty acids.

nLDs could also serve as sites of nuclear lipid storage of precursors for assembly and maintenance of the NE. Most lipid synthesis occurs in the ER, which is contiguous with the outer NE from which lipids could diffuse to the INM through nuclear pore complexes (Barger et al., 2021). The INM is an active site for lipid metabolism in yeast and U2OS cells (Romanauska & Köhler, 2018; Sołtysik et al., 2021) and the INM of hepatocytes harbors of CCTα and LIPIN1, key enzymes in PC and TG synthesis (Aitchison et al., 2015; Kim et al., 2007). However, nuclear lipid synthesis in U2OS cells could be consolidated on nLDs, as important lipid synthesis enzymes have been reported on nLDs such as: CCT, LIPIN1, DGAT 2, ACSL 3, GPAT 3 and 4, and LPCAT1 (Lee et al., 2020; Sołtysik et al., 2019; Sołtysik et al., 2021).

It is unknown if NE lipid synthesis is coordinated with nLD lipid synthesis. Dephosphorylation of LIPIN1 and CCTα promotes the translocation of these enzymes to both the INM and nLDs, however the precise mechanism behind the partitioning of these enzymes between the two membranes is not known (Lee et al., 2020; Wang & Kent, 1995; Yue et al., 2020). The increase in nLDs that occurs when cells are exposed to excess fatty acids suggests that TG and PL synthesis occurs on nLDs or that there is lipid exchange between the NE and nLDs and the ability of nLDs to be degraded suggests that these lipids can later be mobilized (Lagrutta et al., 2017; Ohsaki et al., 2016). It is thus apparent that nLDs are sites of nuclear lipid synthesis and storage, but the relationship of

lipid storage in nLDs to wider nuclear lipid synthesis remains to be determined.

nLDs may also help restore lipid homeostasis by modulating chromatin structure and thus gene expression. Nuclear lipid droplets have minimal presence in the nucleus under normal conditions (Lagrutta et al., 2017), and thus a sudden expansion of nLDs in the nucleoplasm could affect gene expression by perturbing chromatin organization and transcription factor activity. While regulation of gene expression is not a major function of LDs, examples of cLDs influencing gene expression do exist.

Although there are no direct studies on nLDs and gene expression, there have been findings linking the two. nLD formation was found to coincide with NE lamin depletion, which could alter chromatin interactions since lamins are essential proteins for chromatin organization (Dechat et al., 2008). nLD proteomic analysis using rat liver identified several histones associated with nLDs, including variants of H2A and H2B, along with H3.3 and H4 (Lagrutta et al., 2021). H3.3 is enriched at active sites of gene transcription and is a regulator of H3 histone methylation (Kato et al., 2015), therefore the accumulation of H3.3 on nLDs may aberrate gene expression and epigenetic modifications. Furthermore, PML NBs have been connected to histone H3.3. The PML NB protein DAXX is a chaperone of H3.3 and PML NBs and DAXX coordinate H3.3 integration into DNA, promoting transcription (Corpet et al., 2014; Drané et al., 2010). PML NB regulation of H3.3 is DAXX-dependent and may not apply to LAPS given their limited DAXX colocalization, however DAXX-positive LAPS could also be a unique subpopulation of LAPS with important histone-handling given that H3.3 has been identified on their surface via proteomic screening.

Direct interactions between chromatin and nLDs are another potential avenue for nLDs to modulate gene expression. PLs on the surface of nLDs, including PC, have been shown to interact with chromatin in rat hepatocytes (Albi et al., 1994). Studies in *C.elegans* have shown direct interaction between nLDs and DNA, however it was not determined whether these interactions were facilitated by proteins or lipids and if these associations altered gene expression (Mosquera et al., 2021). While it has not yet been investigated, understanding the interplay between nLDs and chromatin appears to be a promising way to better understand nLD function.

Another potential mechanism for nLDs to restore lipid homeostasis is by providing lipid ligands for the activation of nuclear receptors and by helping recruit proteins with transcriptional coactivation activity. Lipids such as fatty acids, retinol and cholesterol are precursors of cofactors that activate several nuclear transcription factors, including LXRs, PPARs, RXRs and hepatic nuclear factors (HNFs) (Chawla et al., 2001; Hertz et al., 1998). It is noteworthy that nLDs that exist under basal conditions are enriched in sterol esters, which could serve as precursors for RA or oxysterols (Layerenza et al., 2013). Interestingly, two lipid-activated nuclear receptors, HNF4α and PPARγ, are coactivated by the nLD-associated protein LIPIN1.

The significance of LIPIN1 on nLDs is twofold: LIPIN1 possesses catalytic activity essential for TG synthesis and nuclear LIPIN1 acts as a transcriptional coactivator and repressor (Finck et al., 2006; Peterson et al., 2011). Mutation of either LIPIN1 catalytic activity or transcriptional coactivation activity were found to reduce nLDs in U2OS cells, suggesting that both functions are relevant to nLD formation

(Sołtysik et al., 2021). Thus, LIPIN1 could couple nLDs to wider cellular metabolism and signalling and lipid metabolic gene regulation.

LIPIN1 localization is primarily regulated by phosphorylation. Insulin signalling promotes LIPIN1 phosphorylation and retention in the cytoplasm through direct phosphorylation of LIPIN1 by mechanistic target of rapamycin (mTOR) C1, resulting in reduced LIPIN1-nLD association and nLD formation (Harris et al., 2007; Peterson et al., 2011; Sołtysik et al., 2021). The mTOR-LIPIN1 signalling axis thus connects nLDs to wider cellular nutrition and metabolism. The AAA+ ATPase Torsin A, an important regulator of lipid metabolism, also affects LIPIN1 translocation to the nucleus. LIPIN1 is dephosphorylated by the complex of CTDNEP1 and nuclear envelope protein 1 regulatory subunit1 (NEP1R1) (Kim et al., 2007). In *Drosophila*, Torsin was shown to promote NEP1R1-CTDNEP1 dissociation from the NE, resulting in increased LIPIN1 phosphorylation and exclusion from the nucleus. Mice with impaired torsin A signalling displayed hepatic steatosis, impaired lipid oxidation and VLDL secretion and massive nLD accumulation (Jacquemyn et al., 2021; Shin et al., 2019). Torsin A regulation of LIPIN1 could serve as another mechanism to coordinate nLD function with wider lipid metabolism.

Nuclear LIPIN1 can exert effects on lipid gene regulation as both a transcriptional coactivator and co-repressor. Nuclear LIPIN1 activates and inhibits lipolytic and lipogenic gene transcription, respectively, promoting the oxidation of fatty acids. LIPIN1 expression is enhanced by PGC1α; LIPIN1 then promotes PPARα expression and acts as a PPARα coactivator, thus the transcription of FA oxidation genes (Finck et al., 2006). LIPIN1 also influences lipid metabolic gene expression through its direct interaction with

HNF4α to enhance its binding to promoters of lipid catabolism genes (Chen et al., 2012). Both signalling pathways involve LIPIN1-protein interactions and thus nLD sequestration of LIPIN1 could modulate the activation of these pathways. Nuclear LIPIN1 also acts as a repressor of the lipogenic transcription factor sterol regulatory element binding protein (SREBP) 1c through an unknown mechanism that requires its PA phosphatase activity (Peterson et al., 2011). Although LIPIN1 inhibition of SREBP1C does not involve protein-protein interactions, nLDs may still modulate SREBP1C inhibition given that nLDs contain PA, the substrate of LIPIN1 (Peterson et al., 2011; Sołtysik et al., 2021).

PML offers another mechanism to connect transcription factors to LAPS. Like LIPIN1, PML NBs also affect SREBPs and PGC1α activity and thus LAPS could serve to coordinate these effects. SREBP2, but not SREBP1, has been noted to localize to PML NBs (Zoumi et al., 2005), while loss of PML in mouse prostate cancer led to hyperactive SREBP1 and 2 activity and thus transcription of lipogenic genes, suggesting an SREBP-suppressive role for PML (Chen et al., 2018). Additionally, PML can promote the oxidation of lipids by preventing the inhibitory acetylation of PGC1α (Carracedo et al., 2012). This results in greater PGC1α coactivation of PPARγ and therefore expression of lipid oxidation genes. Both PML and LIPIN1 promote lipid oxidative transcription and inhibit lipogenic gene transcription through different mechanisms and thus their dual presence on LAPS could serve coordinate synergistic suppression of lipogenesis and activation of oxidation, although neither PGC1α nor SREBPs have been reported on LAPS (Mcphee et al., 2022). Whether these PML transcription factor regulation

mechanism also apply to PML on LAPS remains unknown but serves as an interesting avenue for future research.

While the functions of nLDs remains mostly speculative, our knowledge of these enigmatic organelles is constantly expanding. My research aims to contribute to this body of knowledge by providing the first insight into the temporal dynamics of PML, LIPIN1 and CCTα association with nLDs and the mechanistic details of CCTα translocation. These findings help to better understand how nLDs recruit key proteins, possibly as a response to quell lipotoxic accumulation of FAs. Additionally, I have conducted preliminary investigations demonstrating the presence of APOL6 on nLDs providing a new potential avenue of nLD function to explore.

Chapter 2: Materials and Methods

2.1 Cell Culture

U2OS and PML-KO U2OS female osteosarcoma cells (courtesy of Graham Dellaire (Lee et al., 2020)) and human embryonic kidney (HEK) 293T cells (courtesy of Graham Dellaire (Lee et al., 2020)) were cultured in Dulbecco's modified Eagle's media (DMEM; Invitrogen 12800-082) containing 10% fetal bovine serum (FBS). Huh7 male hepatocellular carcinoma cells (JCRB0403) were cultured in low-glucose (1000 mg/L) DMEM (Invitrogen 11054-020) containing 10% FBS. CHOK1 and MT58 cells were cultured in DMEM containing 5% FBS and proline (34 μg/mL). All cells were cultured in 5% CO_2 at 37˚C except CHOK1 and CHOK1 MT58 cells, which were cultured at 33˚C unless otherwise noted. Oleate/bovine serum albumin (BSA) complexes (6:1 mol/mol) were prepared as previously reported and stored at -20˚C (Goldstein et al., 1983). Palmitate/BSA complexes (6:1 mol/mol) were prepared using the same protocol except were heated to 70˚C to dissolve palmitate and had a final concentration of 10 mM. Cells were treated with 0.4 mM FA/BSA complex unless otherwise noted.

U2OS and Huh7 cells were transfected at 60-70% confluency. Transfection mix was prepared by incubating lipofectamine (LF) 2000 with plasmid DNA (2 μL LF/1 μg DNA for U2OS, 2.5 μL LF/1 μg DNA for Huh7) for 30 minutes at room temperature. Mock transfected control cells were treated with only LF. Cells had fresh culture media added and transfection mixtures were added dropwise to cells. Experiments were initiated 16-24 h post-transfection.

Plasmids used for transfection include: pcDNA3.1-APOL6-HA (**Section 2.7**), pGFP-C1(2)δ-2xNLS (Lee et al., 2020), pLIPIN-1α-V5 and pLIPIN-1β-V5 (Khalil et al.,

2009), pCMV-rCCTα-V5 and pCCTα-K122A-V5 (Lagace & Ridgway, 2005), pCCTα-3EQ-V5 and pCCTα-8KQ-V5 (Johnson et al., 2003), pCCTα-16SA-V5, pCCTα-16SE-V5 and pCCTα-ΔP-V5 (Wang & Kent, 1995), pCMV-rCCTα-1A-V5 and pCMV-rCCTα-1D-V5 (Yue et al., 2020) and pCMV-rCCTα-V5 S→A and S→D P-domain mutants (**Section 2.7**).

2.2 Lentiviral production and cell transduction

shCTDNEP lentivirus was produced in HEK293T cells (70% confluent in 10 cm dishes). Cells were co-transfected with polyethyleneimine complexed with 3.3 µg of pLKO.1-shCTDNEP1 (Horizon Discovery RHS3979), 2 µg psPAX.2 and 1 µg pMD2.G. shCTDNEP shRNAs were from the RNAi consortium and had clone numbers TRC0000006911, TRC0000006912 and TRC0000006914 (listed as shRNAs 4, 5 and 7 in figures). Media was replaced with fresh DMEM+10% FBS 18 h post-transfection. Virus-containing media was collected 48 h post-transfection and filtered using a 0.45-micron polysterene filter. Virus-containing media had polybrene added (final concentration 10 µg/mL), was flash frozen using liquid nitrogen and stored at -80˚C.

To produce cell lines stably expressing non-targeting shRNA (shNT) and shCTDNEP1 in U2OS and Huh7 cells, 1 mL of virus-containing media was added to 50-70% confluent cells in 35 mm dishes for 4 h and then 1 mL of culture media was added. Cells were selected for 24 h after virus was initially added using 1 µg/mL puromycin for U2OS cells and 2 µg/mL for Huh7 cells. Selection was deemed complete after complete cell death of puromycin-treated non-transduced cells. After selection, cells were maintained in culture media with the same puromycin concentrations used for selection.

2.3 SDS-PAGE and immunoblotting

Prior to cell lysis, media was removed, cells were washed twice with ice-cold phosphate-buffered saline (PBS), pelleted and lysed for 15 minutes on ice using RIPA (0.05 M Tris-HCl pH 7.4, 0.15 M sodium chloride, 0.25% (w/v) deoxycholate, 1% NP40, 1 mM EDTA, 1x protease inhibitor, 1 mM sodium metavanadate and 2.5 mM sodium fluoride). Lysates were centrifuged to pellet debris, supernatants collected, and concentrations were measured using a Pierce BCA protein assay kit. Lysate supernatants had 1/5 volume 5X SDS reducing buffer added resulting in a 1X final concentration (62.5 mM Tris-HCL pH 6.8, 10% glycerol, 2% SDS, 0.05% bromophenol blue, and 5% β-mercaptoethanol). Lysates were heated at 95°C for 3-5 minutes. All samples were stored at -20°C.

Samples were separated using SDS-polyacrylamide gels (8, 10 or 12.5%) at 60 V until past the stacking gel and then 100 V in SDS-PAGE running buffer (3 mM SDS, 200 mM glycine, 25 mM Tris-base) until the dye ran off the gel. Proteins were transferred to nitrocellulose membranes in transfer buffer (25 mM Tris-base, 192 mM glycine, 20% (v/v) methanol) at 100 V for 60-90 minutes.

Nitrocellulose membranes were incubated at room temperature for 60 minutes or overnight at 4°C with gentle shaking in 4:1 TBS-T (20 mM Tris-base, pH of 7.4, 500 mM NaCl, 0.05% Tween 20): Licor Odyssey blocking buffer. Primary antibodies used include: anti-APOL6 polyclonal (1/1000, Sigma Prestige HPA029165 or HPA029167, used interchangeably), anti-β-actin (1/15,000, 15 minutes at room temperature, Sigma Aldrich AC-15), anti-CCTα polyclonal (1/1000, genScript), anti-CCTα phosphoserine 319 (pS319) polyclonal (1/1000, Kinexus, (Yue et al., 2020)), anti-CCTα

phosphotyrosine 359/phosphoserine 362 (Y359/S362) polyclonal (Kinexus, 1/1000, (Yue et al., 2020)), anti-CTDNEP1 polyclonal (1/500, Sigma Prestige HPA037439), anti-Lipin1 polyclonal (1/1000, Abcam ab181389), anti-OSBP/ORP2 polyclonal (1:1000-1:10,000, in-house ab170) and anti-V5 monoclonal (1/1000, BioRad MCA1360GA and Invitrogen PA1-993, used interchangeably). Primary antibody incubations were conducted at 4°C overnight unless otherwise noted. Membranes were washed twice and secondary antibodies were incubated for 1 h at room temperature. Secondary antibodies used include: IRdye 800CW (1/15,000, LiCOR Biosciences) and 680LT (1/20,000, LiCor Biosciences). Membranes were washed twice with TBS-T and once with TBS (20 mM Tris-base, pH of 7.4, 500 mM NaCl). Nitrocellulose membranes were scanned using a Licor Odyssey and fluorescence was quantified using Licor Odyssey software v3.0.

2.4 Immunofluorescence

Cells cultured on 1-mm glass coverslips were fixed with 4% (w/v) paraformaldehyde in PBS for 15 minutes at room temperature, washed twice with 5 mM NH_4Cl and permeabilized with 0.5% Triton X-100 in PBS at 4°C for 15 minutes. Coverslips were blocked at room temperature for 1 h using 1% BSA in PBS. Primary antibodies used include: anti-APOL6 polyclonal (1/1000, Sigma Prestige HPA029165 or HPA029167, used interchangeably), anti-CCTα polyclonal (1/1000, genScript), anti-CCTα pS319 polyclonal (1/1000, Kinexus, (Yue et al., 2020)), anti-CCTα pY359/pS362 polyclonal (Kinexus, 1/1000, (Yue et al., 2020)), anti-PML monoclonal (1/200, Santa Cruz E11) and anti-V5 monoclonal (1/1000, BioRad MCA1360GA and Invitrogen PA1-993, used interchangeably). Primary antibodies were diluted in 1% BSA in PBS and

incubated overnight at 4°C, either in 750 mL antibody solution in 6 well plates with gentle shaking (anti-CCTα, anti-CCTα pS319, anti-CCTα pY359/pS362, anti-V5) or on 75 µL of antibody solution on parafilm in a humid chamber (anti-APOL6, anti-PML). Coverslips were washed twice with 1% BSA in PBS. Secondary antibodies used include: goat anti-mouse and goat anti-rabbit antibodies conjugated to Alexafluor 488, 594 or 647 (all 1/4000, Thermo Scientific). Secondary antibodies were diluted in 1% BSA in PBS and incubations were at room temperature for 1 h. Cover slips were washed twice with 1% BSA in PBS and LDs were visualized using BODIPY 493/503 (1/500, Thermo Scientific) or LipidTox red (1/1000, Invitrogen) diluted in PBS. Coverslips were rinsed with PBS and nuclei visualized using propidium iodide (1/1000) for 10 minutes at room temperature. Coverslips were mounted on glass slides using Mowiol and confocal slices of cells were imaged using Zeiss LSM710 and Leica SP8 laser scanning microscopes with Plan-Apochromat 63x (1.4 NA) oil immersion objectives. Quantification of nLDs, LAPS, APOL6 puncta and protein association was done manually using the Leica application suite X annotations software.

2.5 Statistical significance

Statistical significance of data was determined from 3 or more independent experiments using a two-tailed student t-test computed by GraphPad Prism 6.0 software or one- or two-way ANOVA. Figure legends indicate how data are presented and how significance was calculated. Significance reported for p-values as follows:

*p<0.05 **p<0.01 ***p<0.001 ****p<0.0001

2.6 Molecular Biology

The APOL6 gene was amplified from U2OS genomic DNA with the 5' primer including a *Kpn1* cut site at 5' end and the 3' end of the 3' primer including an HA-tag followed by a *Xho*1 site. The amplification product was ligated into pCR-Blunt-II-TOPO (Invitrogen) and sequenced. APOL6-HA was then cut from the TOPO vector was cloned into pcDNA3.1 using *Bam*HI and *Xba*I.

pCMV-rCCTα-V5, pCMV-rCCTα-1A-V5 and pCMV-rCCTα-1D-V5 were mutated using mutagenic primers (see **Figure 3.17A** and **Figure 3.18A**). The same primers were used on all constructs to mutate tracts 3 and 4. However, another set of 5' primers were needed to mutate tract 2 on constructs with tract 1 mutated, due to the proximity of the two tracts. Site-directed mutagenesis PCR was used to mutate rCCTα-V5, with melting temperature determined through trial and error. PCR products were incubated with *Dpn*I to cleave the methylated template DNA and transformed in Sig10 cells (Sigma Aldrich) per the manufacturer's protocol. Colonies were selected on carbenicillin plates, grown in 50 mL LB broth plasmids were isolated using a Qiagen Plasmid Miniprep Kit and sequenced. Successful mutants were then sequentially mutagenized with another mutagenic primer to produce double, triple and quadruple mutants.

2.7 Primers used

Primer name	Primer sequence (5'→3')
1A rCCT 2A fwd	CCCAAGCAGGCTCCCGCCGCCGCCCCTACTCATGAG CGC
1A rCCT 2A rev	GCGCTCATGAGTAGGGGCGGCGGCGGGAGCCTGCTTG GG
1D rCCT 2D fwd	GCTGCAGGCCATCGATCCCAAGCAGGCATCCTACGAC GACCCC
1D rCCT 2D rev	GGGGTCGTCGTCGGGATCCTGCTTGGGATCGATGGCCT GCAGC
APOL6-HA fwd	GGTACCGGCACCATGGACAACCAGGCGGAGAGA
APOL6-HA rev	CTCGAGTTAAGCGTAATCTGGAACATCGTATGGGTATG TAAACTGTACATACAC
WT 2A fwd	CCCAAGCAGAGTCCCGCCGCCGCCCCTACTCATGAGC GC
WT 2A rev	GCGCTCATGAGTAGGGGCGGCGGCGGGACTCTGCTTG GG
WT 2D fwd	CCCAAGCAGAGTCCCGACGACGACCCTACTCATGAGC GC
WT 2D rev	GCGCTCATGAGTAGGGTCGTCGTCGGGACTCTGCTTGG G
WT 3A fwd	CTCATGAGCGCGCCCCCGCCCCCGCCTTTCGGTGGCCC
WT 3A rev	GGGCCACCGAAAGGCGGGGGCGGGGGCGCGCTCATGA G
WT 3D fwd	CTCATGAGCGCGACCCCGACCCCGACTTTCGGTGGCCC
WT 3D rev	GGGCCACCGAAAGTCGGGGTCGGGGTCGCGCTCATGA G
WT 4A fwd	GGCAAGACTTCCCCAGCTGCCGCCCCAGCAAGTCTCT CTAGG
WT 4A rev	CCTAGAGAGACTTGCTGGGGCGGCAGCTGGGGAAGT CTTGCC
WT 4D fwd	GGCAAGACTTCCCCAGATGACGACCCAGCAAGTCTCT CTAGG
WT 4D rev	CCTAGAGAGACTTGCTGGGTCGTCATCTGGGGAAGTC TTGCC

Chapter 3: Results

3.1 Exploring the temporal dynamics of nLDs and nLD proteins

3.1.1 Saturated fatty acids induce CCTα translocation to nLDs but not the INM

All studies on nLD formation used the unsaturated FA oleate (OA) to induce nLD formation. However, saturated FAs are inducers of ER stress and are more lipotoxic than OA and thus nLDs could potentially serve a role in buffering excess saturated FAs. To investigate whether saturated FAs can also induce nLD formation, Huh7 cells were treated with the saturated FA palmitate for 24 h. Like oleate, palmitate induced the formation of nLDs (**Figure 3.1, middle panel**). Additionally, a combination of the two FAs in a 3:1 OA:palmitate ratio also induced nLD formation (**Figure 3.1, bottom panel**). OA, palmitate and OA/palmitate nLDs were all capable of recruiting CCTα, although OA promoted the greatest shift of CCTα from soluble to nLD-associated. This differential translocation could be due to either differing cell signalling activated in response to FA stimulation or differing CCTα lipid activators. It was found that nLDs induced by OA- or palmitate treatment were rich in DAG, a lipid activator of the CCTα M-domain (**Figure 3.2**). It was next determined whether could stimulate CCTα translocation to the INM and thus dephosphorylation in Huh7 cells. As expected, OA induced translocation of CCTα to the INM within 15 minutes of addition (**Figure 3.3A**). CCTα phosphorylated at Y359 and/or S362 translocated to the INM, whereas CCTα phosphorylated at S319 did not. Additionally, the pS319 signal began to dissipate at 30 minutes, indicative of dephosphorylation at this site. However, palmitate was not able to induce CCTα translocation and there was no change in pS319 signal between 0 and 30 minutes

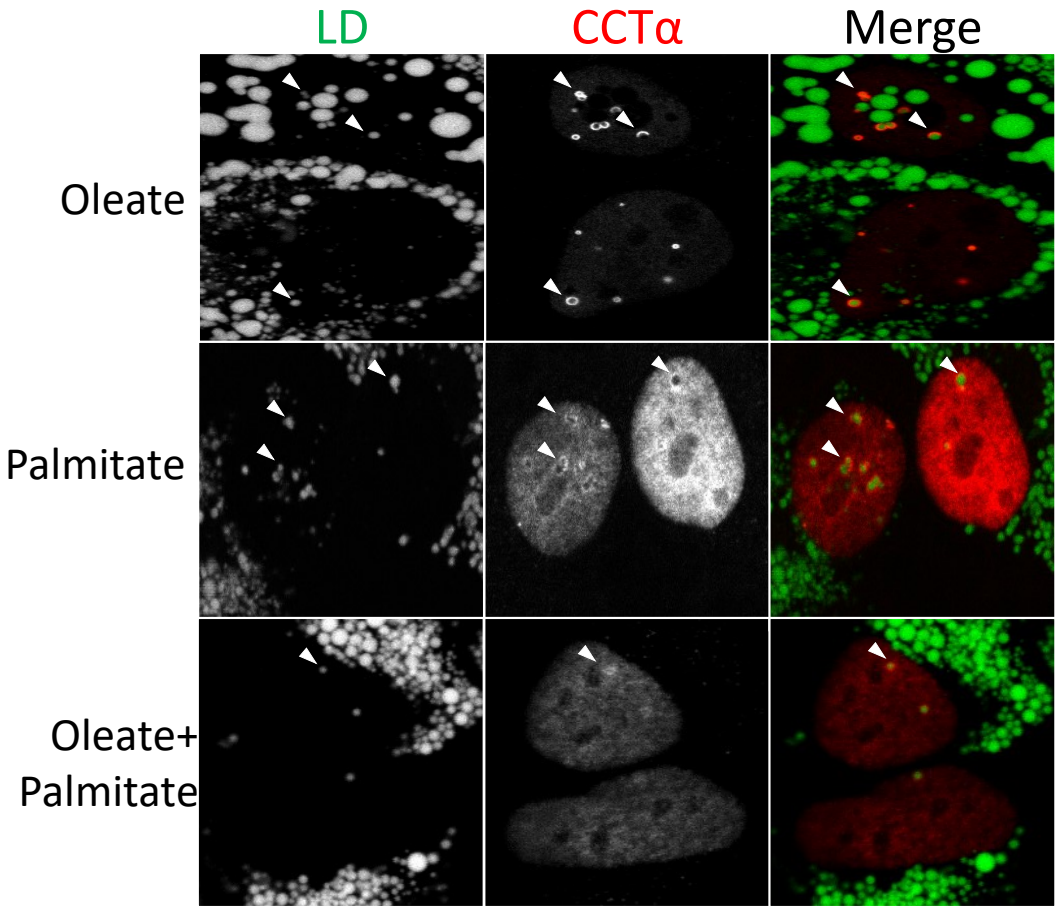

Figure 3.1. nLDs in palmitate-treated Huh7 cells recruit CCTα. Huh7 cells were treated with oleate (0.4 mM), palmitate (0.4 mM) or oleate+palmitate (0.3 and 0.1 mM, respectively) for 24 h. Cells were immunostained with CCTα antibody and LDs were visualized with BODIPY 493/503. Arrowheads indicate CCTα-positive nLDs.

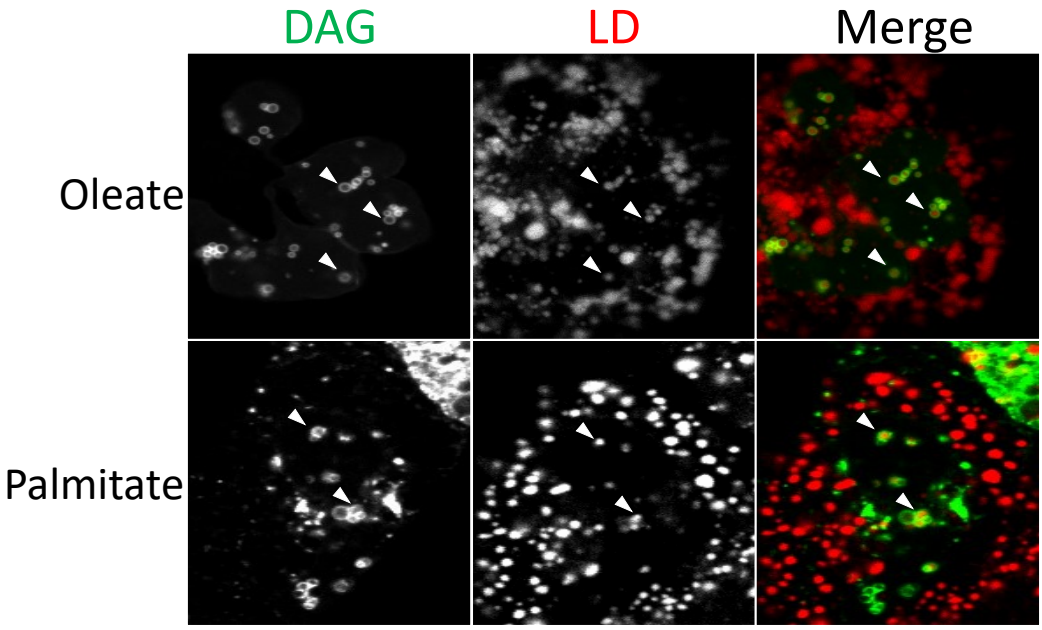

Figure 3.2. nLDs in palmitate-treated Huh7 cells contain DAG. Huh7 cells transiently expressing the nuclear DAG sensor GFP-C1(2)δ-NLS were treated with oleate (0.4 mM) or palmitate (0.4 mM) for 24 h. LDs were visualized with LipidTox red. Arrowheads indicate DAG-positive nLDs.

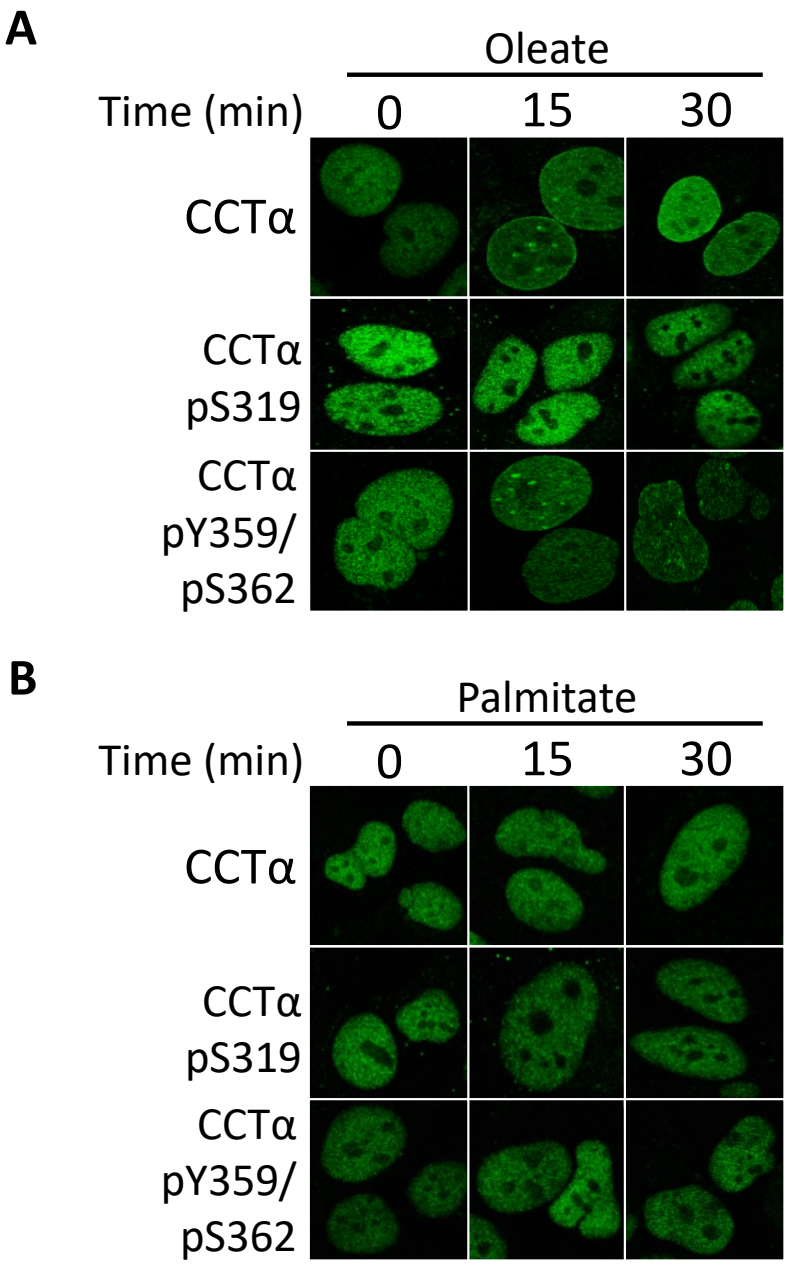

Figure 3.3. Oleate, but not palmitate, induces CCTα translocation to the nuclear envelope in Huh7 cells. Huh7 cells were treated with **(A)** oleate (0.4 mM) or **(B)** palmitate (0.4 mM) for the indicated duration. Cells were immunostained with antibodies against CCTα, CCTα pS319 and CCTα pY359+pS362.

(**Figure 3.3B**). These results demonstrate that OA is a stronger inducer of CCTα translocation, as it promoted translocation to both the INM and nLDs and pS319 dephosphorylation, whereas palmitate did not induce INM translocation, had weaker CCTα staining surrounding nLDs and did not affect pS319. This is also the first example of nLDs forming in response to a stimulus other than OA. Previous studies noted that nLD formation and CCTα recruitment in response to OA acted as a mechanism to enhance PC synthesis (Sołtysik et al., 2019). However, the limited recruitment of CCTα on nLDs in response to palmitate treatment makes the efficacy of these nLDs as a response to lipotoxicity limited, if not questionable.

3.1.2 PML, CCTα and Lipin1 are differentially recruited to nLDs

Previous studies have demonstrated association of PML and CCTα with nLDs after 24 h (Lee et al., 2020; Ohsaki et al., 2016), however little is known about when nLD proteins are recruited. Knowing when nLDs acquire proteins helps to understand how nLD formation may be coordinated with lipid synthesis. To investigate when the nLD proteins PML and CCTα are recruited, Huh7 cells were treated with oleate for 0, 3, 6, 12 or 24 h (**Figure 3.4**). As previously reported, some nLDs were present in Huh7 cells under basal conditions. Interestingly, these basal nLDs were almost always LAPS (PML-positive nLDs) and lacked CCTα association (**Figure 3.5A**), despite DAG being present on surface of these nLDs (**Figure 3.6**). In contrast, nLDs at 24 h had both CCTα and PML, with a plurality of nLDs containing both (**Figure 3.5A**). The quantity of nLDs per cell increased from 0 to 3 h before plateauing around 7 nLD/cell at 6 h (**Figure 3.5B, upper panel**). However, the number of PML- and CCTα-positive nLDs continually increased over 24 h despite the number of nLDs staying constant (**Figure 3.5B, bottom**

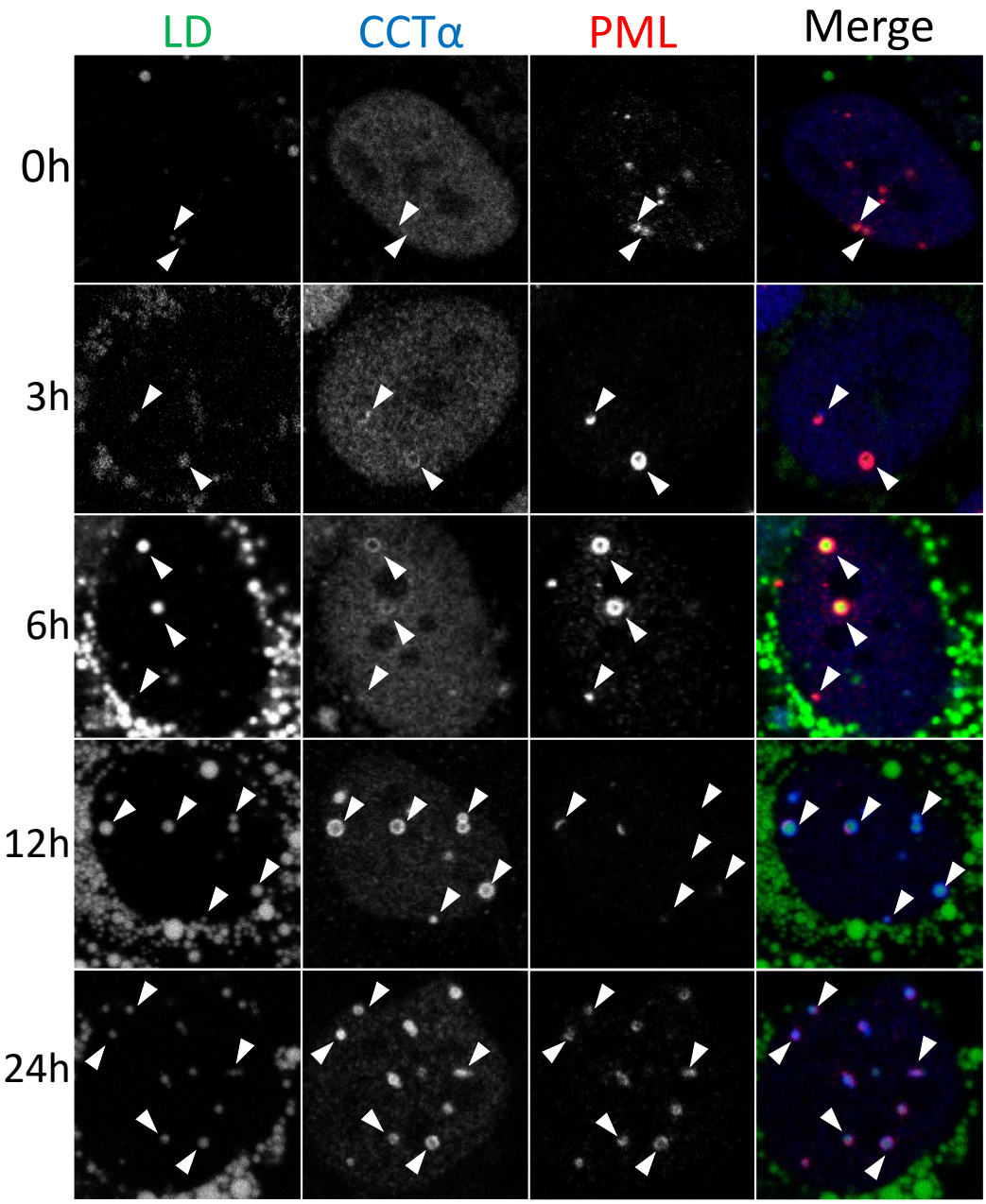

Figure 3.4. PML association with nLDs precedes that of CCTα in Huh7 cells. Huh7 cells were treated with oleate (0.4 mM) for the indicated duration. Cells were immunostained with antibodies against CCTα and PML and LDs were visualized with BODIPY 493/503. Arrowheads denote nLDs.

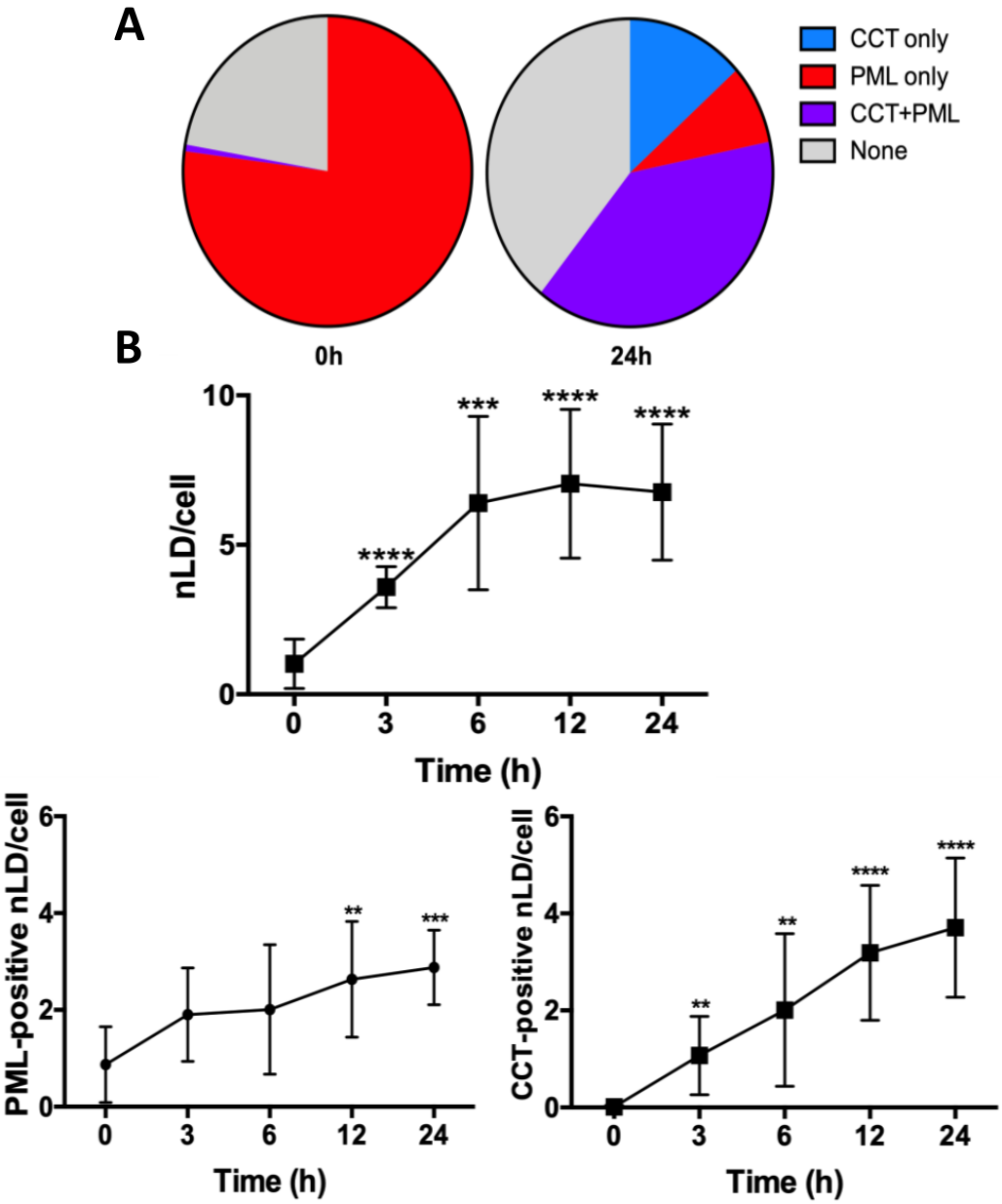

Figure 3.5. Quantification of oleate time points in Huh7 cells. Quantification of images in Figure 3.4. CCTα and PML association with nLDs in oleate-treated Huh7 cells was quantified from 3-5 fields of cells from 3 independent experiments. **(A)** Percent of nLDs at 0 and 24 hours with CCTα, PML or both associated. Data includes all nLDs quantified from all experiments for both time points. **(B)** Number of nLD/cell, PML-positive nLD/cell and CCTα-positive nLD/cell presented as mean with SD. Significance was tested between each time vs 0h using student's T-test. **p<0.01 ***p<0.001 ****p<0.0001

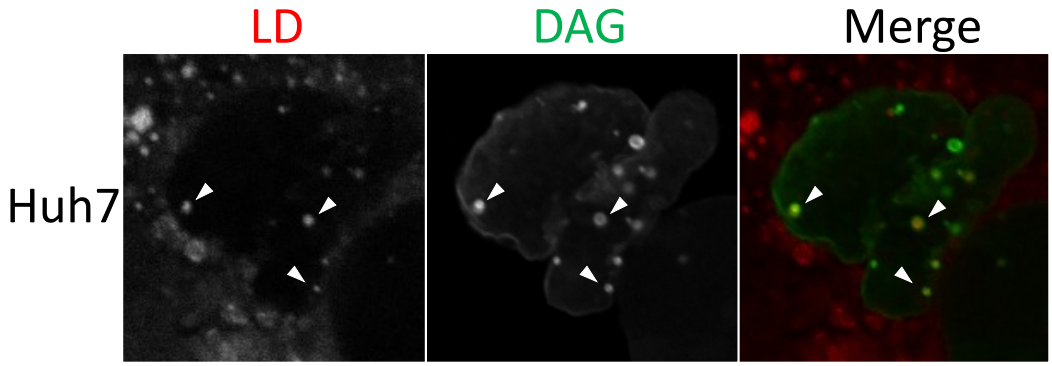

Figure 3.6. DAG is present on nLDs under basal conditions in Huh7 cells. Huh7 cells transiently expressing the nuclear DAG-sensor GFP-C1(2)δ-NLS were cultured in low-glucose DMEM with 10% FBS. LDs were visualized with LipidTox red. Arrowheads indicate DAG-positive nLDs.

panels). This demonstrates that CCTα and PML are differentially recruited to nLDs over time, with PML being omnipresent on nLDs (even under basal conditions) and CCTα requiring OA stimulation for nLD association. As previously reported (Yue et al., 2020), CCTα phosphorylated at Y359 or S362, but not S319, was recruited to nLDs as early as 3 h (**Figure 3.7**). Previous findings by our lab noted that the presence of PML on nLDs increased CCTα recruitment in U2OS cells (Lee et al., 2020). These results demonstrate that PML recruitment to nLDs also precedes that of CCTα. Additionally, the relatively small increase in total LAPS after 24 h and the slow rate of LAPS increase relative to nLD increase suggests that the LAPS pool is a less flexible subset of the entire nLD pool.

Next, LIPIN1 translocation to nLDs over time was determined. Like CCTα, LIPIN1 association with nLDs was shown to be increased by the presence of PML in U2OS cells (Lee et al., 2020). Due to a lack of antibodies detecting endogenous LIPIN1 for immunofluorescence, V5-tagged LIPIN1α and 1β were overexpressed in Huh7 cells that were then treated with OA for 0, 3, 6, 12 or 24 h. Both LIPIN1α (**Figure 3.8, left panel**) and 1β (**Figure 3.8, right panel**) were found to translocate to nLDs upon oleate addition and both isoforms had similar levels of association with nLDs at 0 and 24 h (**Figure 3.9A**). However, LIPIN1α translocation preceded 1β translocation, with there being more LIPIN1α nLDs at 3, 6 and 12 h. The more rapid translocation of LIPIN1α to nLDs could be due to its nuclear localization, as hepatic LIPIN1α has previously been reported to have a more nuclear distribution than 1β (Péterfy et al., 2005). This was observed during these experiments, with about 70% of LIPIN1α-expressing Huh7 cells having a predominantly nuclear LIPIN1α distribution at 0 and 24 h (**Figure 3.9B**). In contrast, LIPIN1β-expressing Huh7 cells tended to have LIPIN1β more evenly

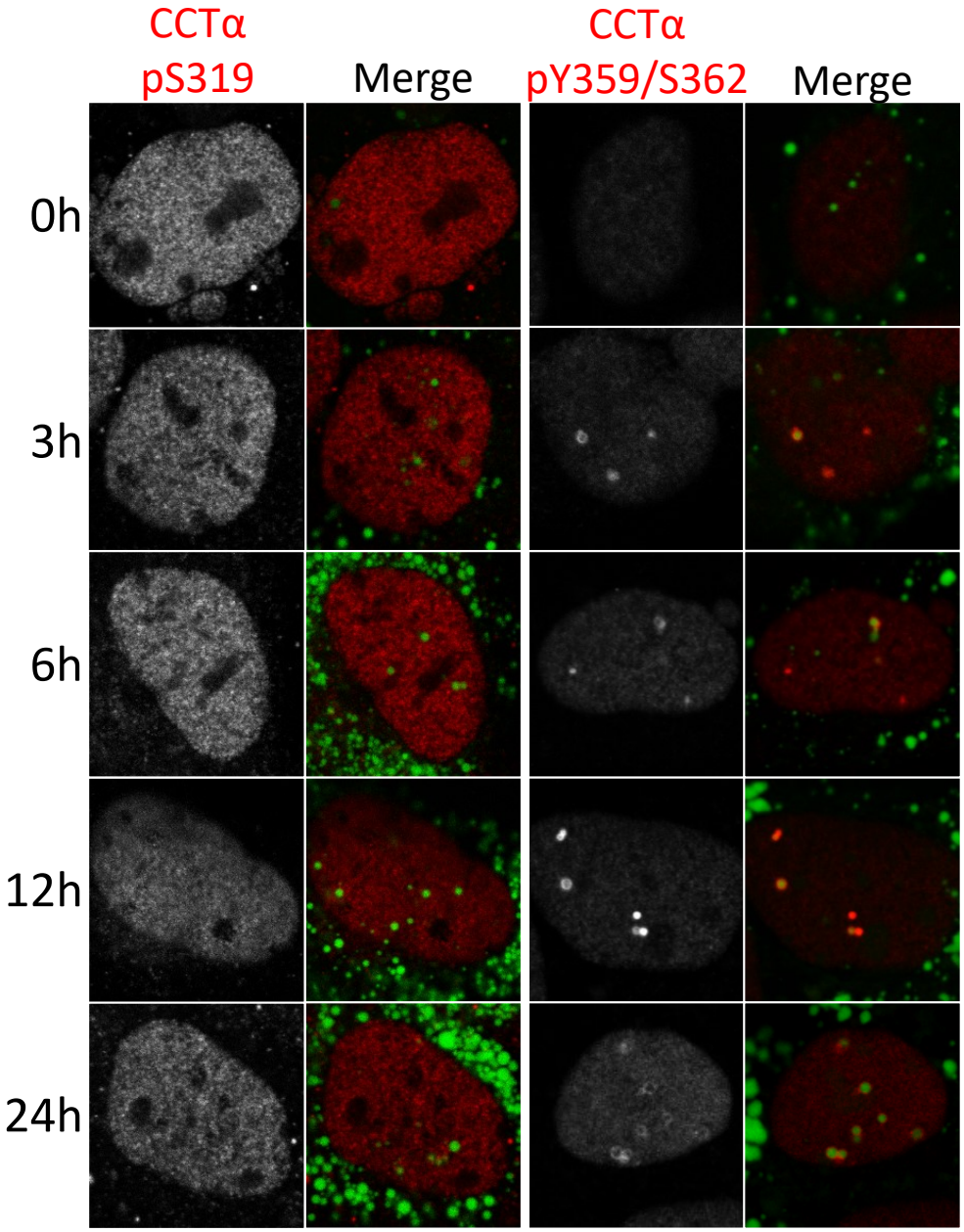

Figure 3.7. CCTα phosphorylated at S319 and Y359/S362 differentially associates with nLDs in Huh7 cells. Huh7 cells were treated with oleate (0.4 mM) for the indicated duration. Cells were immunostained with antibodies against CCTα pS319 and pY359/pS362 and LDs were visualized with BODIPY 493/503. LD=green

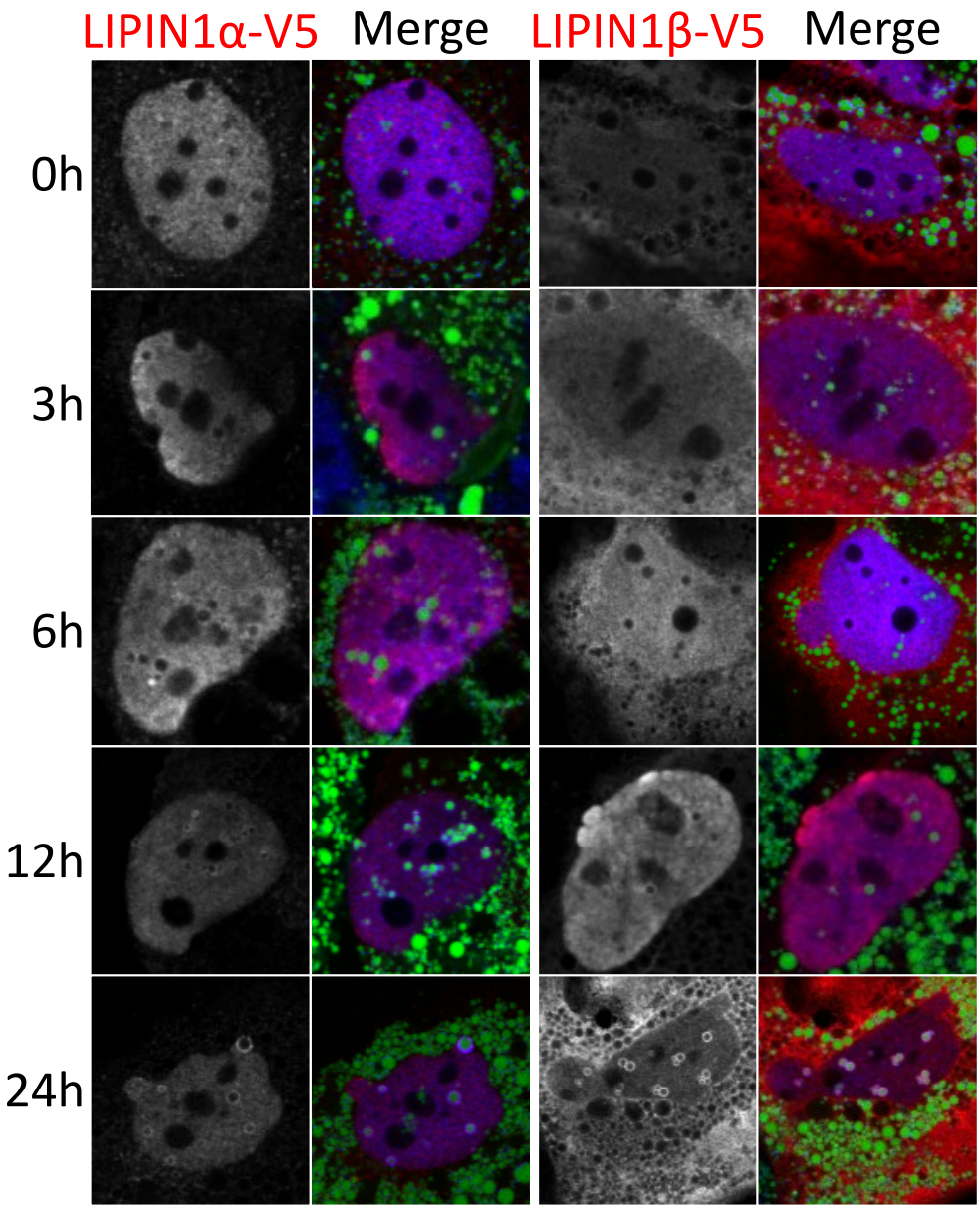

Figure 3.8. LIPIN1α and LIPIN1 β associate with nLDs in Huh7 cells. Huh7 cells transiently expressing LIPIIN1α-V5 or LIPIN1β-V5 were treated with oleate (0.4 mM) for the indicated duration. Cells were immunostained with antibodies against V5 and CCTα and LDs were visualized with BODIPY 493/503. LD=green V5=red CCTα=blue

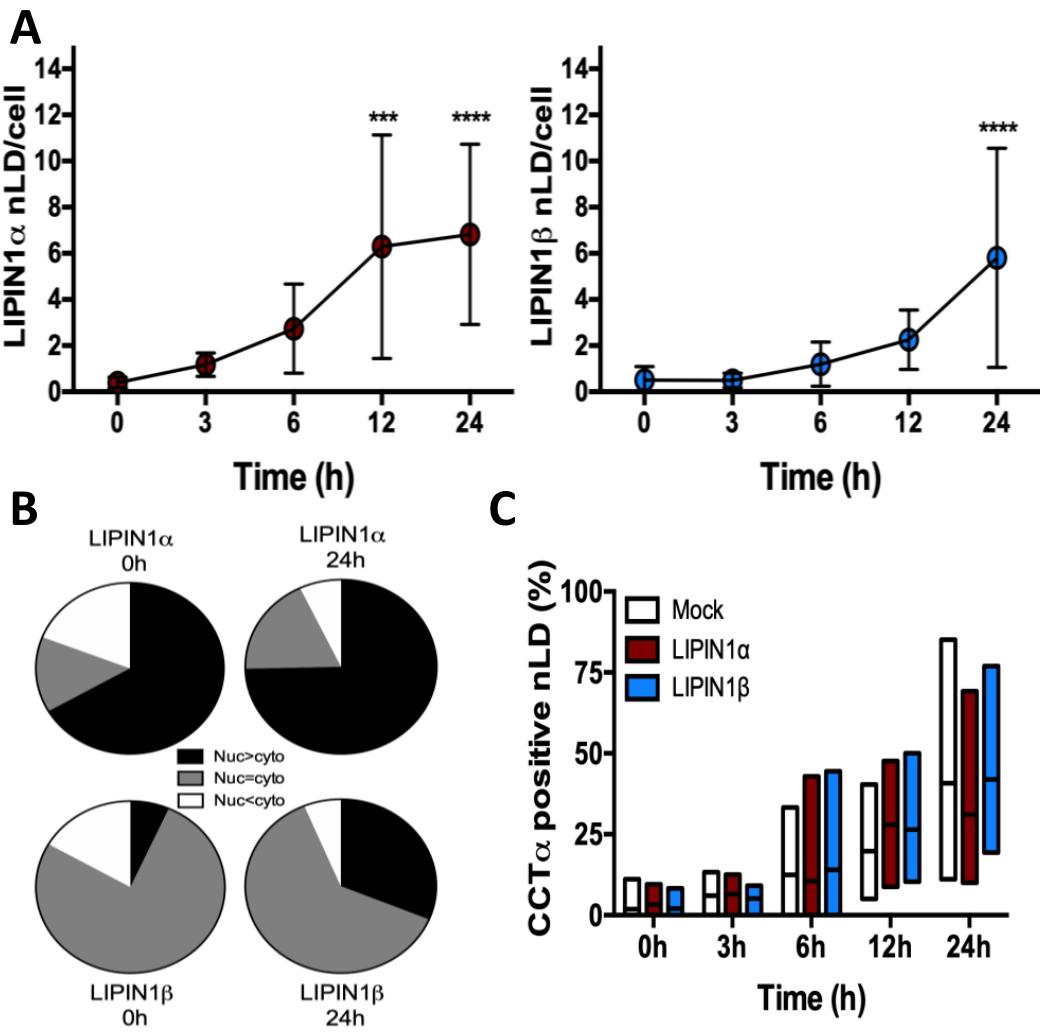

Figure 3.9. Quantification of LIPIN1α/β association with nLDs in Huh7 cells during oleate treatment. Quantification of images from images in Figure 3.8. LIPIN1α/β and CCTα association with nLDs and LIPIN1α/β in oleate-treated Huh7 cells was quantified from 3-5 fields of cells from 2-3 independent experiments. **(A)** LIPIN1α/β-positive nLDs per cell presented as a mean with one standard deviation. Significance was tested between each time point vs 0h using T-test. **(B)** Relative distribution of LIPIN1α/β in transfected cells at 0 and 24 h. LIPIN1 in cells was classified as more nuclear than cytoplasmic (Nuc>cyto), equally partitioned (Nuc=cyto) or more cytoplasmic (Nuc<cyto). **(C)** CCTα-nLD association presented as floating bar charts showing mean and 5th-95th percentile. Significance was tested between mock, LIPIN1α and LIPIN1β cells at each time point using two-way ANOVA. **p<0.01 ***p<0.001 ****p<0.0001

distributed between the cytoplasm and nucleus. This differs from a previous study reporting more LIPIN1β than LIPIN1α in the nucleus of U2OS cells treated with oleate and mTOR inhibitors (Sołtysik et al., 2021). Expression of either LIPIN1 isoform had no effect on the rate of CCTα association with nLDs versus mock transfected cells (**Figure 3.9C**). While it might be expected that increasing expression of LIPIN1 would increase CCTα association given that LIPIN catalyzes the production of the CCTα-activating lipid DAG, a previous report from our lab showed no correlation between the presence of DAG and CCTα on nLDs in U2OS cells (Lee et al., 2020). Lipin1 thus appears to translocate to nLDs in a manner similar to CCTα and unlike PML, with low association under basal conditions and early OA timepoints but with continually increasing association over 24 h of OA treatment.

Additionally, overexpression of LIPIN1α or 1β in Huh7 cells doubled the number of nLDs per cell compared to mock transfected cells (**Figure 3.10A**). Lipin1α-expressing cells had significantly more nLDs than LIPIN1β-expressing cells at 6 and 12 h of OA treatment but not 24 h (**Figure 3.10B**). Overexpression of LIPIN1α or 1β was also demonstrated to increase nLDs in U2OS cells (Sołtysik et al., 2021). Given the earlier association of LIPIN1α with nLDs along with its greater effect on their total and its greater expression in hepatic tissue, it appears that LIPIN1α is the more important LIPIN1 isoform for nLD interaction in liver.

3.1.3 Determining if CTDNEP1 is a regulator of nLD proteins

The NE phosphatase CTDNEP1 is a known LIPIN1 phosphatase (Kim et al., 2007). It was investigated whether it is also involved in CCTα dephosphorylation. Given the role of both LIPIN1 and CCTα as nLD proteins central to TG and PC biosynthesis,

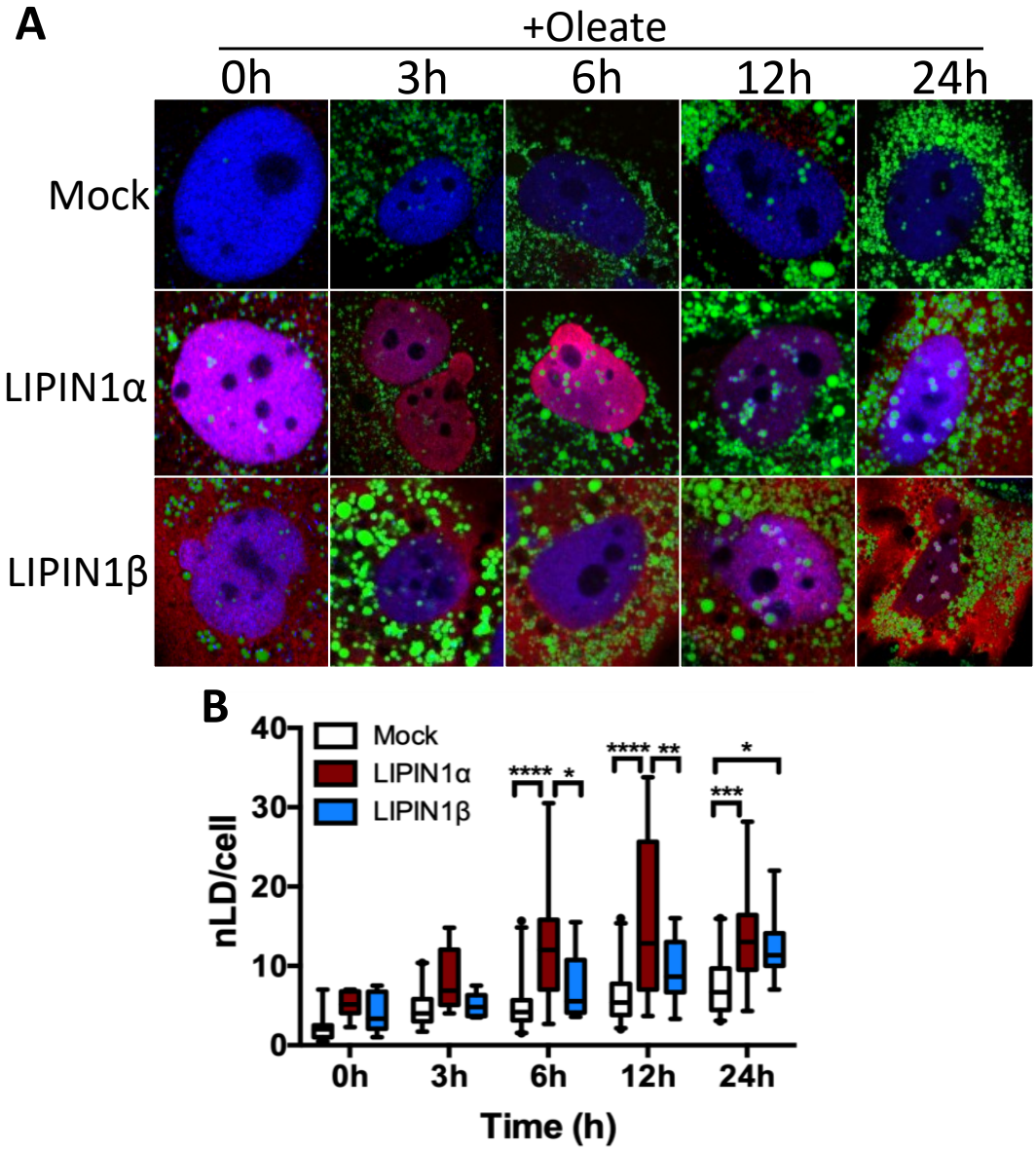

Figure 3.10. LIPIN1 overexpression increases nLD number in Huh7 cells. (A) Huh7 cells transiently expressing LIPIN1α- or β-V5 were treated with oleate (0.4 mM) for the indicated duration. Cells were immunostained with antibodies against V5 and CCTα and LDs were visualized with BODIPY 493/503. LD=green V5=red CCTα=blue **(B)** Quantification of images in panel A. nLDs were quantified from 3-5 fields of cells from 2-3 independent experiments in mock cells and cells expressing LIPIN1α or β. Data presented as box and whisker plots showing the mean and 5th-95th percentile Significance was tested between mock, LIPIN1α and β cells at each time point using two-way ANOVA and Tukey's multiple comparison.
*p<0.05 **p<0.05 ***p<0.001 ****p<0.0001

preliminary experiments were conducted to investigate its role in regulating nLDs in U2OS and Huh7 cells. CTDNEP1 was knocked down using shRNA in U2OS cells resulting in an 80% reduction in expression (**Figure 3.11A**). shCTDNEP1 U2OS cells treated with OA for 1 h had reduced dephosphorylation of LIPIN1 versus shNT cells, as evidenced by the reduction in LIPIN1 band shift below the phosphorylated LIPIN (p-Lipin) (**Figure 3.11B**). A similar reduction in band shift was not observed for CCTα, suggesting that CTDNEP1 knockdown does not affect short-term CCTα dephosphorylation in U2OS cells. CTDNEP1 was also knocked down in Huh7 cells using shRNA, achieving a 60% reduction in expression (**Figure 3.12A**). However, CTDNEP1 knockdown was not sufficient to prevent association of overexpressed LIPIN1α or 1β with nLDs, as both isoforms still associated with nLDs after 24 h (**Figure 3.12B**). These experiments confirm that CTDNEP1 dephosphorylates LIPIN1 but show CTDNEP1 is not necessary for LIPIN1 association with nLDs. Future experiments quantifying LIPIN1 and CCTα association with nLDs over time will be essential to understand whether CTDNEP1 affects nLD protein recruitment.

3.2 A mechanistic analysis of how CCTα association with nLDs is regulated

3.2.1 CCTα association with nLDs is regulated by its M- and P-domains

The role of the CCTα M- and P-domains as regulators of INM association have been well-characterized (Cornell & Ridgway, 2015). To determine whether CCTα association with nLDs is also regulated by these domains, V5-tagged rat CCTα mutants were expressed in U2OS cells (**Figure 3.13A**). The mutants tested included a catalytically dead enzyme (K122A), a hyperactive enzyme with 3 inhibitory glutamate

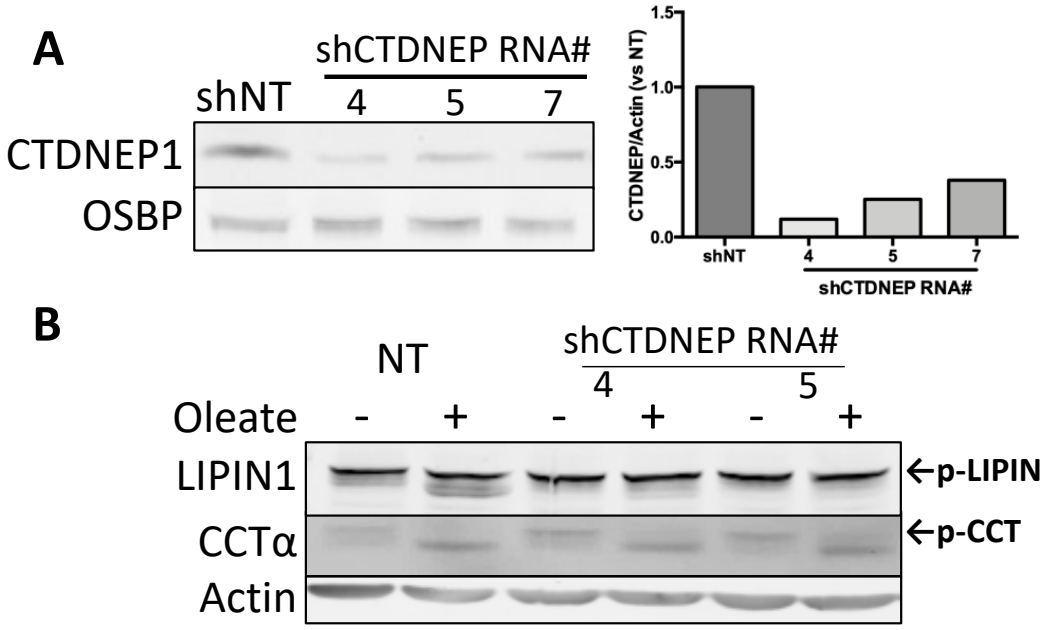

Figure 3.11. CTDNEP1 knockdown reduces LIPIN1 but not CCTα dephosphorylation in U2OS cells. (A) U2OS cells stably expressing non-targeting shRNA (shNT) or shCTDNEP1 shRNAs had expression quantified versus actin (n=1). Total cell lysates were immunoblotted with antibodies against CTDNEP1 and OSBP (load control). **(B)** shNT and shCTDNEP1 U2OS cells were treated with oleate (0.4 mM) for 1 h. p-LIPIN and p-CCTα indicate phosphorylated protein bands. Total cell lysates were immunoblotted with antibodies against LIPIN1, CCTα and actin.

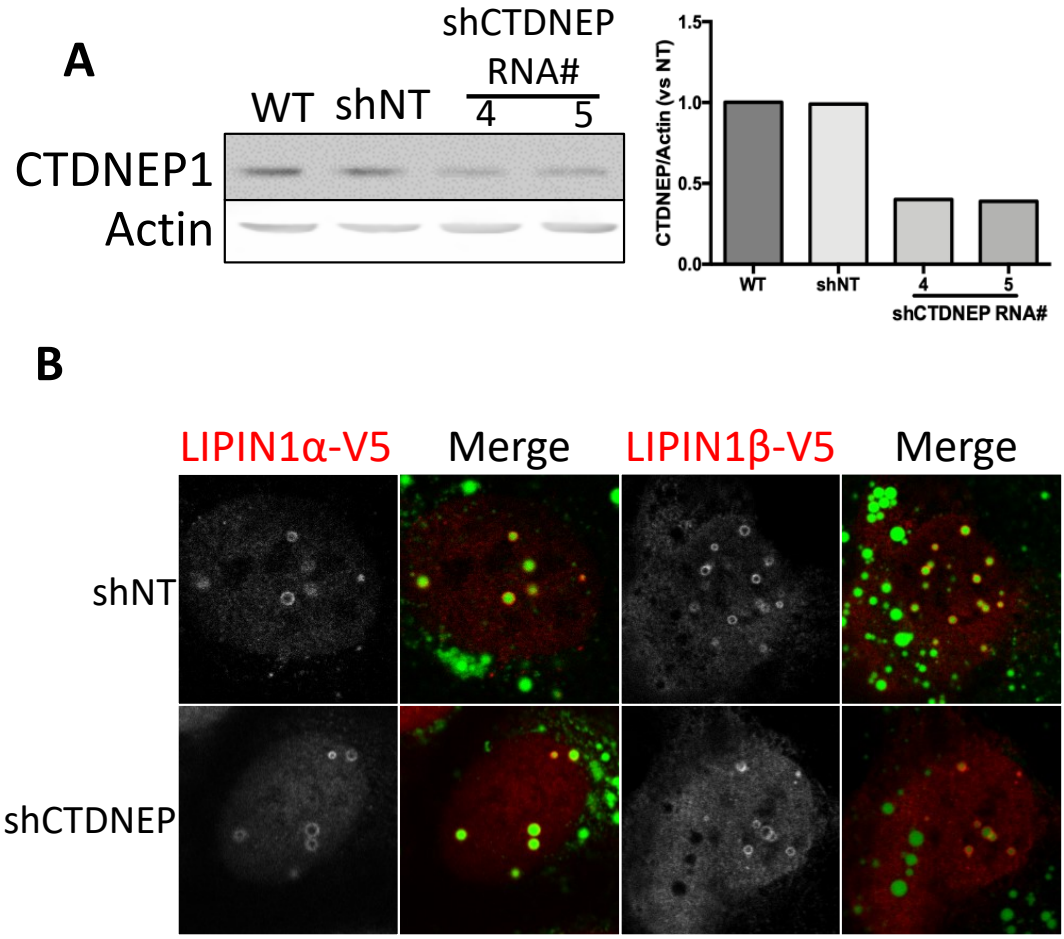

Figure 3.12. CTDNEP1 knockdown does not prevent LIPIN1 association with nLDs in Huh7 cells. (A) Huh7 cells stably expressing non-targeting shRNA (shNT) or shCTDNEP1 shRNAs had expression quantified versus actin (n=1). Total cell lysates were immunoblotted with antibodies against CTDNEP1 and actin. **(B)** shNT and shCTDNEP1 Huh7 cells expressing LIPIN1α- or β-V5 were treated with oleate (0.4 mM) for 24 h. Cells were immunostained with V5 antibody and LDs were visualized with BODIPY 493/503. LD=green V5=red

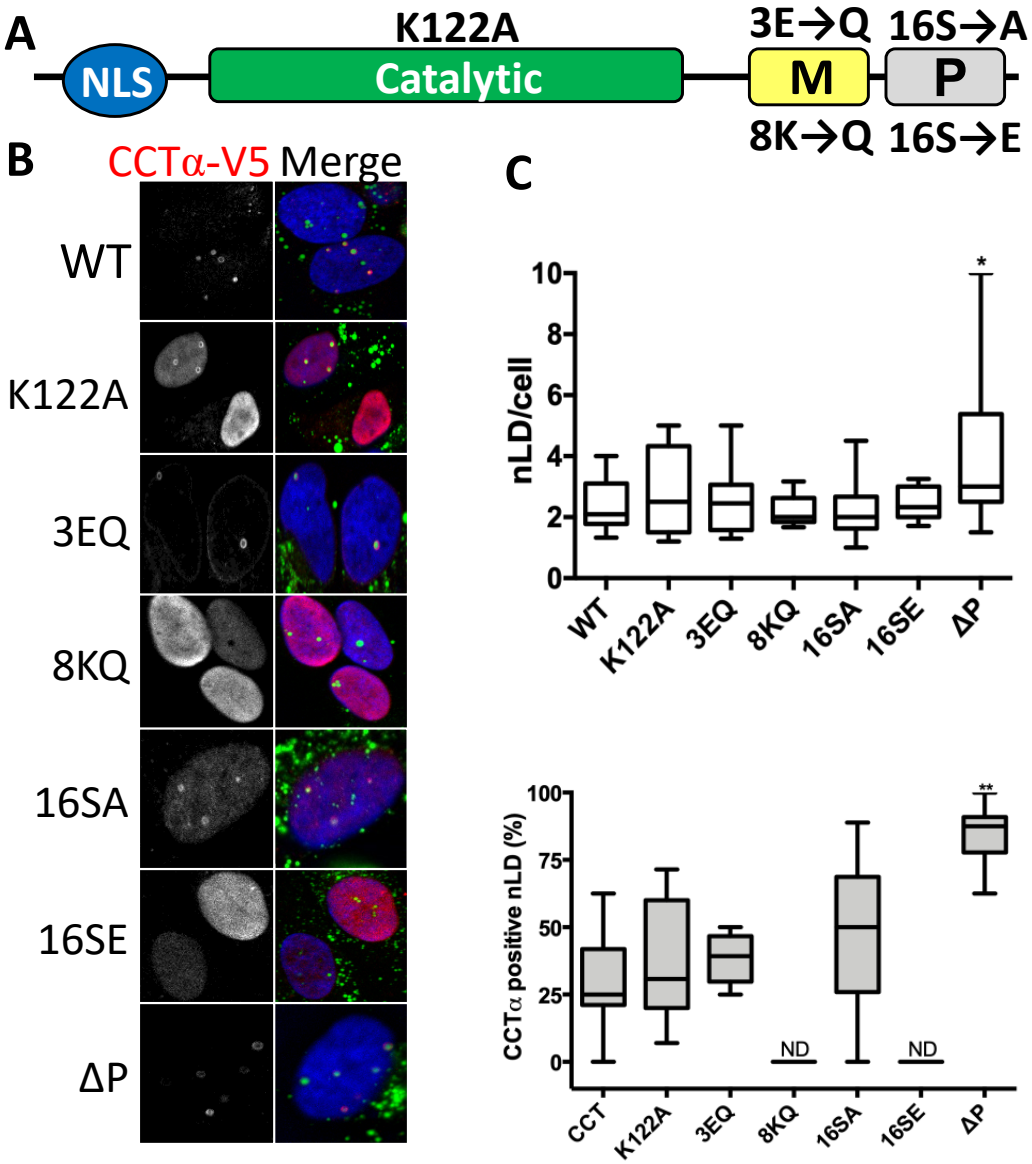

Figure 3.13. M- and P-domains regulate CCTα association with nLDs. **(A)** Domain structure of CCTα showing where each mutant is altered. ΔP mutant (not shown) is truncated at the P-domain. **(B)** U2OS cells transiently expressing CCTα-V5 mutants were treated with oleate (0.4 mM) for 24 h. Cells were immunostained with antibodies against V5, LDs were visualized with BODIPY 493/503 and nuclei with propidium iodide. LD=green V5=red nucleus=blue **(C)** Quantification of images in panel B. nLD number and percentage of nLDs CCTα -V5-positive were quantified from 10-15 fields of cells from 2-3 independent experiments. Data shown as box and whisker plots showing mean and 5th-95th percentile, significance tested using one-way ANOVA and Tukey's multiple comparison vs WT. ND: not detected *p<0.05 **p<0.01

residues on the M-domain mutated to glutamine (3EQ), an enzyme with 8 lysines on the basic face of the helical M-domain mutated to glutamine (8KQ) that had reduced INM association, a phospho-null mutant with all 16 P-domain serines mutated to alanine (16SA) with enhanced INM translocation, a phosphomimetic mutant with all 16 P-domain serines mutated to glutamate (16SE) with reduced INM translocation, and a mutant with the P-domain removed (ΔP). U2OS cells expressing these mutants were treated with OA for 24 h to induce nLD formation (**Figure 3.13B**) and nLD total and CCTα-V5 association were quantified. Cells expressing each mutant had similar levels of nLD formation as wild type CCTα (**Figure 3.13C, top panel**), except for CCTα-ΔP which showed increased nLD formation. Interestingly, the 8KQ and phosphomimetic 16SE mutations completely prevented nLD association (**Figure 3.13C, bottom panel**). In contrast, these mutants were still able to associate with membranes despite these mutations (Gehrig et al., 2008; Wang & Kent, 1995). This demonstrates the necessity of the M-domain for nLD association and suggests that P-domain phosphorylation inhibits nLD association. Conversely, preventing P-domain phosphorylation by mutating all serines to alanines resulted in increased nLD association (although not significant) and complete removal of the P-domain enhanced nLD association threefold, even though removal of the P-domain significantly reduced CCTα-V5 expression (**Figure 3.14A and B, left panel**). The reduction in expression of the ΔP suggests that the P-domain may possess stabilizing effects. Additionally, the lower (albeit not statistically significant) expression of the phospho-null mutant suggests that it is the lack of P-domain phosphorylation that results in reduced expression of these mutants. This corroborates a previous report showing that CCTα dephosphorylation reduces protein stability

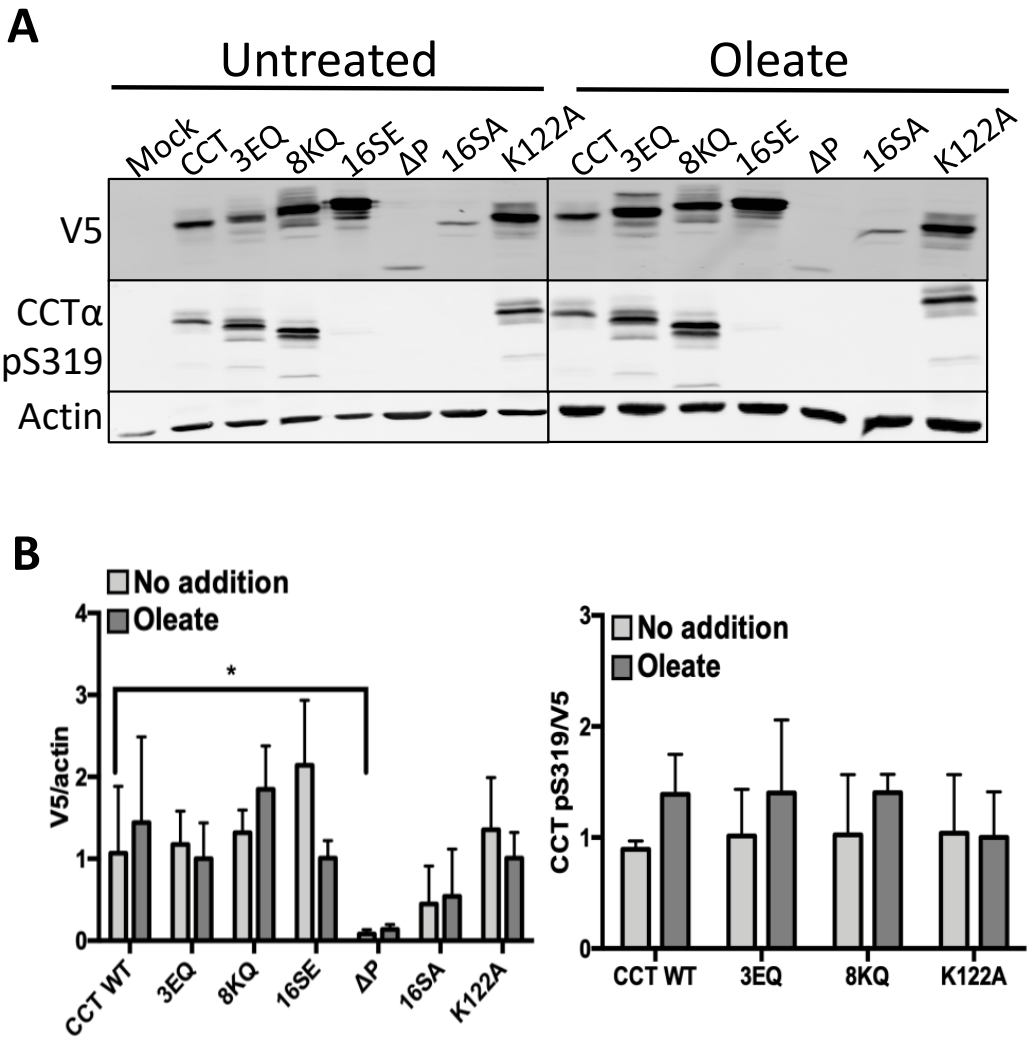

Figure 3.14. Deletion of the P-domain reduces CCTα-V5 expression. **(A)** U2OS cells transiently expressing CCTα-V5 tagged mutants were untreated or treated with oleate (0.4 mM) for 24 h. Total cell lysates were immunoblotted with antibodies against V5, CCTα pS319 and actin. **(B)** Quantification of CCTα-V5, CCTα pS319 and actin from panel A. Data shown as mean and SD, n=3. Significance tested between all mutants of the same treatment versus WT CCTα using one-way ANOVA and Tukey's multiple comparison. Significance between untreated and treated within a pair tested using T-test. *p<0.05

(Groblewski et al., 1995). Additionally, mutants with the S319 site intact (K122A, 3EQ and 8KQ) had no change in S319 phosphorylation, suggesting that mutations of these residues do not affect long-term phosphorylation at this site. Additional mutants were then tested to better analyze how specific residues contribute to nLD association. A less extreme version of the 8KQ mutant with only 5 M-domain lysines mutated to glutamine (5KQ) also failed to associate with nLDs (**Figure 3.15**), while a mutant that had the casein kinase II phosphorylation site S362 mutated to phospho-null alanine (S362A) or phosphomimetic aspartate (S362D) had no difference in association versus wild type CCTα (**Figure 3.16**). Overall, these results demonstrate that CCTα association with nLDs is dependent on the same domains as INM association and is also regulated by phosphorylation.

3.2.2 *The CCTα P-domain regulates nLD interactions through cumulative negative charge*

It was thus apparent that phosphorylation of the CCTα P-domain regulated nLD association, however whether this regulation was dependent on the total number of phosphorylated serine residues or was site-specific remained unknown. To investigate whether bulk charge or specific sites regulate nLD association, 4 tracts of 2-3 P-domain serine residues in V5-tagged rat CCTα were mutated to phospho-null alanine (SA) mutants using site-directed mutagenesis (**Figure 3.17A**). U2OS cells expressing these SA mutants were then treated with OA for 24 h to induce nLD formation (**Figure 3.17B**). No differences in nLDs per cell were observed amongst these mutants (**Figure 3.17C, left panel**). Additionally, no mutation of any one tract of serine residues significantly enhanced nLD association (**Figure 3.17C**, **right panel**). However increased nLD

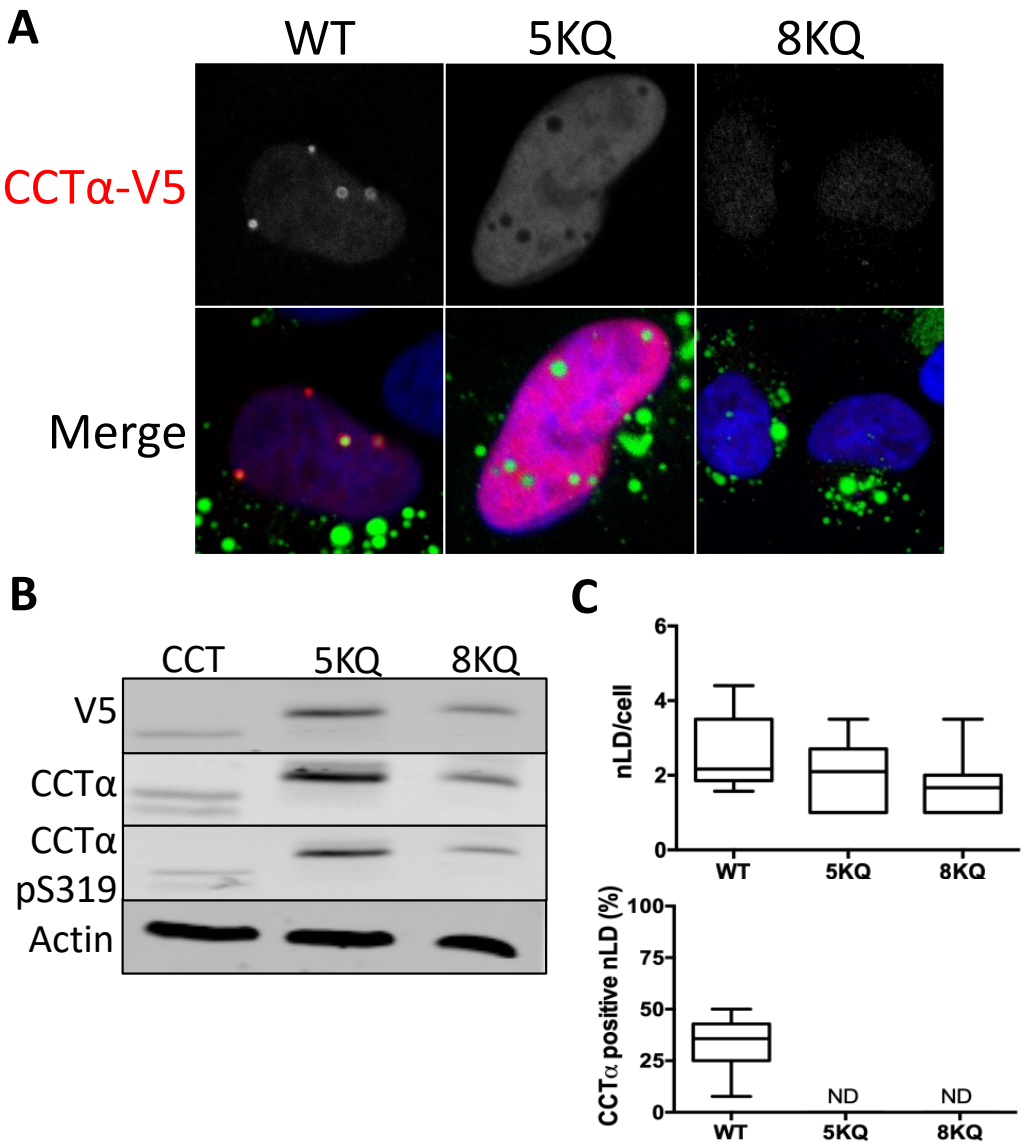

Figure 3.15. M-domain lysines are essential for CCTα association with nLDs. (A) U2OS cells transiently expressing V5-tagged CCTα M-domain K→Q mutants were treated with oleate (0.4 mM) for 24 h. Cells were immunostained with antibodies against V5, LDs were visualized with BODIPY 493/503 and nuclei with propdiuim iodide. LD=green V5=red nucleus=blue **(B)** U2OS cells transiently expressing V5-tagged CCTα M-domain K→Q mutants were treated with oleate (0.4 mM) for 24 h. Total cell lysates were immunoblotted with antibodies against V5, CCTα, CCTα pS319 and actin. **(C)** Quantification of images in panel A. nLD number and percentage of nLDs CCTα-V5-positive were quantified from 10-15 fields of cells from 2-3 independent experiments. Data shown as box and whisker plots showing mean and 5th-95th percentile, significance tested using one-way ANOVA vs WT. ND: not detected

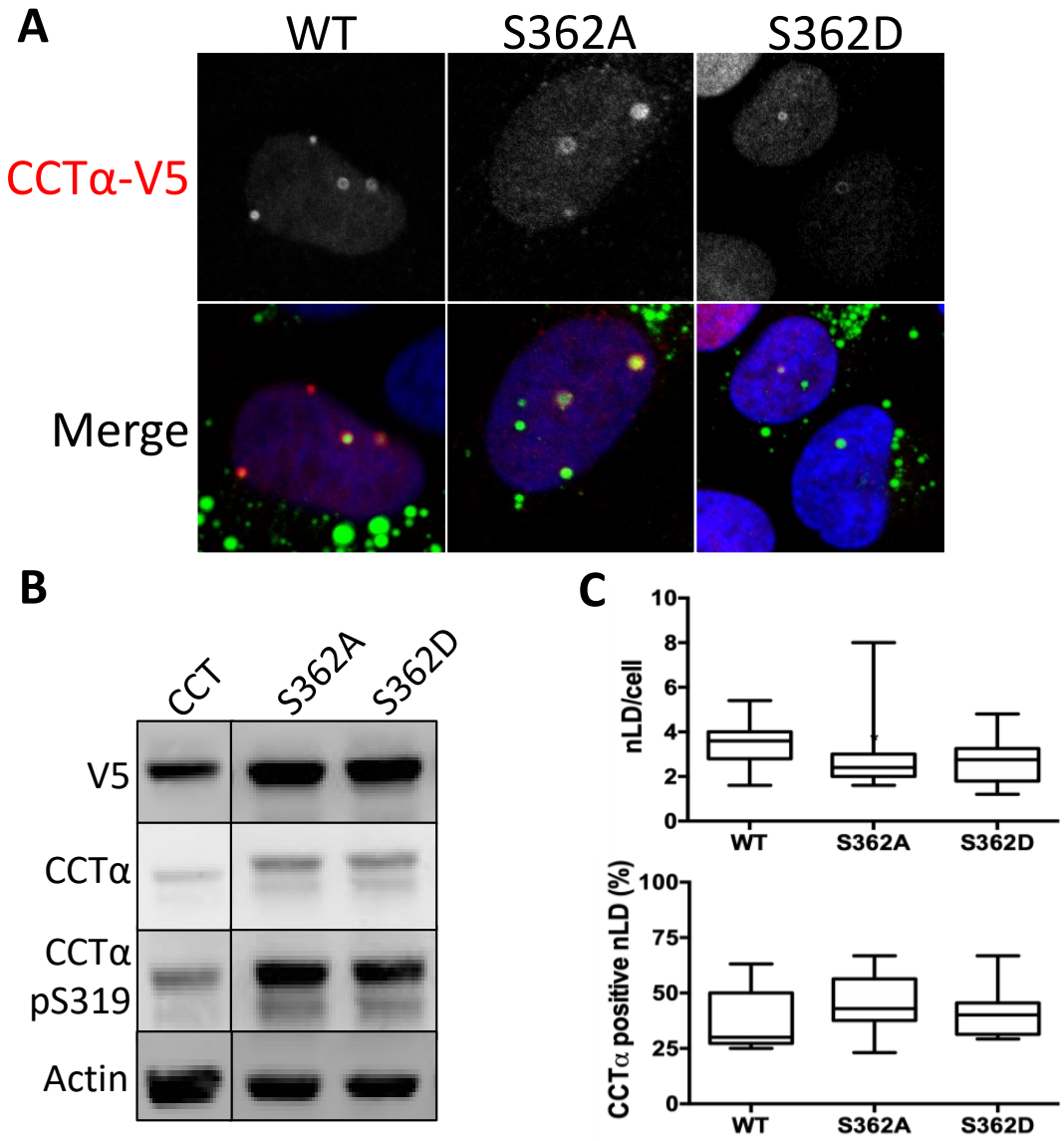

Figure 3.16. CCTα S362 phosphomutations do not affect association with nLDs. (A) U2OS cells transiently expressing V5-tagged CCTα S362A or S362D mutants were treated with oleate (0.4 mM) for 24 h. Cells were immunostained with antibodies against V5, LDs were visualized with BODIPY 493/503 and nuclei with propidium iodide. LD=green V5=red nucleus=blue **(B)** U2OS cells transiently expressing V5-tagged CCTα S362A or S362D mutants were treated with oleate (0.4 mM) for 24 h. Total cell lysates were immunoblotted with antibodies against V5, CCTα, CCTα pS319 and actin. **(C)** Quantification of images in panel A. nLD number and percentage of nLDs CCTα-V5-positive were quantified from15 fields of cells from 3 independent experiments. Data shown as box and whisker plots showing mean and 5th-95th percentile, significance tested using one wayANOVA vs WT.

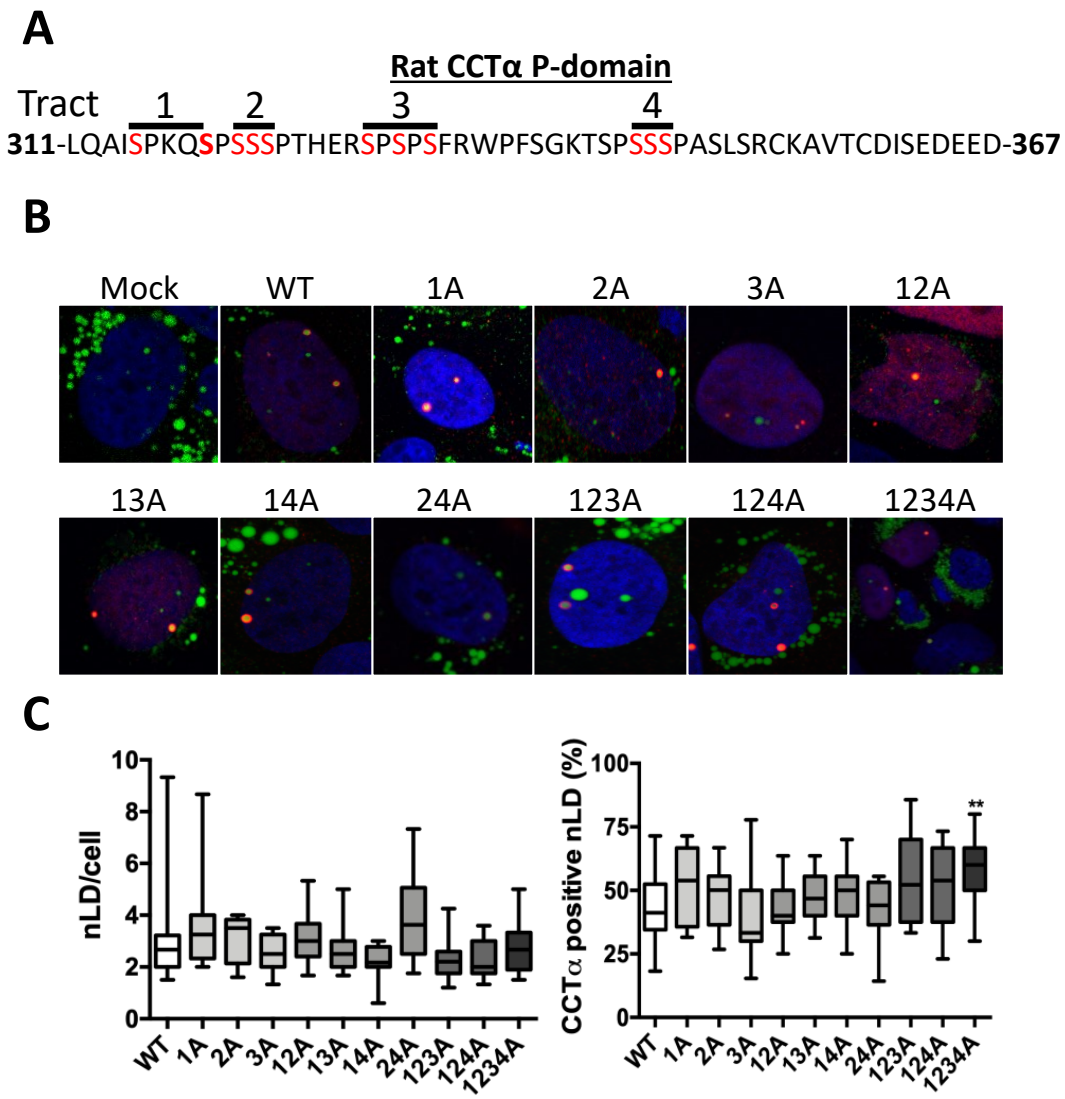

Figure 3.17. CCTα association with nLDs is enhanced by P-domain serine to alanine mutations. (A) Amino acid sequence of the rat CCTα P-domain and the mutated serine tracts. Mutated serines are shown in red, with S319 in tract 1 bolded. Mutant names include all mutated tracts and A to specify mutation to alanine. **(B)** U2OS cells transiently expressing CCTα-V5 mutants were treated with oleate (0.4 mM) for 24 h. Cells were immunostained with antibodies against V5, LDs were visualized with BODIPY 493/503 and nuclei with propidium iodide. LD=green V5=red nucleus=blue **(C)** Quantification of images in panel B. nLD number and percentage of nLDs CCTα-V5-positive were quantified from 15 fields of cells from 3 independent experiments. Data shown as box and whisker plots showing mean and 5th-95th percentile, significance tested using one-way ANOVA and Tukey's multiple comparison vs WT. **p<0.01

association was noted when all four tracts (totalling 11 serines) were mutated, suggesting that CCTα association with nLDs is primarily inhibited by bulk P-domain negative charge. The same serine tracts were then mutated to phosphomimetic aspartate (SD) mutants (**Figure 3.18A**), expressed in U2OS cells and treated with OA for 24 h (**Figure 3.18B**). Like SA mutations, SD mutations had no effect on nLD number (**Figure 3.18C, left panel**) and no single mutation greatly impacted nLD association (**Figure 3.18, right panel**). Significant reduction in nLD association was only observed when all four tracts were mutated to aspartate. CCTα P-domain regulation of nLD association is thus dictated by the bulk charge of the P-domain and not by any specific residue. Furthermore, large amounts of P-domain phosphorylation are needed to completely inhibit nLD association as 11 serine to aspartate were not sufficient to prevent nLD translocation (**Figure 3.18C**) whereas mutating all 16 to glutamate silenced CCTα association with nLDs (**Figure 3.13C**). Interestingly, despite the 16SA and ΔP mutants having less expression on account of their low phosphorylation (**Figure 3.14B, left panel**) the 1234A mutant had similar expression to wild type CCTα and the 1234D mutant (**Figure 3.19A**). This suggests that a high degree of P-domain dephosphorylation is required to reduce CCTα stability.

3.2.3 *Phosphorylation of CCTα P-domain S319 is regulated by adjacent serine phosphosites*

It has been suggested that phosphorylation of sites in the CCTα P-domain are dependent on other sites (Cornell et al., 1995), however no evidence of this has been reported. To investigate whether mutation of P-domain phosphosites affects serine 319, CCTα SA mutants were expressed in CHOK1 MT58 cells, which have a temperature-

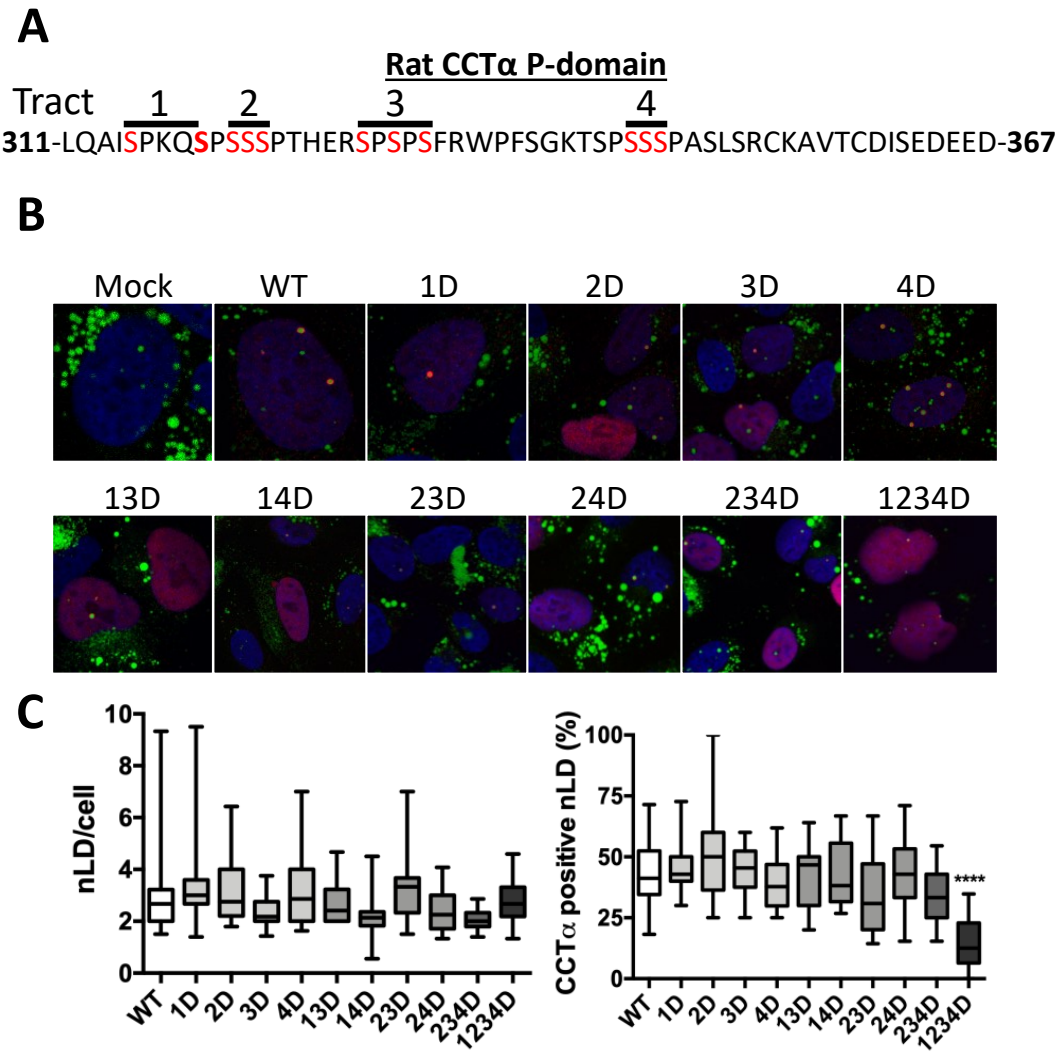

Figure 3.18. CCTα association with nLDs is inhibited by P-domain negative charge density. (A) Amino acid sequence of the rat CCTα P-domain and the mutated serine tracts. Mutated serines are shown in red, with S319 in tract 1 bolded. Mutant names include all mutated tracts and D to specify mutation to aspartate. **(B)** U2OS cells transiently expressing CCTα-V5 mutants were treated with oleate (0.4 mM) for 24 h. Cells were immunostained with antibodies against V5, LDs were visualized with BODIPY 493/503 and nuclei with propidium iode. LD=green V5=red nucleus=blue **(C)** Quantification of images in panel B. nLD number and percentage of nLDs CCTα-V5-positive were quantified from 15 fields of cells from 3 independent experiments. Data shown as box and whisker plots showing mean and 5th-95th percentile, significance tested using one-way ANOVA and Tukey's multiple comparison vs WT. ****p<0.0001

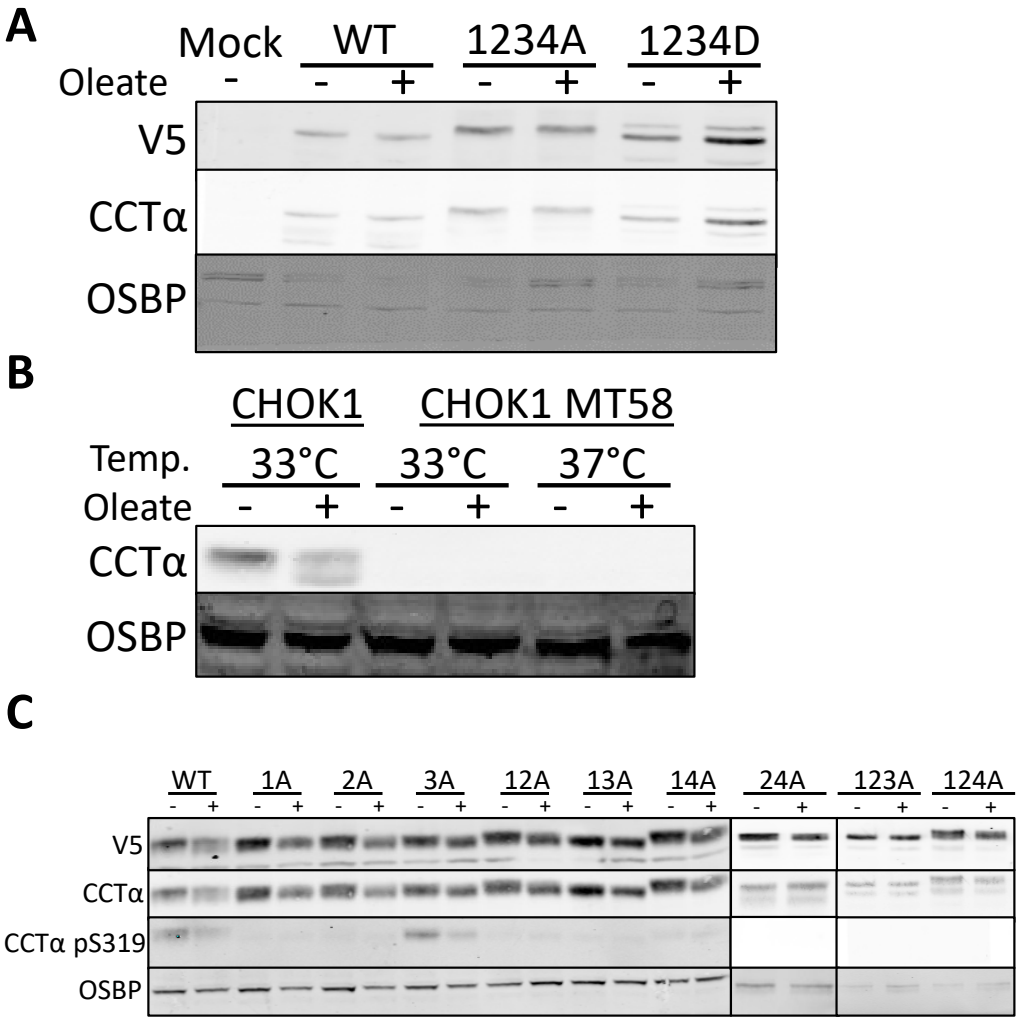

Figure 3.19. Expression of CCTα P-domain S→A mutants in MT58 cells. (A) Mock U2OS cells and U2OS cells expressing V5-tagged CCTα mutants were treated with oleate for 24 h. Total cell lysates were immunoblotted with antibodies against V5, CCTα and OSBP (load control). **(B)** CHOK1 MT58 cells have a temperature-sensitive CCTα mutation that destabilizes its expression. Total cell lysates were immunoblotted with antibodies against CCTα and OSBP (load control). **(C)** MT58 cells expressing a selection of V5-tagged CCTα S→A mutants were cultured in serum-free media for 1 hour and then treated with oleate (0.4 mM0 for 1 h. Total cell lysates were immunoblotted with antibodies against V5, CCTα, CCTα pS319 and OSBP (load control).

sensitive CCTα mutation that reduces its stability and expression (**Figure 3.19B**). MT58 cells expressing SA mutants were treated with OA for 1 h to induce dephosphorylation (**Figure 3.19C**). As expected, the wild type CCTα and 3A mutant had reduced S319 signal in response to OA versus untreated, indicative of their dephosphorylation. Additionally, the SA mutants mutated at tract 1 lacked S319 phosphorylation due to this site being mutated (**Figure 3.20A**). Surprisingly, the 2A and 24A mutants also lacked S319 signal under basal conditions (**Figure 3.19C**) even though the site is intact and there is no interference with antibody binding, since the pS319 antibody epitope does not include any of these sites (**Figure 3.20A**). Interestingly, S319 was phosphorylated when tract 2 serines were mutated to aspartate to mimic the phosphorylated state (**Figure 3.20B**). Thus, S319 phosphorylation requires phosphorylation at adjacent downstream serines 321-323. This is the first example of a CCTα phosphosite being dependent on another and suggests that other CCTα phosphosites could also be regulated by hierarchical phosphorylation.

3.3 Investigating apolipoprotein L6 as a potential LAPS protein

3.3.1 Verification of an APOL6 antibody

Given the limited publications on APOL6, I first validated a commercial APOL6 antibody for its specificity. The antibody was used to probe a panel of human tissue lysates and an APOL6 band was detected in liver and kidney tissue corresponding to 38 kDa (**Figure 3.21A**), the predicted molecular weight of APOL6 (Page et al., 2001). A C-terminal HA-tagged APOL6 construct was amplified from U2OS genomic DNA, sequenced to confirm its identity and then expressed in U2OS cells. The antibody was

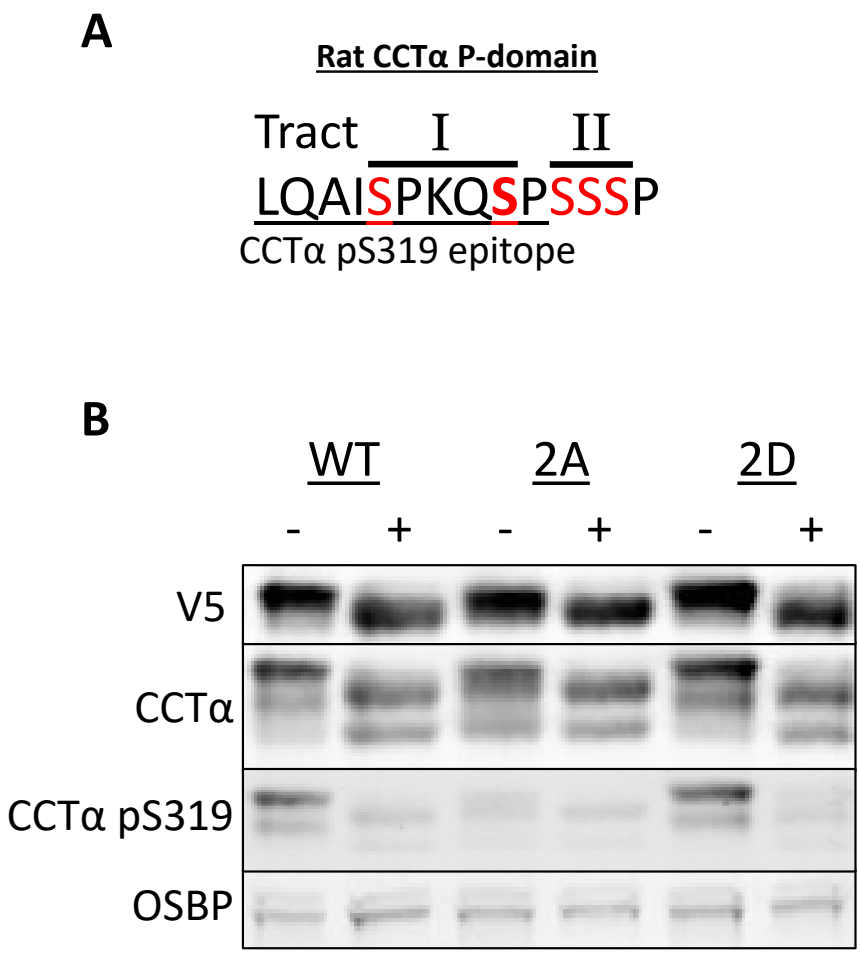

Figure 3.20. CCTα phosphorylation at S319 is dependent on phosphorylation at adjacent serine residues. (A) Part of the CCTα P-domain sequence showing the epitope of CCTα pS319 antibody (underlined) and mutated serines mutated in tracts I and II. Mutated serines are shown in red with S319 bolded. **(B)** MT58 cells expressing V5-tagged CCTα mutants were cultured in serum-free media for 1 h and then treated with oleate (0.4 mM) for 1 h. Total cell lysates were immunoblotted with antibodies against V5, CCTα, CCTα pS319 and OSBP (load control).

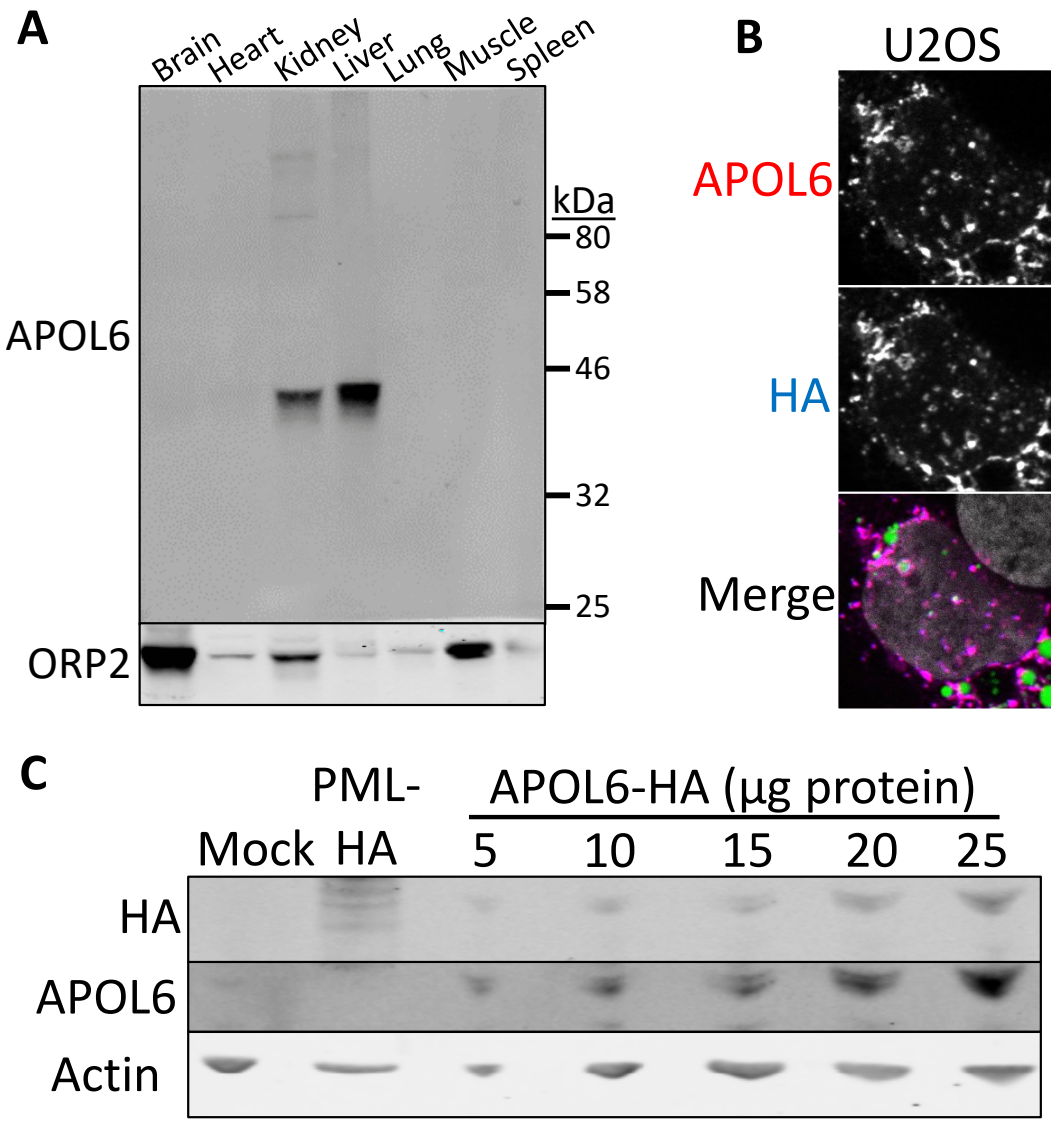

Figure 3.21. Detection of APOL6 in tissue and U2OS cells. (A) Tissue panel screen consisting of the respective tissue homogenates (10 µg). Homogenates were immunoblotted with antibodies against APOL6 and ORP2 (load control). **(B)** U2OS cells expressing an APOL6-HA construct were immunostained with antibodies against HA and APOL6, LDs were visualized with BODIPY 493/503 and nuclei with propidium iodide. LD=green APOL6=red HA=blue Nucleus=gray **(C)** U2OS cells expressing PML-HA (control) or APOL6-HA construct were probed to confirm WB antibody specificity. Total cell lysates were immunoblotted with antibodies against HA, APOL6 and actin.

then used to probe for overexpressed APOL6-HA using immunofluorescence (**Figure 3.21B**) and immunoblotting (**Figure 3.21C**). The APOL6 antibody co-stained with anti-HA for both techniques, confirming its specificity.

3.3.2 Interferon γ induces APOL6 expression in Huh7 and U2OS cells

Previous studies have reported increased APOL6 expression in response to IFNγ treatment of macrophages (Zhaorigetu et al., 2011). In light of this result I determined whether APOL6 expression is altered by FAs, LPS or IFNγ treatment of U2OS and Huh7 cells for up to 24 h (**Figure 3.22A**). APOL6 was expressed in both cell lines at 3 h, with full induction being reached at 6 h and continuing through 12 and 24 h. The bacterial outer membrane component lipopolysaccharide (LPS) was also tested as a potential regulator of APOL6 expression, given the role of apoL family members in innate immunity. However, LPS failed to induce APOL6 expression in Huh7 and U2OS cells (**Figure 3.22B**). Finally, OA and palmitate were tested for their effects on APOL6 expression in Huh7 cells but neither FA induced APOL6 expression (**Figure 3.22C**).

It was then tested whether combining FAs and IFNγ could amplify the induction of APOL6 expression in U2OS and Huh7 cells. U2OS and PML-KO U2OS cells were treated with OA, IFNγ or OA and IFNγ for 24 h (**Figure 3.23A**). The addition of oleate and IFNγ to cells did not increase the induction of APOL6 (**Figure 3.23B**). PML knockout resulted in a small but insignificant decrease in APOL6 induction. However, IFNγ and OA did result in a significant 2.5-fold increase in APOL6 expression in Huh7 cells (**Figure 3.24B**). This is particularly interesting in Huh7 cells, where the combination of inflammatory IFNγ signalling and excess FAs in liver tissue is implicated in the development of NASH (Li et al., 2021).

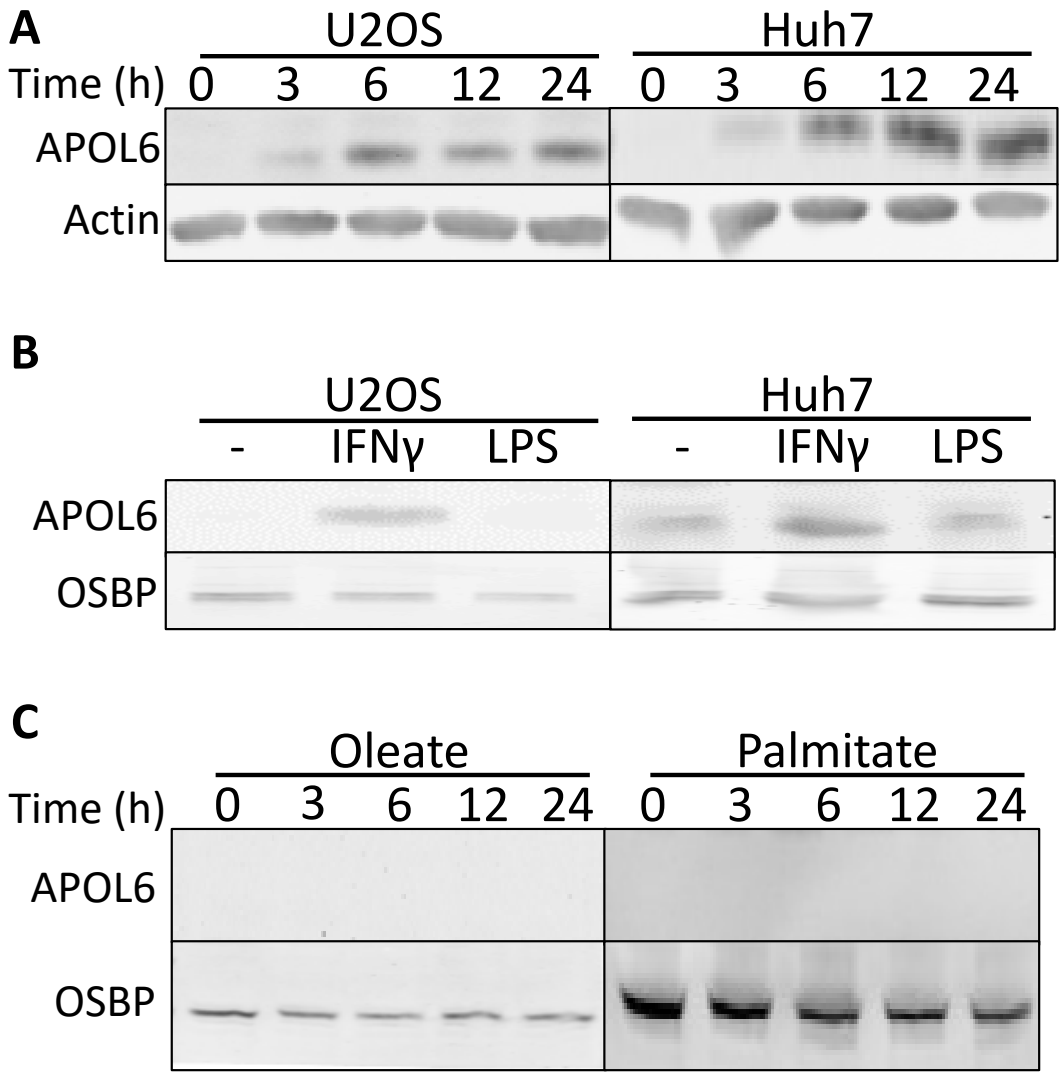

Figure 3.22. Effects of IFNγ, LPS and fatty acids on endogenous APOL6 expression in Huh7 and U2OS cells. (A) U2OS and Huh7 cells were treated with IFNγ (1000U/mL) for the indicated duration. Total cell lysates were immunoblotted with antibodies against APOL6 and actin. **(B)** U2OS and Huh7 cells were treated with IFNγ (1000U/mL) or lipopolysaccharide (LPS, 5 μg/mL) for 24 h. Total cell lysates were immunoblotted with antibodies against APOL6 and actin. **(C)** Huh7 cells were treated with oleate (0.4 mM) or palmitate (0.4 mM) for the indicated duration. Total cell lysates were immunoblotted with antibodies against APOL6 and actin.

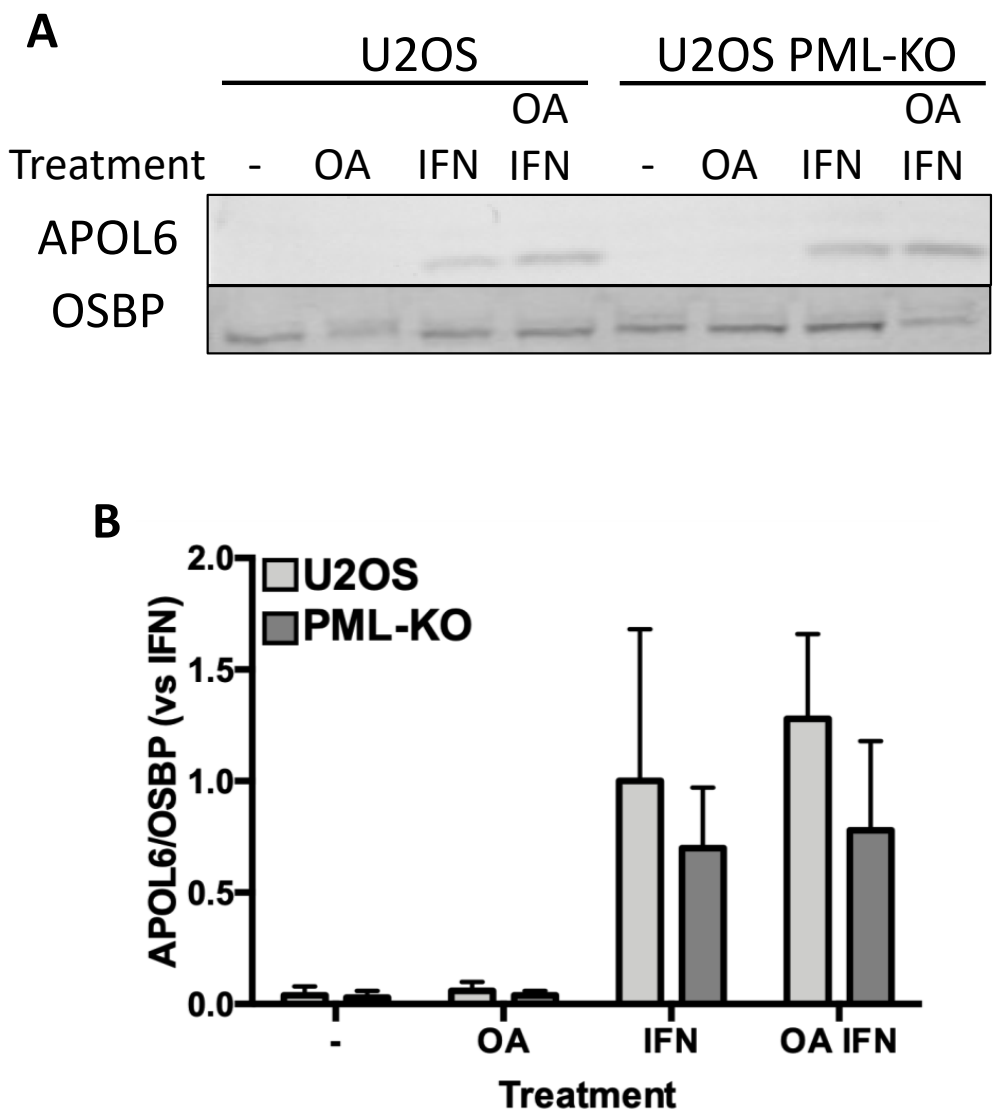

Figure 3.23. IFNγ induces endogenous APOL6 expression independent of PML in U2OS cells. (A) U2OS and PML-KO U2OS cells were treated with oleate (0.4 mM), IFNγ (1000 U/mL) or both for 24 h. Total cell lysates were immunoblotted with antibodies against APOL6 and OSBP (load control). **(B)** Quantification of APOL6 expression relative to IFNγ-U2OS cells . Mean shown with SD, n=2-5. Significance compared between U2OS and PML-KO cells and IFNγ and OA+IFNγ treatments using two-way ANOVA.

A

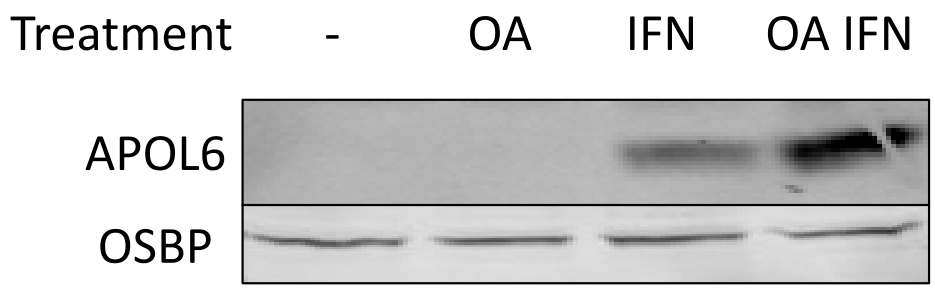

B

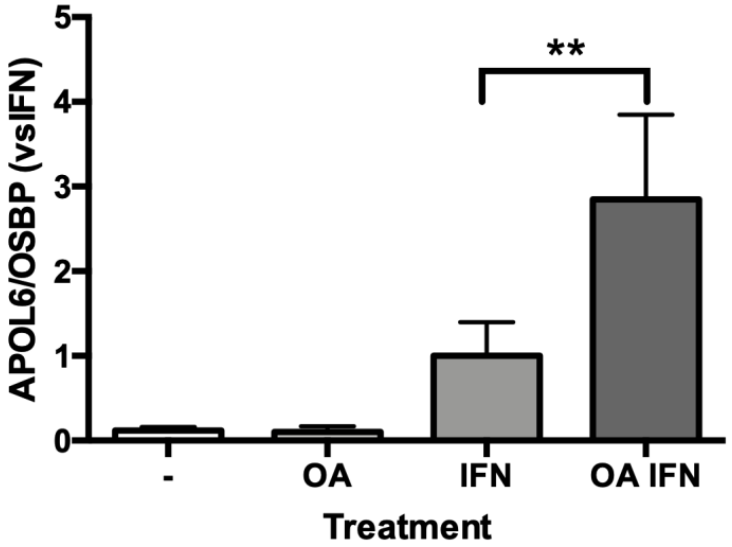

Figure 3.24. Combination of IFNγ and OA increases endogenous APOL6 levels in Huh7 cells. (A) Huh7 cells were treated with oleate (0.4 mM), IFNγ (1000 U/mL) or both for 24 h. Total cell lysates were immunoblotted with antibodies against APOL6 and OSBP (load control). **(B)** Quantification of APOL6 expression relative to IFNγ-treated Huh7 cells. Mean shown with error bars representing SD, n=4-5, significance compared between IFNγ and OA+IFNγ using T-test. **$p<0.01$

Overexpression of APOL6 induces apoptosis in macrophages and colorectal adenocarcinoma cells (Liu et al., 2005; Zhaorigetu et al., 2011), and so I tested whether this would also occur in U2OS and Huh7 cells. U2OS and PML-KO U2OS cells expressing APOL6-HA were treated with OA, IFNγ or both for 24 h (**Figure 3.25A**). Both cell lines showed some increase in response to OA, however the addition of IFNγ resulted in decreased APOL6-HA expression but not endogenous APOL6. It has been speculated that IFNγ signalling could induce apoptosis by promoting APOL6-mediated apoptosis (Zhaorigetu et al., 2011). While this may not have been sufficient to induce cell death in U2OS and PML-KO U2OS cells, overexpressing APOL6-HA could have a stronger apoptotic response to IFNγ by combining endogenous and overexpressed APOL6, resulting in the death of cells expressing APOL6-HA. Alternatively, IFNγ could have attenuated APOL6-HA expression given that the APOL6-HA vector contains a viral promoter (Harms & Splitter, 1995). Future experiments monitoring for apoptotic markers can determine why APOL6-HA expression is reduced.

3.3.3 APOL6 associates with LAPS

It was next investigated whether APOL6 associates with LAPS. Huh7 cells were treated with OA, IFNγ or both for 24 h (**Figure 3.26**). APOL6 was found to be associated with PML NBs under basal conditions and with LAPS upon OA, IFNγ and dual OA/IFNγ treatment. This was the first reported instance of nLD formation stimulated by IFNγ signalling. Interestingly, IFNγ induced a similar level of nLD formation as OA (**Figure 3.27A**). However, IFNγ combined with OA resulted in an additive effect, with 50% more nLDs per cell than either treatment alone. IFN, but not oleate, also increased the number of APOL6 puncta (including both PML and non-PML associated APOL6 puncta) per cell

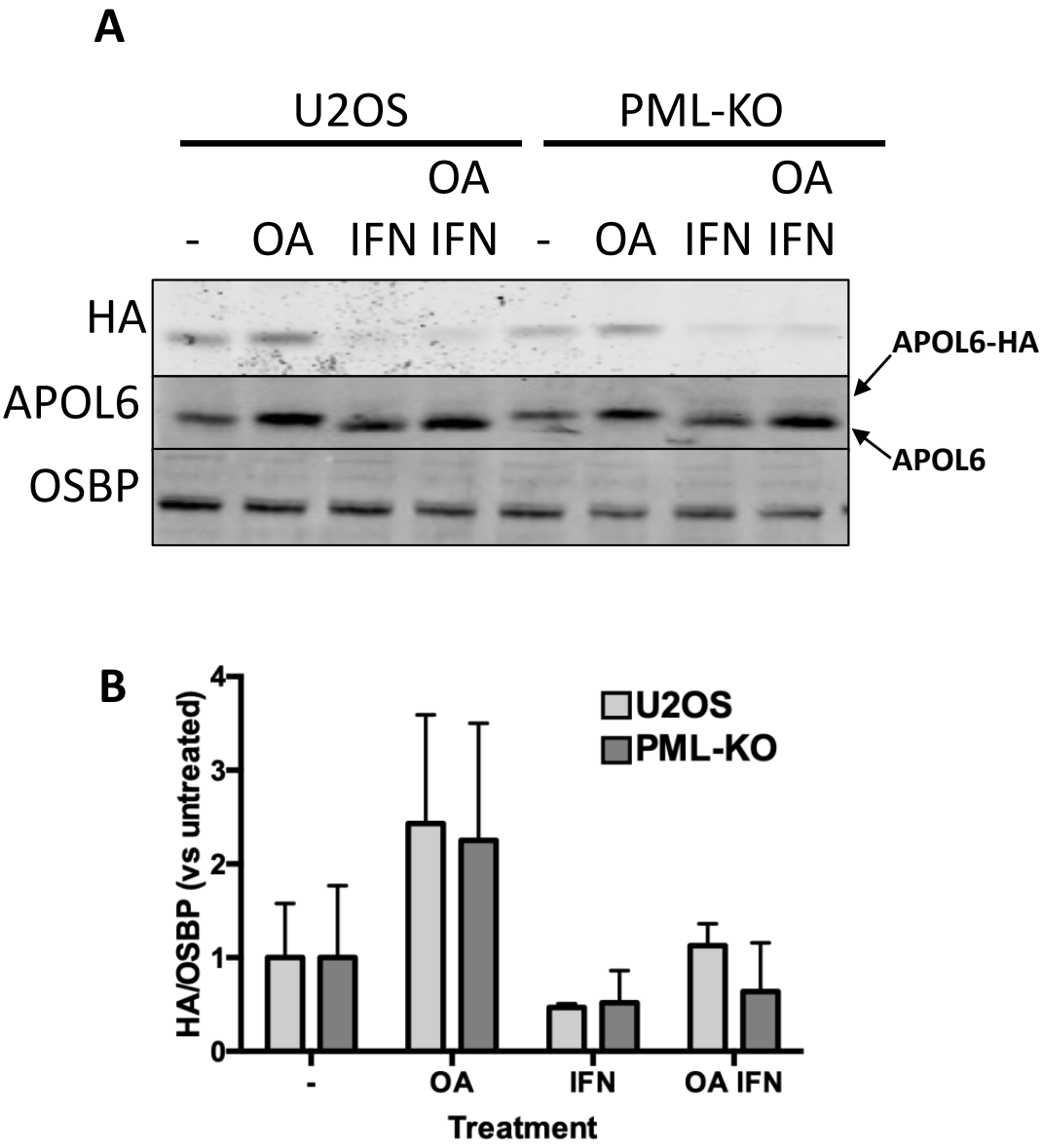

Figure 3.25. IFNγ reduces expression of overexpressed APOL6 in U2OS cells. (A) U2OS and PML-KO U2OS cells expressing APOL6-HA were treated with oleate (0.4 mM), IFNγ (1000 U/mL) or both for 24 h. Total cell lysates were immunoblotted with antibodies against HA, APOL6 and OSBP (load control). **(B)** Quantification of HA expression relative to untreated U2OS or PML-KO. Mean shown with SD, n=3. Significance tested versus untreated U2OS or PML-KO using one-way ANOVA.

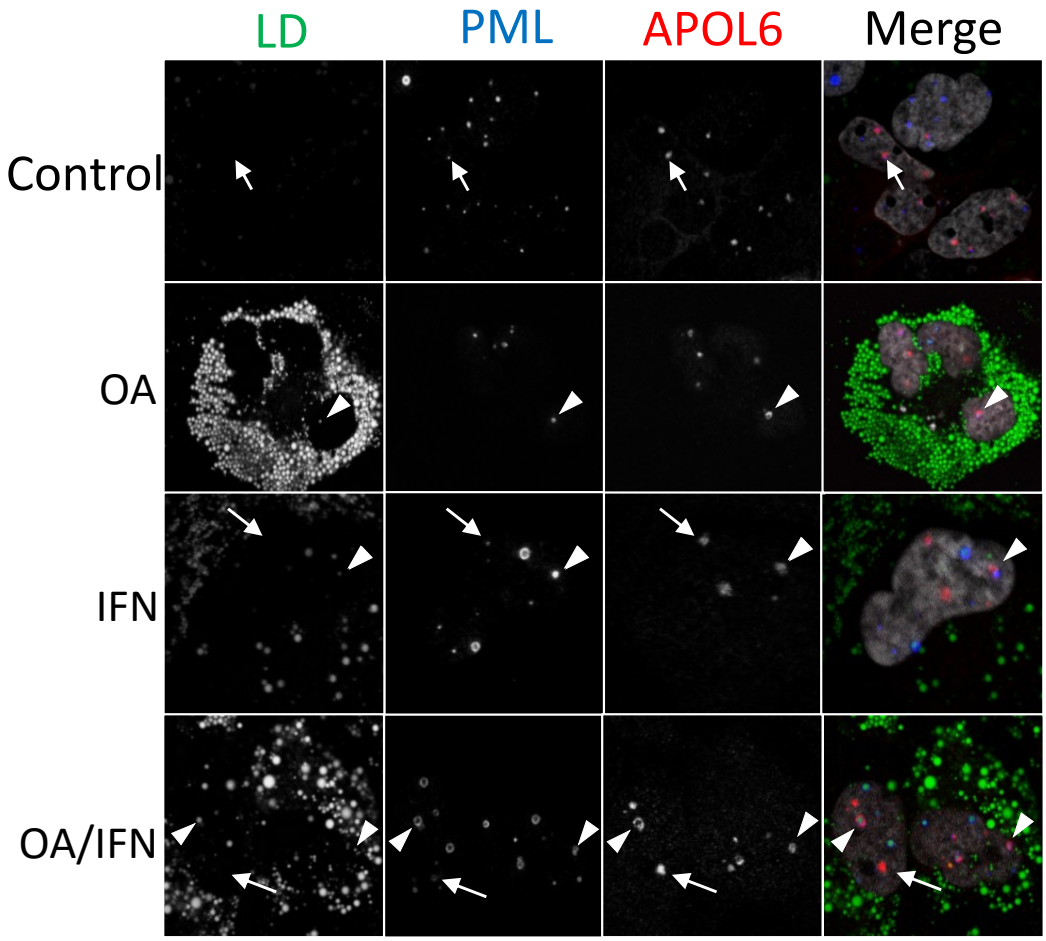

Figure 3.26. Endogenous APOL6 associates with LAPS. Huh7 cells were treated with oleate (0.4 mM), IFNγ (1000 U/mL) or both. Arrows indicate PML-positive APOL6 and arrowheads indicate APOL6-positive LAPS. Cells were immunostained with antibodies against HA and APOL6, LDs were visualized with BODIPY 493/503 and nuclei with propidium iodide. Nucleus=gray

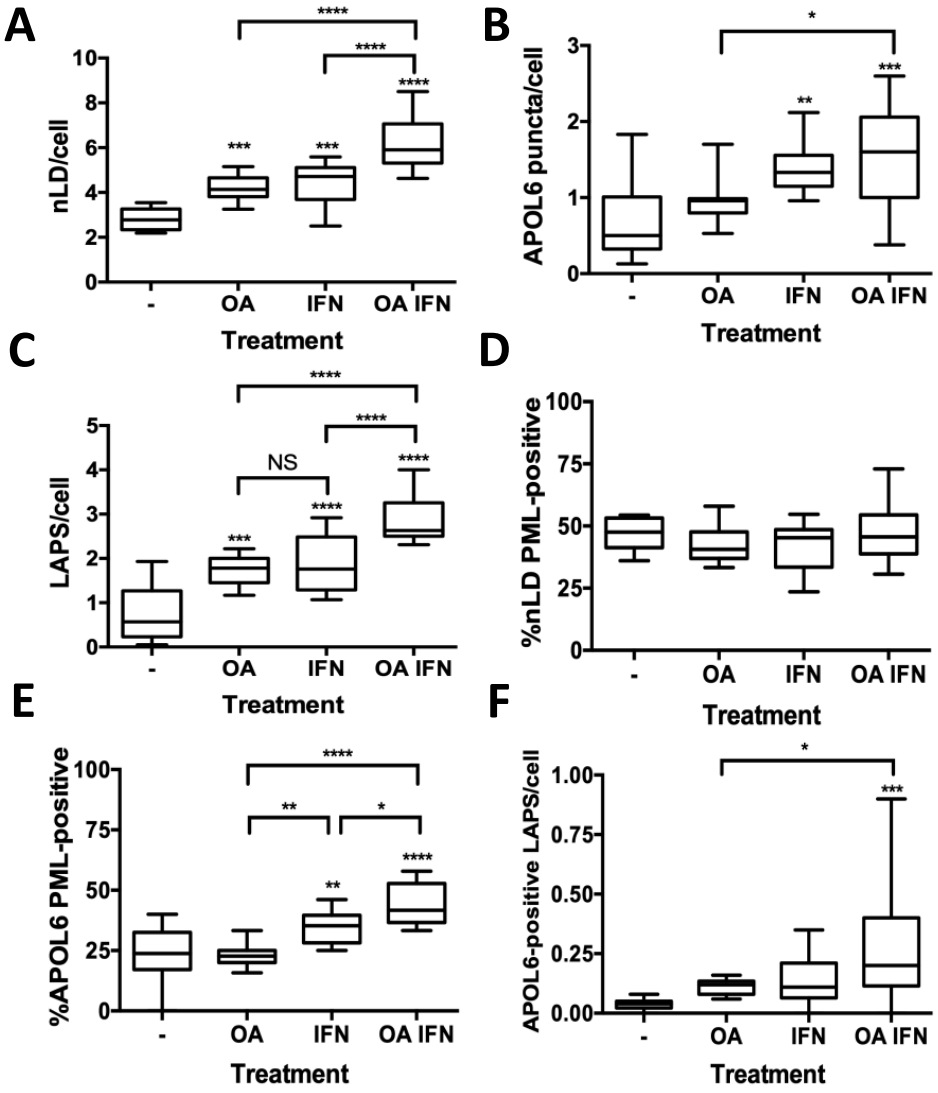

Figure 3.27. Quantification of APOL6 association with LAPS in Huh7 cells. Quantification of Z-stack images from Figure 3.26. nLDs, LAPS, total APOL6 puncta, APOL6 puncta associated with PML NBs and APOL6 puncta associated with LAPS were quantified from 11 fields of cells from 1 experiment. Calculated data shown includes: **(A)** nLDs per cell, **(B)** total APOL6 puncta per cell, **(C)** LAPS per cell, **(D)** percentage of nLDs with PML associated, **(E)** percentage of APOL6 puncta associated with PML (NBs+LAPS) and **(F)** APOL6 associated with LAPS per cell. Data shown as box and whisker plots showing mean and 5^{th}-95^{th} percentile. Significance between treatments tested using one-way ANOVA and Tukey's multiple comparison, with asterisks above plots showing significance versus untreated (-). *p<0.05 **p<0.01 ***p<0.001 ****p<0.0001

(**Figure 3.27B**), supporting the immunoblot data from **Figure 3.24**. However, unlike results shown in **Figure 3.24,** no significant increase was observed when cells were treated with IFNγ and IFNγ plus OA. This difference could be due to a change in the size of APOL6 puncta, rather than the total number. Both OA and IFNγ increased the number of LAPS per cell to a similar degree (**Figure 3.27C**), with OA plus IFNγ resulting in a significantly greater level of LAPS formation than either treatment alone. This increase in LAPS appears to be driven by increased levels of nLD formation and PML expression rather than a redistribution of existent PML, as the percentage of nLDs that are PML positive did not change between samples (**Figure 3.27D**). IFNγ signalling also promotes greater APOL6 association with PML, as the percentage of APOL6 associated with PML structures (both NBs and LAPS) was increased, with even more pronounced effects with the combination of IFNγ and OA (**Figure 3.27E**). Dual OA/IFNγ treatment also enhanced the number of APOL6-positive LAPS per cell compared to OA or IFNγ alone (**Figure 3.27F**), suggesting that the increase in association between APOL6 and PML association is driven by APOL6 association with LAPS rather than NBs (**Figure 3.28**). Overall, these data demonstrate that the combination of OA and IFNγ induce a synergistic response that results in greater nLD and LAPS formation and APOL6 recruitment to PML structures, primarily LAPS.

3.3.4 LAPS induced by interferon γ do not recruit CCTα

Given that this is the first reported instance of IFNγ-induced nLD formation, it was next tested whether IFNγ-induced nLDs have a different profile of associated proteins compared to oleate induced nLDs. nLDs induced by IFNγ in Huh7 cells (**Figure 3.29**) and U2OS (**Figure 3.30, upper panel**) lacked the canonical nLD-associated protein

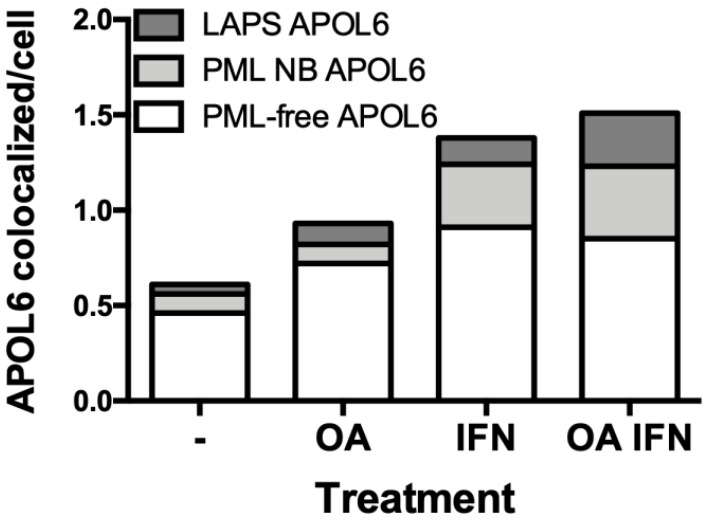

Figure 3.28. Distribution of APOL6 puncta in Huh7 cells.
Distribution of APOL6 puncta quantified in Figure 3.27. APOL6 was classified as being unassociated with PML (PML-free APOL6), associated with PML NBs (PML NB APOL6) or associated with LAPS (LAPS APOL6) and the quantity of each puncta per cell was calculated. Data includes all APOL6 puncta counted from all fields of cells for each treatment.

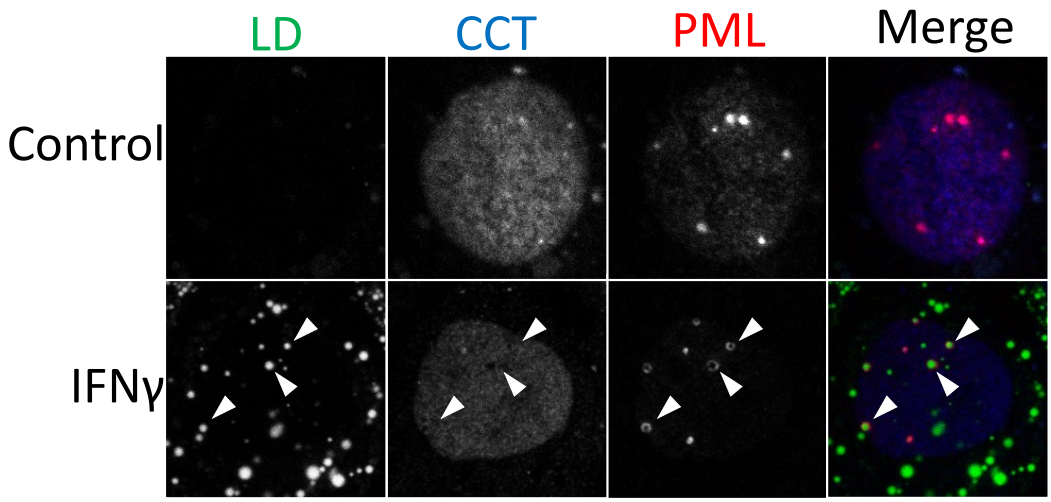

Figure 3.29. CCTα does not translocate to LAPS in IFNγ-treated Huh7 cells. Huh7 cells were treated with IFNγ (1000 U/mL) for 24 h. Cells were immunostained with antibodies against PML and CCTα and LDs were visualized with BODIPY 493/503. Arrowheads denote LAPS.

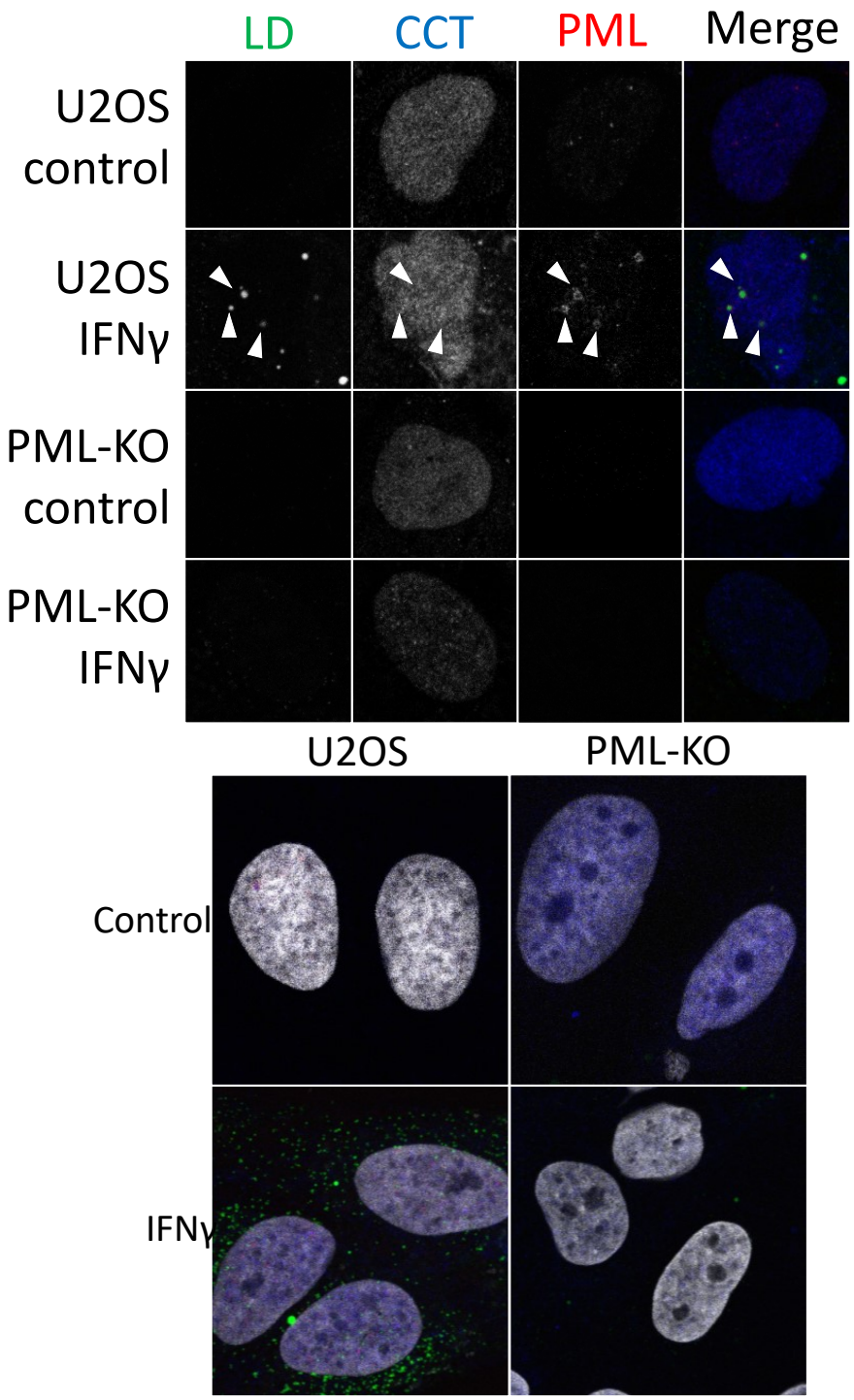

Figure 3.30. PML knockout prevents LAPS and LD formation in IFNγ-treated U2OS cells. U2OS and PML-KO U2OS cells were treated with IFNγ (1000 U/mL) for 24 h. Shown are **(A)** nuclei and **(B)** fields of cells. Cells were immunostained with antibodies against PML and CCTα, LDs were visualized with BODIPY 493/503 and nuclei with propidium iodide. Nucleus=gray Arrowheads denote LAPS.

CCTα, despite having PML on their surface. Thus, IFNγ induced nLDs appear to have a different associated protein profile than their OA-induced brethren. Additionally, PML-KO U2OS cells did not form nLDs in response to IFNγ (**Figure 3.30, upper panel**) and had reduced cLD formation as well (**Figure 3.30, lower panel**). This suggests that PML has an essential function in both IFNγ-induced lipid synthesis and nLD formation.

Chapter 4: Discussion

My research goal was to contribute to our understanding of how nLDs originate and how specific proteins are recruited to their surface. More specifically, my research aims were to 1) characterize nLD protein recruitment over time, 2) analyze how CCTα domains regulate its ability to associate with nLDs and 3) investigate APOL6 as a potential LAPS-associated protein. I was able to make progress on each of these questions, providing novel insight that could help understand nLD functions and how proteins are recruited to assist those functions.

4.1 PML association with nLDs precedes that of CCTα and LIPIN1

One aim of my research was to characterize when specific proteins associate with nLDs during treatment of cells with FAs. I found that PML was recruited on nLDs before CCTα or LIPIN1, with PML commonly being found on nLDs under basal conditions. This suggests that LAPS could have a function under basal conditions and that they are not strictly a response mechanism that occurs upon exposure to excess FAs. It was noted that the LAPS pool had a smaller increase in response to OA treatment versus the CCTα- or LIPIN1-nLD pool (**Figures 3.5B** and **3.9A**). It was similarly noted by other reports that the percentage of nLDs that are PML-positive is negatively correlated with the total nLD number (Ohsaki et al., 2016). This could be because LAPS are a distinct pool of nLDs whose number is more stable than the total nLD pool at large.

The recruitment of PML prior to CCTα and LIPIN1 complements previous findings by our lab that PML-positive nLDs have enhanced CCTα and LIPIN1 recruitment (Lee et al., 2020). The early recruitment of PML in Huh7 cells could be due

to its presence as part of PML patches on the INM (Ohsaki et al., 2016). eLDs entering the nucleoplasm through type 1 NR defects preferentially do so at sites enriched in PML-II and this process could result in PML-II and other isoforms associating with the nascent eLD-turned-nLD. Future experiments using live cell imaging could confirm this hypothesis. How LAPS enhance CCTα and LIPIN1 recruitment is unknown. One explanation is that it could be due to the greater size of LAPS relative to PML-free nLDs, as previous findings demonstrated CCTα preferentially located to larger nLDs (Lee et al., 2020). However, it also could be due to an as-of-yet unknown protein or lipid activators on the surface of the LAPS. The increased recruitment could reflect the increase in OA on the surface of LAPS, which is known to activate and enhance CCTα binding to membranes (Wang et al., 1993). Regardless, these results demonstrate that PML recruitment precedes that of CCTα and LIPIN1 temporally in cells undergoing oleate treatment. The lack of CCTα and LIPIN1 on basal nLDs and their high degree of increased recruitment relative to PML in response to OA implies that their function on nLDs is limited to serving as a response to FAs, whereas the omnipresence of PML on nLDs and its relatively small increased rate of recruitment suggests that LAPS could have a function independent of resolving excess FAs.

I also demonstrated for the first time that nLD formation occurs in response to exposure to saturated PA. Previous studies have focused on nLD formation strictly in response to OA or OA and inducers of ER stress (Lee et al., 2020; Sołtysik et al., 2019; Sołtysik et al., 2021). It has been speculated that nLDs, like cLDs, could help buffer cells from FA-induced cytotoxicity, either by acting as sites of lipid synthesis or as signalling mechanisms. The increased presence of nLDs in nucleus in response to excess FAs has

been demonstrated to enhance PC synthesis by enhancing CCTα translocation to the nLD surface, which would provide more PC for packaging TG into VLDL and LDs and thus quelling the lipotoxic effects of FAs (Sołtysik et al., 2019). This response was found to be magnified by inducing ER stress, which is relevant to palmitate treatment since it also induces ER stress (Hetherington et al., 2016; Karaskov et al., 2006). However, the limited recruitment of CCTα to nLDs in response to palmitate treatment suggests that this mechanism is not as applicable to saturated FAs. Saturated FAs have been shown to induce less lipid storage and LD formation than their unsaturated counterparts (Listenberger et al., 2003) and this can be clearly seen comparing the cLDs in OA- versus PA-treated Huh7 cells (**Figure 3.1)**, where OA-treated cells have significantly larger LDs than PA-treated cells. One potential mechanism for nLD formation to act as a response to excess palmitate is by altering the pro-β-oxidation activity of PML and transcriptional coactivator activity of the nLD protein LIPIN1. OA has been shown to mitigate PA-induced ER stress and lipotoxicity in part by diverting excess palmitate towards β-oxidation (Henique et al., 2010). Both PML and LIPIN1 have been shown to enhance PGC1α activity by preventing inhibitory acetylation and coactivation, respectively, and nLDs induced by palmitate treatment could coordinate these effects to achieve a synergistic response (Carracedo et al., 2012; Finck et al., 2006). If nLDs induced by palmitate formation promote greater activation of β-oxidation then it could act as a mechanism for nLDs formed by saturated FAs to resolve lipotoxicity. Future experiments determining if nLD formation induced by OA and palmitate increases LIPIN1 and PML recruitment to nLDs and the effect on pro-β-oxidation gene expression would determine whether this indeed occurs.

4.2 CCTα association with nLDs is inhibited by P-domain phosphorylation

Another research aim investigating how the CCTα M- and P-domains regulate nLD association revealed that CCTα recruitment to nLDs requires M-domain lysines and is antagonized by P-domain phosphorylation. Neither of these results were particularly surprising given that these M- and P-domains have well characterized roles in association with the INM. However, the more interesting results were that high levels of P-domain phosphorylation completely inhibited nLD association and that large shifts in P-domain charge are needed to alter CCTα translocation to nLDs.

Previous reports have demonstrated that phosphomimetic 16SE-CCTα was still able to bind to the INM of CHO MT58 cells, albeit at a reduced level (Wang & Kent, 1995). However, the same mutant showed no ability to bind nLDs (**Figure 3.13C**). This is especially surprising since CCTα appears to preferentially translocate to nLDs rather than the INM in oleate-treated Huh7 and U2OS cells. Most cells lacking nLDs have CCTα on the INM during OA treatment (Gehrig et al., 2008; Lagace & Ridgway, 2005), however cells with nLDs usually have CCTα on nLDs with little CCTα on the INM. This contrast is apparent in **Figure 3.3A** and **Figure 3.4** where images show OA-treated Huh7 cells after short- and long-term OA treatment, respectively. In **Figure 3.3A**, CCTα translocates to the INM after 15-30 minutes of OA treatment. However, after 3 h there is no CCTα on the INM, corresponding to increased nLD association and CCTα recruitment to nLDs. Why CCTα is preferentially recruited to nLDs remains unknown and why phosphorylation can completely inhibit this recruitment (but not recruitment to the INM) is also unknown. One explanation for why CCTα is preferentially-recruited to nLDs is different biophysical properties of the membrane versus surface monolayer of nLDs. The

CCTα M-domain preferentially inserts into membranes with packing defects and the more sharply curved membrane of an nLD would thus contain more packing defects than the flatter INM. However, this would not explain why CCTα-16SE has been shown to associate with membranes and not nLDs. This could be explained by the presence of lipid activators of CCTα in the INM, but not nLDs, that can overcome the negative effects of P-domain phosphorylation. CCTα M-domain insertion into membranes is facilitated by the presence of lipid activators such as FAs and DAG. DAG is present on nLDs, as both basal nLDs (**Figure 3.6**) and nLDs induced by palmitate treatment (**Figure 3.1**) were bound by a DAG-sensor. Despite this, these nLDs had poor CCTα recruitment. Additionally, previous reports showed DAG and CCTα association on nLDs was not correlated (Lee et al., 2020). This suggests that DAG, at least on nLDs, is a poor recruiter of CCTα. The INM, on the contrary, could possess lipid activators absent on nLDs that allow the M-domain to insert into it despite a heavily phosphorylated P-domain. It is difficult to tell what this lipid activator could be, given that only one study on the nLD lipidome has been conducted (Layerenza et al., 2013) and it only looked at broad classes of lipids.

My results also showed that significant changes in nLD association only occurred with large shifts in P-domain charge. Extreme phenotypes were observed when all 16 P-domain serines were mutated to glutamate (**Figure 3.13C**) resulting in no nLD association and when the P-domain was completely removed resulting in 80% of nLDs being CCTα-positive. However, the more moderate SA and SD mutations shown in **Figure 3.16C** and **Figure 3.17C**, respectively, only resulted in significant differences when all four tracts totalling 11 serine residues were mutated. This indicates that large

scale CCTα phosphorylation is necessary to inhibit nLD association, as even the 234D mutant with 9 serine residues mutated to aspartate had no significant difference in nLD association versus the wild type (**Figure 3.18C**). There is also likely a critical threshold between 11 and 16 serine phosphorylations or another critical residue(s) that completely inhibits nLD association, as the 16SE mutant had complete inhibition of nLD association.

While my findings demonstrate the CCTα P-domain regulates nLD association through bulk negative charge, it is still unknown how these phosphosites are regulated. CCTα dephosphorylation in response to short-term OA treatment is characterized by a band shift (for example **Figure 3.20B**) that corresponds to its dephosphorylation. Likewise, S319 is also dephosphorylated. I have demonstrated the first example of a CCTα phosphosite (S319) being regulated by phosphorylation of the adjacent tract 2, which opens up the possibility that large scale phosphorylation of the P-domain is turned on or off by phosphorylation at a subset of sites in a form of hierarchical phosphorylation. This model is supported by previous findings that have shown that preventing phosphorylation by casein kinase II of serine 362 resulted in a 20% reduction in total enzyme phosphorylation (Cornell et al., 1995); however, I found that S362A mutation had no effect on nLD association (**Figure 3.16**). Understanding these "master sites", if they exist, would be crucial for studying the kinase(s) responsible for CCTα phosphorylation and potential signalling pathways that regulate phosphorylation.

4.3 APOL6, IFNγ and NASH: A novel avenue for nLD function

The final aim of my thesis project was determining whether APOL6 is associated with LAPS. APOL6 was identified as a possible PML-regulated gene by cross-

referencing a list of genes identified as possibly PML NB-regulated by chromatin immunoprecipitation and immune-TRAP (Wang et al., 2020) against RNA sequencing data from PML-knockdown U2OS cells (Salsman et al., 2017), although PML knockout in U2OS cells had no effect on the induction of APOL6 expression by INFγ (**Figure 3.23B**). Regardless, APOL6 was found to associate with LAPS in response to OA and IFNγ, confirming that it is indeed a *bona fide* LAPS protein. However, the 70-90% of APOL6 was found in nuclear puncta that were associated with neither PML NBs or LAPS (**Figure 3.28**), even when induced with IFNγ and OA/IFNγ in Huh7 cells. Given the limited research on APOL6, the identity of these non-PML structures remains unknown. The total APOL6-positve puncta approximately doubled in response to IFNγ treatment, suggesting that PML-positive and PML-free APOL6 structures are both IFNγ regulated.

The formation of nLDs was stimulated in response to IFNγ treatment in U2OS and Huh7 cells. IFNγ is primarily involved in immune signalling and response against viruses and other pathogens, although connections between IFNγ and cLDs have been previously reported. Bacterial-infected macrophages were found to have increased LD formation in response to IFNγ (Knight et al., 2018) and IFNγ-induced *de novo* lipogenesis was necessary to achieve the full effects of IFNγ transcription of anti-viral genes in pancreatic beta cells (Truong et al., 2019). The addition of nLD formation as part of IFNγ signalling adds another interesting dimension to nLD function, suggesting a possible immune modulation. LDs have been previously implicated in immunity, providing lipid precursors for eicosanoid production, being assembly platforms for

viruses such as hepatitis C and being targeting sites for IFNγ-stimulated genes (Boucher et al., 2021). The presence of nLDs in the nucleus could affect these and other functions.

Interestingly, IFNγ induced nLD formation in both Huh7 (**Figure 3.29**) and U2OS cells (**Figure 3.30**) despite nLDs in these cells being formed by two different mechanisms. An explanation for why greater nLD formation occurred in Huh7 cells is that IFNγ increases TG synthesis and induces PML expression (Stadler et al., 1995). Greater TG synthesis would promote eLD formation in Huh7 cells, while PML-II overexpression was found to increase nLD number (Ohsaki et al., 2016). The combination of both greater eLD formation and PML upregulation would thus increase nLD entry from the type 1 NR. However, U2OS cells form nLDs via *in situ* TG synthesis on the INM in a mechanism that is not dependent on PML-II (Sołtysik et al., 2021), although knockout of all PML isoforms did reduce nLD formation (Lee et al., 2020). This mechanism of nLD formation appears to be driven by TG synthesis and thus IFNγ-induced TG synthesis, rather than increased PML expression, is likely driving the formation of nLDs in U2OS cells. I also found that PML knockout in U2OS cells prevented the formation of both cLDs and nLDs (**Figure 3.30**), suggesting that PML is necessary for the IFNγ-mediated induction of TG synthesis. This aligns with a previously-described function of PML expression enhancing IFNγ signalling (El Bougrini et al., 2011; Maarifi et al., 2014). The mechanistic details of how PML enhances TG synthesis via IFNγ signalling is unknown. The most likely explanation is that PML promotes IFNγ-induced TG synthesis via signal transducer and activator of transcription (STAT) 1 phosphorylation. IFNγ-stimulated TG synthesis is dependent on SREBP1C activation via STAT1 signalling (Hao et al., 2013; Truong et al., 2019), which

is at least partially dependent on PML (El Bougrini et al., 2011). However, while PML knockdown decreases STAT1 phosphorylation and thus IFNγ-stimulated gene expression, it was insufficient to completely block IFNγ-stimulated gene induction (El Bougrini et al., 2011). This could be due to some residual PML in the knockdown cells, however my finding that induction of APOL6 expression is unaffected by PML-KO in U2OS cells (**Figure 3.23B**) suggests that not all IFNγ-induced genes require PML for upregulation. Re-expression of specific PML isoforms in PML-KO U2OS cells could help resolve how PML and IFNγ-stimulated TG synthesis are linked.

The connection between nLDs, IFNγ and immunity is made more interesting by the presence of PML. PML and PML NB proteins such as SP100 are upregulated by IFNγ signalling and involved in anti-viral response (Dellaire & Bazett-Jones, 2004), while the PML NB protein DAXX has been implicated in IFNγ-induced apoptosis and anti-viral response (Ullman & Hearing, 2008; Yun et al., 2011). Although LAPS had significantly reduced content of DAXX and SP100 in oleate-treated U2OS cells compared to PML NBs, about a quarter of LAPS retained these proteins (Lee et al., 2020). It has been speculated that this population of LAPS could be distinct from DAXX- and SP100-free LAPS and PML-free nLDs (Mcphee et al., 2022). Future experiments should investigate whether IFNγ-induced nLDs recruit DAXX and SP100 better than OA-induced nLDs and whether DAXX- and SP100-positive LAPS also colocalize with APOL6.

Another interesting angle on IFNγ signalling and nLD formation is the synergistic increase in nLD and LAPS formation when combined with OA in Huh7 cells (**Figure 4.1A**). More nLDs were observed when IFNγ signalling was coupled to OA treatment in

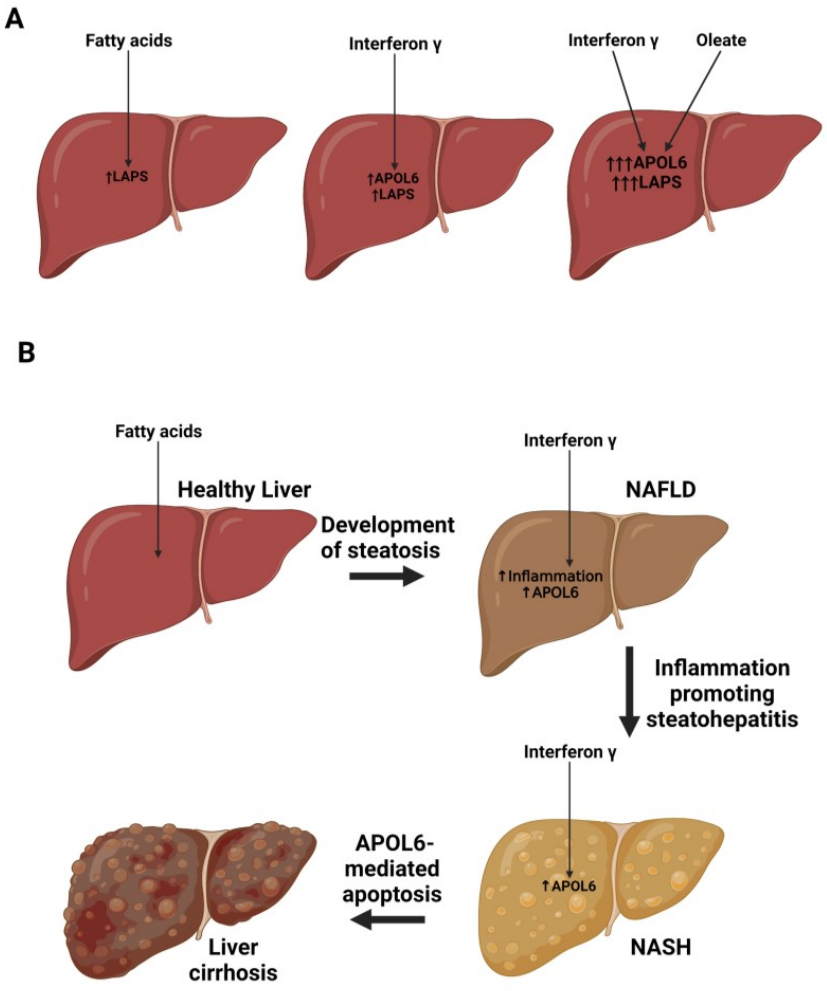

Figure 4.1. Graphical abstract. (A) In liver tissue fatty acids (FAs) induce LAPS formation, while interferon (IFN) γ induces LAPS formation and APOL6 expression. The combination of FAs and IFNγ produces an additive effect that significantly increases APOL6 and LAPS. **(B)** A proposed model for APOL6 in the progression of NAFLD. In healthy liver, FAs lead to NAFLD. NAFLD coupled with inflammatory IFNγ signalling progresses to NASH. Chronic IFNγ signalling leads to elevated levels of the pro-apoptotic protein APOL6, which mediates cell death and NASH progression to liver cirrhosis. Image made using Biorender.

Huh7 cells compared to either treatment alone (**Figure 3.27A**). Additionally, greater expression of the IFNγ-induced gene APOL6 was also noted in Huh7 cells treated with the dual combination of OA and IFNγ versus IFNγ alone (**Figure 3.24**). This suggests that the FA-IFNγ combination exacerbates IFNγ-induced upregulation target genes while also promoting a degree of LAPS formation not seen in either OA- or IFNγ-treated cells. This observation reveals an interesting connection between LAPS formation and NAFLD. Interferon signalling and excess lipid accumulation are often seen in cases of NAFLD that develop into NASH (Møhlenberg et al., 2019), although most studies have identified IFNs other than IFNγ as being responsible. However, IFNγ too has been implicated in NASH. IFNγ signalling was more pronounced in livers of rats on a high-fat diet and drove the progression of NAFLD towards NASH (Li et al., 2021). As well, phosphorylation of STAT1 occurred in livers of NASH rats, which could be connected to PML and LAPS, as PML expression has been shown to enhance IFNγ signalling by promoting the phosphorylation of STAT1 (El Bougrini et al., 2011). However, despite the role of PML as an enhancer of IFNγ-induced gene expression, PML knockout did not prevent the induction of APOL6 expression by IFNγ in U2OS cells (**Figure 3.23B**). This suggests that APOL6 induction occurs through a PML-independent mechanism.

APOL6 overexpression caused apoptosis in previous studies (Liu et al., 2005; Zhaorigetu et al., 2011) and my own findings in U2OS cells found that overexpression of APOL6-HA resulted in a large decrease in APOL6-HA expression when cells were treated with IFNγ (**Figure 3.25**), possibly due to increased cell death. Severe cases of NASH are characterized by apoptotic cell death that causes the formation of scar tissue and organ failure (Kanda et al., 2018) and thus APOL6 could be involved in the

progression of NASH, considering its abundant expression in OA/IFNγ-treated Huh7 cells (**Figure 4.1B**). If and how LAPS fit into this proposed model is speculative.

My findings are the first to demonstrate that IFNγ induces the formation of nLDs and that these nLDs form in a PML-dependent manner. Additionally, the observation that the combination of FAs and IFNγ produce a strong induction of LAPS formation and expression of the pro-apoptotic IFNγ target gene APOL6 in hepatoma cells could provide a fascinating connection between LAPS, APOL6 and NASH.

4.4 Conclusions

nLDs were only recognized as true nuclear entities in the past decade but they have become an area of intensifying research as of late. The only currently-reported function of nLDs is as platforms to increase PC synthesis in response to excess OA and ER stress (Lee et al., 2020). The research presented here better characterizes these enigmatic organelles and provides useful insights into potential nLD functions. I have shown that PML is omnipresent on nLDs and its recruitment precedes that of LIPIN1 and CCTα, suggesting that LAPS could have functions under basal conditions as well as conditions of excess FAs. Furthermore, I have demonstrated that CCTα association with nLDs is inhibited by cumulative P-domain phosphorylation. Finally, I have identified a new LAPS protein connected to IFNγ signalling, providing the groundwork for future research that could connect LAPS to NASH.

References

Aitchison, A. J., Arsenault, D. J., & Ridgway, N. D. (2015). Nuclear-localized CTP: phosphocholine cytidylyltransferase α regulates phosphatidylcholine synthesis required for lipid droplet biogenesis. *Molecular biology of the cell*, *26*(16), 2927-2938.

Albi, E., Mersel, M., Leray, C., Tomassoni, M., & Viola-Magni, M. (1994). Rat liver chromatin phospholipids. *Lipids*, *29*(10), 715-719.

Anand, P., Cermelli, S., Li, Z., Kassan, A., Bosch, M., Sigua, R., Huang, L., Ouellette, A. J., Pol, A., & Welte, M. A. (2012). A novel role for lipid droplets in the organismal antibacterial response. *Elife*, *1*, e00003.

Arnold, R. S., & Cornell, R. B. (1996). Lipid regulation of CTP: phosphocholine cytidylyltransferase: electrostatic, hydrophobic, and synergistic interactions of anionic phospholipids and diacylglycerol. *Biochemistry*, *35*(30), 9917-9924.

Arnold, R. S., DePaoli-Roach, A. A., & Cornell, R. B. (1997). Binding of CTP: phosphocholine cytidylyltransferase to lipid vesicles: diacylglycerol and enzyme dephosphorylation increase the affinity for negatively charged membranes. *Biochemistry*, *36*(20), 6149-6156.

Balmer, J. E., & Blomhoff, R. (2002). Gene expression regulation by retinoic acid. *Journal of Lipid Research*, *43*(11), 1773-1808.

Barger, S. R., Penfield, L., & Bahmanyar, S. (2021). Coupling lipid synthesis with nuclear envelope remodeling. *Trends in biochemical sciences*.

Bartley, J. A., & Ward, R. (1985). Glycerol kinase deficiency inhibits glycerol utilization in phosphoglyceride and triacylglycerol biosynthesis. *Pediatric research*, *19*(3), 313-314.

Bartz, R., Li, W.-H., Venables, B., Zehmer, J. K., Roth, M. R., Welti, R., Anderson, R. G. W., Liu, P., & Chapman, K. D. (2007). Lipidomics reveals that adiposomes store ether lipids and mediate phospholipid traffic. *Journal of Lipid Research*, *48*(4), 837-847. https://doi.org/10.1194/jlr.m600413-jlr200

Boström, P., Andersson, L., Rutberg, M., Perman, J., Lidberg, U., Johansson, B. R., Fernandez-Rodriguez, J., Ericson, J., Nilsson, T., & Borén, J. (2007). SNARE proteins mediate fusion between cytosolic lipid droplets and are implicated in insulin sensitivity. *Nature cell biology*, *9*(11), 1286-1293.

Boström, P., Rutberg, M., Ericsson, J., Holmdahl, P., Andersson, L., Frohman, M. A., Borén, J., & Olofsson, S.-O. (2005). Cytosolic lipid droplets increase in size by microtubule-dependent complex formation. *Arteriosclerosis, thrombosis, and vascular biology*, *25*(9), 1945-1951.

Bronnikov, G. E., Aboulaich, N., Vener, A. V., & Strålfors, P. (2008). Acute effects of insulin on the activity of mitochondrial GPAT1 in primary adipocytes. *Biochemical and biophysical research communications*, *367*(1), 201-207.

Brown, M. S., & Goldstein, J. L. (1997). The SREBP pathway: regulation of cholesterol metabolism by proteolysis of a membrane-bound transcription factor. *Cell*, *89*(3), 331-340.

Cao, J., Li, J.-L., Li, D., Tobin, J. F., & Gimeno, R. E. (2006). Molecular identification of microsomal acyl-CoA: glycerol-3-phosphate acyltransferase, a key enzyme in de novo triacylglycerol synthesis. *Proceedings of the National Academy of Sciences*, *103*(52), 19695-19700.

Carracedo, A., Weiss, D., Leliaert, A. K., Bhasin, M., De Boer, V. C., Laurent, G., Adams, A. C., Sundvall, M., Song, S. J., & Ito, K. (2012). A metabolic prosurvival role for PML in breast cancer. *The Journal of clinical investigation*, *122*(9), 3088-3100.

Caviglia, J. M., de Gómez Dumm, I. N. T., Coleman, R. A., & Igal, R. A. (2004). Phosphatidylcholine deficiency upregulates enzymes of triacylglycerol metabolism in CHO cells. *Journal of Lipid Research*, *45*(8), 1500-1509.

Chakrabarti, P., & Kandror, K. V. (2009). FoxO1 controls insulin-dependent adipose triglyceride lipase (ATGL) expression and lipolysis in adipocytes. *Journal of Biological Chemistry*, *284*(20), 13296-13300.

Chandra, V., Huang, P., Hamuro, Y., Raghuram, S., Wang, Y., Burris, T. P., & Rastinejad, F. (2008). Structure of the intact PPAR-γ–RXR-α nuclear receptor complex on DNA. *Nature*, *456*(7220), 350-356.

Chen, M., Zhang, J., Sampieri, K., Clohessy, J. G., Mendez, L., Gonzalez-Billalabeitia, E., Liu, X.-S., Lee, Y.-R., Fung, J., & Katon, J. M. (2018). An aberrant SREBP-dependent lipogenic program promotes metastatic prostate cancer. *Nature genetics*, *50*(2), 206-218.

Chen, Z., Gropler, M. C., Mitra, M. S., & Finck, B. N. (2012). Complex interplay between the lipin 1 and the hepatocyte nuclear factor 4 α (HNF4α) pathways to regulate liver lipid metabolism. *PloS one*, *7*(12), e51320.

Chitraju, C., Trötzmüller, M., Hartler, J., Wolinski, H., Thallinger, G. G., Lass, A., Zechner, R., Zimmermann, R., Köfeler, H. C., & Spener, F. (2012). Lipidomic analysis of lipid droplets from murine hepatocytes reveals distinct signatures for nutritional stress. *Journal of Lipid Research*, *53*(10), 2141-2152.

Chong, S. S., Taneva, S. G., Lee, J. M., & Cornell, R. B. (2014). The curvature sensitivity of a membrane-binding amphipathic helix can be modulated by the charge on a flanking region. *Biochemistry*, *53*(3), 450-461.

Chorlay, A., Monticelli, L., Verissimo Ferreira, J., Ben M'barek, K., Ajjaji, D., Wang, S., Johnson, E., Beck, R., Omrane, M., Beller, M., Carvalho, P., & Rachid Thiam, A. (2019). Membrane Asymmetry Imposes Directionality on Lipid Droplet Emergence from the ER. *Dev Cell*, *50*(1), 25-42 e27. https://doi.org/10.1016/j.devcel.2019.05.003

Chorlay, A., & Thiam, A. R. (2018). An asymmetry in monolayer tension regulates lipid droplet budding direction. *Biophysical journal*, *114*(3), 631-640.

Choudhary, V., Golani, G., Joshi, A. S., Cottier, S., Schneiter, R., Prinz, W. A., & Kozlov, M. M. (2018). Architecture of Lipid Droplets in Endoplasmic Reticulum Is Determined by Phospholipid Intrinsic Curvature. *Curr Biol*, *28*(6), 915-926 e919. https://doi.org/10.1016/j.cub.2018.02.020

Chung, J., Wu, X., Lambert, T. J., Lai, Z. W., Walther, T. C., & Farese Jr, R. V. (2019). LDAF1 and seipin form a lipid droplet assembly complex. *Developmental Cell*, *51*(5), 551-563. e557.

Cole, L. K., & Vance, D. E. (2010). A role for Sp1 in transcriptional regulation of phosphatidylethanolamine N-methyltransferase in liver and 3T3-L1 adipocytes. *Journal of Biological Chemistry*, *285*(16), 11880-11891.

Cornell, R. (1989). Chemical cross-linking reveals a dimeric structure for CTP: phosphocholine cytidylyltransferase. *Journal of Biological Chemistry*, *264*(15), 9077-9082.

Cornell, R. B. (2016). Membrane lipid compositional sensing by the inducible amphipathic helix of CCT. *Biochimica et Biophysica Acta (BBA)-Molecular and Cell Biology of Lipids*, *1861*(8), 847-861.

Cornell, R. B., Kalmar, G. B., Kay, R. J., Johnson, M. A., Sanghera, J. S., & Pelech, S. L. (1995). Functions of the C-terminal domain of CTP: phosphocholine cytidylyltransferase. Effects of C-terminal deletions on enzyme activity, intracellular localization and phosphorylation potential. *Biochemical Journal*, *310*(2), 699-708. https://doi.org/10.1042/bj3100699

Cornell, R. B., & Ridgway, N. D. (2015). CTP: phosphocholine cytidylyltransferase: Function, regulation, and structure of an amphitropic enzyme required for membrane biogenesis. *Progress in lipid research*, *59*, 147-171.

Corpet, A., Olbrich, T., Gwerder, M., Fink, D., & Stucki, M. (2014). Dynamics of histone H3. 3 deposition in proliferating and senescent cells reveals a DAXX-dependent targeting to PML-NBs important for pericentromeric heterochromatin organization. *Cell cycle*, *13*(2), 249-267.

Dechat, T., Pfleghaar, K., Sengupta, K., Shimi, T., Shumaker, D. K., Solimando, L., & Goldman, R. D. (2008). Nuclear lamins: major factors in the structural organization and function of the nucleus and chromatin. *Genes & development*, *22*(7), 832-853.

Dellaire, G., & Bazett-Jones, D. P. (2004). PML nuclear bodies: dynamic sensors of DNA damage and cellular stress. *Bioessays*, *26*(9), 963-977.

Dellaire, G., Eskiw, C. H., Dehghani, H., Ching, R. W., & Bazett-Jones, D. P. (2006). Mitotic accumulations of PML protein contribute to the re-establishment of PML nuclear bodies in G1. *Journal of cell science*, *119*(6), 1034-1042.

DeLong, C. J., Shen, Y.-J., Thomas, M. J., & Cui, Z. (1999). Molecular distinction of phosphatidylcholine synthesis between the CDP-choline pathway and phosphatidylethanolamine methylation pathway. *Journal of Biological Chemistry*, *274*(42), 29683-29688.

Dennis, M. K., Taneva, S. G., & Cornell, R. B. (2011). The intrinsically disordered nuclear localization signal and phosphorylation segments distinguish the membrane affinity of two cytidylyltransferase isoforms. *Journal of Biological Chemistry*, *286*(14), 12349-12360.

Dolinsky, V. W., Sipione, S., Lehner, R., & Vance, D. E. (2001). The cloning and expression of a murine triacylglycerol hydrolase cDNA and the structure of its corresponding gene. *Biochimica et Biophysica Acta (BBA) - Molecular and Cell Biology of Lipids*, *1532*(3), 162-172. https://doi.org/https://doi.org/10.1016/S1388-1981(01)00133-0

Drané, P., Ouararhni, K., Depaux, A., Shuaib, M., & Hamiche, A. (2010). The death-associated protein DAXX is a novel histone chaperone involved in the replication-independent deposition of H3. 3. *Genes & development*, *24*(12), 1253-1265.

Duchateau, P. N., Pullinger, C. R., Orellana, R. E., Kunitake, S. T., Naya-Vigne, J., O'Connor, P. M., Malloy, M. J., & Kane, J. P. (1997). Apolipoprotein L, a new human high density lipoprotein apolipoprotein expressed by the pancreas: identification, cloning, characterization, and plasma distribution of apolipoprotein L. *Journal of Biological Chemistry*, *272*(41), 25576-25582.

Dunne, S. J., Cornell, R. B., Johnson, J. E., Glover, N. R., & Tracey, A. S. (1996). Structure of the membrane binding domain of CTP: phosphocholine cytidylyltransferase. *Biochemistry*, *35*(37), 11975-11984.

Eichmann, T. O., Kumari, M., Haas, J. T., Farese, R. V., Jr., Zimmermann, R., Lass, A., & Zechner, R. (2012). Studies on the substrate and stereo/regioselectivity of adipose triglyceride lipase, hormone-sensitive lipase, and diacylglycerol-O-acyltransferases. *J Biol Chem*, *287*(49), 41446-41457. https://doi.org/10.1074/jbc.M112.400416

El Bougrini, J., Dianoux, L., & Chelbi-Alix, M. K. (2011). PML positively regulates interferon gamma signaling. *Biochimie*, *93*(3), 389-398.

Fagone, P., & Jackowski, S. (2009). Membrane phospholipid synthesis and endoplasmic reticulum function. *Journal of Lipid Research*, *50*, S311-S316.

Finck, B. N., Gropler, M. C., Chen, Z., Leone, T. C., Croce, M. A., Harris, T. E., Lawrence Jr, J. C., & Kelly, D. P. (2006). Lipin 1 is an inducible amplifier of the hepatic PGC-1α/PPARα regulatory pathway. *Cell Metabolism*, *4*(3), 199-210.

Flis, V. V., & Daum, G. (2013). Lipid transport between the endoplasmic reticulum and mitochondria. *Cold Spring Harbor perspectives in biology*, *5*(6), a013235.

Gallardo-Montejano, V. I., Saxena, G., Kusminski, C. M., Yang, C., McAfee, J. L., Hahner, L., Hoch, K., Dubinsky, W., Narkar, V. A., & Bickel, P. E. (2016). Nuclear Perilipin 5 integrates lipid droplet lipolysis with PGC-1α/SIRT1-dependent transcriptional regulation of mitochondrial function. *Nature communications*, *7*(1), 1-14.

Galsgaard, K. D., Pedersen, J., Knop, F. K., Holst, J. J., & Wewer Albrechtsen, N. J. (2019). Glucagon receptor signaling and lipid metabolism. *Frontiers in physiology*, *10*, 413.

Gaudet, R. G., Zhu, S., Halder, A., Kim, B.-H., Bradfield, C. J., Huang, S., Xu, D., Mamiñska, A., Nguyen, T. N., & Lazarou, M. (2021). A human apolipoprotein L with detergent-like activity kills intracellular pathogens. *Science*, *373*(6552), eabf8113.

Gehrig, K., Cornell, R. B., & Ridgway, N. D. (2008). Expansion of the nucleoplasmic reticulum requires the coordinated activity of lamins and CTP: phosphocholine cytidylyltransferase α. *Molecular biology of the cell*, *19*(1), 237-247.

Gehrig, K., Lagace, T. A., & Ridgway, N. D. (2009). Oxysterol activation of phosphatidylcholine synthesis involves CTP: phosphocholine cytidylyltransferase α translocation to the nuclear envelope. *Biochemical Journal*, *418*(1), 209-217.

Gluchowski, N. L., Becuwe, M., Walther, T. C., & Farese, R. V. (2017). Lipid droplets and liver disease: from basic biology to clinical implications. *Nature reviews Gastroenterology & hepatology*, *14*(6), 343-355.

Goeritzer, M., Vujic, N., Schlager, S., Chandak, P. G., Korbelius, M., Gottschalk, B., Leopold, C., Obrowsky, S., Rainer, S., & Doddapattar, P. (2015). Active autophagy but not lipophagy in macrophages with defective lipolysis. *Biochimica et Biophysica Acta (BBA)-Molecular and Cell Biology of Lipids*, *1851*(10), 1304-1316.

Goldstein, J. L., Basu, S. K., & Brown, M. S. (1983). [19] Receptor-mediated endocytosis of low-density lipoprotein in cultured cells. In *Methods in enzymology* (Vol. 98, pp. 241-260). Elsevier.

Greenberg, A. S., Egan, J. J., Wek, S. A., Garty, N. B., Blanchette-Mackie, E. J., & Londos, C. (1991). Perilipin, a major hormonally regulated adipocyte-specific phosphoprotein associated with the periphery of lipid storage droplets. *Journal of Biological Chemistry*, *266*(17), 11341-11346.

Groblewski, G. E., Wang, Y., Ernst, S. A., Kent, C., & Williams, J. A. (1995). Cholecystokinin Stimulates the Down-regulation of CTP: Phosphocholine Cytidylyltransferase in Pancreatic Acinar Cells (∗). *Journal of Biological Chemistry*, *270*(3), 1437-1442.

Hao, J., Zhang, Y.-j., Lv, X., Xu, N., Liu, Q.-j., Zhao, S., Feng, X.-j., Xing, L.-l., Kang, P.-p., & Li, G.-y. (2013). IFN-γ induces lipogenesis in mouse mesangial cells via the JAK2/STAT1 pathway. *American Journal of Physiology-Cell Physiology*, *304*(8), C760-C767.

Harms, J. S., & Splitter, G. A. (1995). Interferon-γ inhibits transgene expression driven by SV40 or CMV promoters but augments expression driven by the mammalian MHC I promoter. *Human gene therapy*, *6*(10), 1291-1297.

Harris, T. E., Huffman, T. A., Chi, A., Shabanowitz, J., Hunt, D. F., Kumar, A., & Lawrence, J. C. (2007). Insulin controls subcellular localization and multisite phosphorylation of the phosphatidic acid phosphatase, lipin 1. *Journal of Biological Chemistry*, *282*(1), 277-286.

Hedtke, V., & Bakovic, M. (2019). Choline transport for phospholipid synthesis: An emerging role of choline transporter-like protein 1. *Experimental Biology and Medicine*, *244*(8), 655-662.

Helmink, B. A., Braker, J. D., Kent, C., & Friesen, J. A. (2003). Identification of lysine 122 and arginine 196 as important functional residues of rat CTP: phosphocholine cytidylyltransferase alpha. *Biochemistry*, *42*(17), 5043-5051.

Henique, C., Mansouri, A., Fumey, G., Lenoir, V., Girard, J., Bouillaud, F., Prip-Buus, C., & Cohen, I. (2010). Increased mitochondrial fatty acid oxidation is sufficient to protect skeletal muscle cells from palmitate-induced apoptosis. *Journal of Biological Chemistry*, *285*(47), 36818-36827.

Henne, M., Goodman, J. M., & Hariri, H. (2020). Spatial compartmentalization of lipid droplet biogenesis. *Biochimica et Biophysica Acta (BBA)-Molecular and Cell Biology of Lipids*, *1865*(1), 158499.

Hetherington, A. M., Sawyez, C. G., Zilberman, E., Stoianov, A. M., Robson, D. L., & Borradaile, N. M. (2016). Differential lipotoxic effects of palmitate and oleate in activated human hepatic stellate cells and epithelial hepatoma cells. *Cellular Physiology and Biochemistry*, *39*(4), 1648-1662.

Hörl, G., Wagner, A., Cole, L. K., Malli, R., Reicher, H., Kotzbeck, P., Köfeler, H., Höfler, G., Frank, S., & Bogner-Strauss, J. G. (2011). Sequential synthesis and methylation of phosphatidylethanolamine promote lipid droplet biosynthesis and stability in tissue culture and in vivo. *Journal of Biological Chemistry*, *286*(19), 17338-17350.

Houweling, M., Jamil, H., Hatch, G., & Vance, D. (1994). Dephosphorylation of CTP-phosphocholine cytidylyltransferase is not required for binding to membranes. *Journal of Biological Chemistry*, *269*(10), 7544-7551.

Hsieh, K., Lee, Y. K., Londos, C., Raaka, B. M., Dalen, K. T., & Kimmel, A. R. (2012). Perilipin family members preferentially sequester to either triacylglycerol-specific or cholesteryl-ester-specific intracellular lipid storage droplets. *Journal of cell science*, *125*(17), 4067-4076.

Jacquemyn, J., Foroozandeh, J., Vints, K., Swerts, J., Verstreken, P., Gounko, N. V., Gallego, S. F., & Goodchild, R. (2021). Torsin and NEP1R1-CTDNEP1 phosphatase affect interphase nuclear pore complex insertion by lipid-dependent and lipid-independent mechanisms. *The EMBO journal*, *40*(17), e106914.

Janowski, B. A., Willy, P. J., Devi, T. R., Falck, J., & Mangelsdorf, D. J. (1996). An oxysterol signalling pathway mediated by the nuclear receptor LXRα. *Nature*, *383*(6602), 728-731.

Jensen, K., Shiels, C., & Freemont, P. S. (2001). PML protein isoforms and the RBCC/TRIM motif. *Oncogene*, *20*(49), 7223-7233.

Jocken, J. W., & Blaak, E. E. (2008). Catecholamine-induced lipolysis in adipose tissue and skeletal muscle in obesity. *Physiology & behavior*, *94*(2), 219-230.

Johnson, J. E., Xie, M., Singh, L. M., Edge, R., & Cornell, R. B. (2003). Both acidic and basic amino acids in an amphitropic enzyme, CTP: phosphocholine cytidylyltransferase, dictate its selectivity for anionic membranes. *Journal of Biological Chemistry*, *278*(1), 514-522.

Kanda, T., Matsuoka, S., Yamazaki, M., Shibata, T., Nirei, K., Takahashi, H., Kaneko, T., Fujisawa, M., Higuchi, T., & Nakamura, H. (2018). Apoptosis and non-alcoholic fatty liver diseases. *World journal of gastroenterology*, *24*(25), 2661.

Karasaki, S. (1969). The fine structure of proliferating cells in preneoplastic rat livers during azo-dye carcinogenesis. *The Journal of Cell Biology*, *40*(2), 322-335.

Karasaki, S. (1973). Passage of cytoplasmic lipid into interphase nuclei in preneoplastic rat liver. *Journal of ultrastructure research*, *42*(5-6), 463-478.

Karaskov, E., Scott, C., Zhang, L., Teodoro, T., Ravazzola, M., & Volchuk, A. (2006). Chronic palmitate but not oleate exposure induces endoplasmic reticulum stress, which may contribute to INS-1 pancreatic β-cell apoptosis. *Endocrinology*, *147*(7), 3398-3407.

Karim, M., Jackson, P., & Jackowski, S. (2003). Gene structure, expression and identification of a new CTP: phosphocholine cytidylyltransferase β isoform. *Biochimica et Biophysica Acta (BBA)-Molecular and Cell Biology of Lipids*, *1633*(1), 1-12.

Kato, S., Ishii, T., & Kouzmenko, A. (2015). Point mutations in an epigenetic factor lead to multiple types of bone tumors: role of H3. 3 histone variant in bone development and disease. *BoneKEy Reports*, *4*.

Kaushik, S., & Cuervo, A. M. (2015). Degradation of lipid droplet-associated proteins by chaperone-mediated autophagy facilitates lipolysis. *Nature cell biology*, *17*(6), 759-770.

Kaushik, S., & Cuervo, A. M. (2016). AMPK-dependent phosphorylation of lipid droplet protein PLIN2 triggers its degradation by CMA. *Autophagy*, *12*(2), 432-438.

Kaushik, S., Rodriguez-Navarro, J. A., Arias, E., Kiffin, R., Sahu, S., Schwartz, G. J., Cuervo, A. M., & Singh, R. (2011). Autophagy in hypothalamic AgRP neurons regulates food intake and energy balance. *Cell Metabolism*, *14*(2), 173-183.

Khalil, M. B., Sundaram, M., Zhang, H.-Y., Links, P. H., Raven, J. F., Manmontri, B., Sariahmetoglu, M., Tran, K., Reue, K., & Brindley, D. N. (2009). The level and compartmentalization of phosphatidate phosphatase-1 (lipin-1) control the assembly and secretion of hepatic VLDL s. *Journal of Lipid Research*, *50*(1), 47-58.

Kim, Y., Gentry, M. S., Harris, T. E., Wiley, S. E., Lawrence, J. C., & Dixon, J. E. (2007). A conserved phosphatase cascade that regulates nuclear membrane biogenesis. *Proceedings of the National Academy of Sciences*, *104*(16), 6596-6601.

Knight, M., Braverman, J., Asfaha, K., Gronert, K., & Stanley, S. (2018). Lipid droplet formation in Mycobacterium tuberculosis infected macrophages requires IFN-γ/HIF-1α signaling and supports host defense. *PLoS pathogens*, *14*(1), e1006874.

Krahmer, N., Guo, Y., Wilfling, F., Hilger, M., Lingrell, S., Heger, K., Heather, Schmidt-Supprian, M., Dennis, Mann, M., Robert, & Tobias. (2011). Phosphatidylcholine Synthesis for Lipid Droplet Expansion Is Mediated by Localized Activation of CTP:Phosphocholine Cytidylyltransferase. *Cell Metabolism*, *14*(4), 504-515. https://doi.org/10.1016/j.cmet.2011.07.013

Kumanski, S., Viart, B. T., Kossida, S., & Moriel-Carretero, M. (2021). Lipid droplets are a physiological nucleoporin reservoir. *Cells*, *10*(2), 472.

Lagace, T. A., Miller, J. R., & Ridgway, N. D. (2002). Caspase processing and nuclear export of CTP: phosphocholine cytidylyltransferase α during farnesol-induced apoptosis. *Molecular and cellular biology*, *22*(13), 4851-4862.

Lagace, T. A., & Ridgway, N. D. (2005). The rate-limiting enzyme in phosphatidylcholine synthesis regulates proliferation of the nucleoplasmic reticulum. *Molecular biology of the cell*, *16*(3), 1120-1130.

Lagrutta, L. C., Layerenza, J. P., Bronsoms, S., Trejo, S. A., & Ves-Losada, A. (2021). Nuclear-lipid-droplet proteome: carboxylesterase as a nuclear lipase involved in lipid-droplet homeostasis. *Heliyon*, *7*(3), e06539.

Lagrutta, L. C., Montero-Villegas, S., Layerenza, J. P., Sisti, M. S., García de Bravo, M. M., & Ves-Losada, A. (2017). Reversible nuclear-lipid-droplet morphology induced by oleic acid: A link to cellular-lipid metabolism. *PloS one*, *12*(1), e0170608.

Lands, W. E. (1958). Metabolism of glycerolipides: a comparison of lecithin and triglyceride synthesis. *Journal of Biological Chemistry*, *231*(2), 883-888.

Layerenza, J. P., González, P., De Bravo, M. G., Polo, M. P., Sisti, M. S., & Ves-Losada, A. (2013). Nuclear lipid droplets: a novel nuclear domain. *Biochimica et Biophysica Acta (BBA)-Molecular and Cell Biology of Lipids*, *1831*(2), 327-340.

Leduc, E., & Wilson, J. W. (1959). A histochemical study of intranuclear inclusions in mouse liver and hepatoma. *Journal of Histochemistry & Cytochemistry*, *7*(1), 8-16.

Lee, J., Johnson, J., Ding, Z., Paetzel, M., & Cornell, R. B. (2009). Crystal structure of a mammalian CTP: phosphocholine cytidylyltransferase catalytic domain reveals novel active site residues within a highly conserved nucleotidyltransferase fold. *Journal of Biological Chemistry*, *284*(48), 33535-33548.

Lee, J., & Ridgway, N. D. (2018). Phosphatidylcholine synthesis regulates triglyceride storage and chylomicron secretion by Caco2 cells. *Journal of Lipid Research*, *59*(10), 1940-1950.

Lee, J., & Ridgway, N. D. (2020). Substrate channeling in the glycerol-3-phosphate pathway regulates the synthesis, storage and secretion of glycerolipids. *Biochimica et Biophysica Acta (BBA) - Molecular and Cell Biology of Lipids*, *1865*(1), 158438. https://doi.org/10.1016/j.bbalip.2019.03.010

Lee, J., Salsman, J., Foster, J., Dellaire, G., & Ridgway, N. D. (2020). Lipid-associated PML structures assemble nuclear lipid droplets containing CCTα and Lipin1. *Life science alliance*, *3*(8).

Lee, J., Taneva, S. G., Holland, B. W., Tieleman, D. P., & Cornell, R. B. (2014). Structural basis for autoinhibition of CTP: phosphocholine cytidylyltransferase (CCT), the regulatory enzyme in phosphatidylcholine synthesis, by its membrane-binding amphipathic helix. *Journal of Biological Chemistry*, *289*(3), 1742-1755.

Lee, Y., Hirose, H., Ohneda, M., Johnson, J., McGarry, J. D., & Unger, R. H. (1994). Beta-cell lipotoxicity in the pathogenesis of non-insulin-dependent diabetes mellitus of obese rats: impairment in adipocyte-beta-cell relationships. *Proceedings of the National Academy of Sciences*, *91*(23), 10878-10882.

Lehner, R., Cui, Z., & Vance, D. E. (1999). Subcellullar localization, developmental expression and characterization of a liver triacylglycerol hydrolase. *Biochemical Journal*, *338*(3), 761-768.

Leikin, S., Kozlov, M. M., Fuller, N. L., & Rand, R. P. (1996). Measured effects of diacylglycerol on structural and elastic properties of phospholipid membranes. *Biophysical journal*, *71*(5), 2623-2632. https://doi.org/10.1016/S0006-3495(96)79454-7

Lewin, T. M., Schwerbrock, N. M., Lee, D. P., & Coleman, R. A. (2004). Identification of a new glycerol-3-phosphate acyltransferase isoenzyme, mtGPAT2, in mitochondria. *Journal of Biological Chemistry*, *279*(14), 13488-13495.

Li, J., Chen, Q., Yi, J., Lan, X., Lu, K., Du, X., Guo, Z., Guo, Y., Geng, M., & Li, D. (2021). IFN-γ contributes to the hepatic inflammation in HFD-induced nonalcoholic steatohepatitis by STAT1β/TLR2 signaling pathway. *Molecular Immunology*, *134*, 118-128.

Li, Z., Johnson, M. R., Ke, Z., Chen, L., & Welte, M. A. (2014). Drosophila lipid droplets buffer the H2Av supply to protect early embryonic development. *Current Biology*, *24*(13), 1485-1491.

Li, Z., & Vance, D. E. (2008). Thematic review series: glycerolipids. Phosphatidylcholine and choline homeostasis. *Journal of Lipid Research*, *49*(6), 1187-1194.

Listenberger, L. L., Han, X., Lewis, S. E., Cases, S., Farese, R. V., Ory, D. S., & Schaffer, J. E. (2003). Triglyceride accumulation protects against fatty acid-induced lipotoxicity. *Proceedings of the National Academy of Sciences*, *100*(6), 3077-3082. https://doi.org/doi:10.1073/pnas.0630588100

Liu, R., Lee, J.-H., Li, J., Yu, R., Tan, L., Xia, Y., Zheng, Y., Bian, X.-L., Lorenzi, P. L., Chen, Q., & Lu, Z. (2021). Choline kinase alpha 2 acts as a protein kinase to promote lipolysis of lipid droplets. *Molecular Cell*, *81*(13), 2722-2735.e2729. https://doi.org/10.1016/j.molcel.2021.05.005

Liu, Z., Lu, H., Jiang, Z., Pastuszyn, A., & Chien-an, A. H. (2005). Apolipoprotein L6, a Novel Proapoptotic Bcl-2 Homology 3–Only Protein, Induces Mitochondria-Mediated Apoptosis in Cancer Cells1 1 Howard Hughes Medical Institute research aids to University of New Mexico Cancer Research and Treatment Center, American Cancer Society ACS-IRG-192 grant 412488-00095, and University of New Mexico Research Allocation Committee grant C-2222-RAC (CA. A. Hu). *Molecular cancer research*, *3*(1), 21-31.

Lykidis, A., Baburina, I., & Jackowski, S. (1999). Distribution of CTP: phosphocholine cytidylyltransferase (CCT) isoforms: identification of a new CCTβ splice variant. *Journal of Biological Chemistry*, *274*(38), 26992-27001.

Lykidis, A., Murti, K. G., & Jackowski, S. (1998). Cloning and characterization of a second human CTP: phosphocholine cytidylyltransferase. *Journal of Biological Chemistry*, *273*(22), 14022-14029.

M'barek, K. B., Ajjaji, D., Chorlay, A., Vanni, S., Forêt, L., & Thiam, A. R. (2017). ER membrane phospholipids and surface tension control cellular lipid droplet formation. *Developmental Cell*, *41*(6), 591-604. e597.

Maarifi, G., Chelbi-Alix, M. K., & Nisole, S. (2014). PML control of cytokine signaling. *Cytokine & Growth Factor Reviews*, *25*(5), 551-561.

Malmberg, P., Karlsson, T., Svensson, H., Lönn, M., Carlsson, N.-G., Sandberg, A.-S., Jennische, E., Osmancevic, A., & Holmäng, A. (2014). A new approach to measuring vitamin D in human adipose tissue using time-of-flight secondary ion mass spectrometry: a pilot study. *Journal of Photochemistry and Photobiology B: Biology*, *138*, 295-301.

Martinez-Lopez, N., Garcia-Macia, M., Sahu, S., Athonvarangkul, D., Liebling, E., Merlo, P., Cecconi, F., Schwartz, G. J., & Singh, R. (2016). Autophagy in the CNS and periphery coordinate lipophagy and lipolysis in the brown adipose tissue and liver. *Cell Metabolism*, *23*(1), 113-127.

Mathur, S. N., BORN, E., MURTHY, S., & FIELD, F. J. (1996). Phosphatidylcholine increases the secretion of triacylglycerol-rich lipoproteins by CaCo-2 cells. *Biochemical Journal*, *314*(2), 569-575.

McIntosh, A. L., Storey, S. M., & Atshaves, B. P. (2010). Intracellular lipid droplets contain dynamic pools of sphingomyelin: ADRP binds phospholipids with high affinity. *Lipids*, *45*(6), 465-477.

Mcphee, M. J., Salsman, J., Foster, J., Thompson, J., Mathavarajah, S., Dellaire, G., & Ridgway, N. D. (2022). Running'LAPS'around nLD: Nuclear lipid droplet form and function. *Frontiers in Cell and Developmental Biology*, 88.

Meegalla, R. L., Billheimer, J. T., & Cheng, D. (2002). Concerted elevation of acyl-coenzyme A: diacylglycerol acyltransferase (DGAT) activity through independent stimulation of mRNA expression of DGAT1 and DGAT2 by carbohydrate and insulin. *Biochemical and biophysical research communications*, *298*(3), 317-323.

Mejhert, N., Kuruvilla, L., Gabriel, K. R., Elliott, S. D., Guie, M.-A., Wang, H., Lai, Z. W., Lane, E. A., Christiano, R., & Danial, N. N. (2020). Partitioning of MLX-family transcription factors to lipid droplets regulates metabolic gene expression. *Molecular Cell*, *77*(6), 1251-1264. e1259.

Minahk, C., Kim, K.-W., Nelson, R., Trigatti, B., Lehner, R., & Vance, D. E. (2008). Conversion of low density lipoprotein-associated phosphatidylcholine to triacylglycerol by primary hepatocytes. *Journal of Biological Chemistry*, *283*(10), 6449-6458.

Mizushima, N., Levine, B., Cuervo, A. M., & Klionsky, D. J. (2008). Autophagy fights disease through cellular self-digestion. *Nature*, *451*(7182), 1069-1075.

Moessinger, C., Klizaite, K., Steinhagen, A., Philippou-Massier, J., Shevchenko, A., Hoch, M., Ejsing, C. S., & Thiele, C. (2014). Two different pathways of phosphatidylcholine synthesis, the Kennedy Pathway and the Lands Cycle, differentially regulate cellular triacylglycerol storage. *BMC cell biology*, *15*(1), 1-17.

Moessinger, C., Kuerschner, L., Spandl, J., Shevchenko, A., & Thiele, C. (2011). Human lysophosphatidylcholine acyltransferases 1 and 2 are located in lipid droplets where they catalyze the formation of phosphatidylcholine. *Journal of Biological Chemistry*, *286*(24), 21330-21339.

Møhlenberg, M., Terczynska-Dyla, E., Thomsen, K. L., George, J., Eslam, M., Grønbæk, H., & Hartmann, R. (2019). The role of IFN in the development of NAFLD and NASH. *Cytokine*, *124*, 154519.

Mosquera, J. V., Bacher, M. C., & Priess, J. R. (2021). Nuclear lipid droplets and nuclear damage in Caenorhabditis elegans. *PLoS Genetics*, *17*(6), e1009602.

Nagle, C. A., Vergnes, L., DeJong, H., Wang, S., Lewin, T. M., Reue, K., & Coleman, R. A. (2008). Identification of a novel sn-glycerol-3-phosphate acyltransferase isoform, GPAT4, as the enzyme deficient in Agpat6−/− mice. *Journal of Lipid Research*, *49*(4), 823-831.

Nguyen, T. B., Louie, S. M., Daniele, J. R., Tran, Q., Dillin, A., Zoncu, R., Nomura, D. K., & Olzmann, J. A. (2017). DGAT1-dependent lipid droplet biogenesis protects mitochondrial function during starvation-induced autophagy. *Developmental Cell*, *42*(1), 9-21. e25.

Ohsaki, Y., Cheng, J., Fujita, A., Tokumoto, T., & Fujimoto, T. (2006). Cytoplasmic lipid droplets are sites of convergence of proteasomal and autophagic degradation of apolipoprotein B. *Molecular biology of the cell*, *17*(6), 2674-2683.

Ohsaki, Y., Kawai, T., Yoshikawa, Y., Cheng, J., Jokitalo, E., & Fujimoto, T. (2016). PML isoform II plays a critical role in nuclear lipid droplet formation. *Journal of Cell Biology*, *212*(1), 29-38.

Ouimet, M., Franklin, V., Mak, E., Liao, X., Tabas, I., & Marcel, Y. L. (2011). Autophagy regulates cholesterol efflux from macrophage foam cells via lysosomal acid lipase. *Cell Metabolism*, *13*(6), 655-667.

Page, N. M., Butlin, D. J., Lomthaisong, K., & Lowry, P. J. (2001). The human apolipoprotein L gene cluster: identification, classification, and sites of distribution. *Genomics*, *74*(1), 71-78.

Pant, J., Giovinazzo, J. A., Tuka, L. S., Peña, D., Raper, J., & Thomson, R. (2021). Apolipoproteins L1-6 share key cation channel-regulating residues but have different membrane insertion and ion conductance properties. *Journal of Biological Chemistry*, *297*(2).

Pelech, S. L., & Vance, D. E. (1984). Regulation of phosphatidylcholine biosynthesis. *Biochimica et Biophysica Acta (BBA)-Reviews on Biomembranes*, *779*(2), 217-251.

Penno, A., Hackenbroich, G., & Thiele, C. (2013). Phospholipids and lipid droplets. *Biochimica et Biophysica Acta (BBA)-Molecular and Cell Biology of Lipids*, *1831*(3), 589-594.

Perea, A., Clemente, F., Martinell, J., Villanueva-Peñacarrillo, M. L., & Valverde, I. (1995). Physiological effect of glucagon in human isolated adipocytes. *Hormone and metabolic research*, *27*(08), 372-375.

Pérez-Morga, D., Vanhollebeke, B., Paturiaux-Hanocq, F., Nolan, D. P., Lins, L., Homblé, F., Vanhamme, L., Tebabi, P., Pays, A., & Poelvoorde, P. (2005). Apolipoprotein LI promotes trypanosome lysis by forming pores in lysosomal membranes. *Science*, *309*(5733), 469-472.

Péterfy, M., Phan, J., & Reue, K. (2005). Alternatively spliced lipin isoforms exhibit distinct expression pattern, subcellular localization, and role in adipogenesis. *Journal of Biological Chemistry*, *280*(38), 32883-32889.

Peterson, T. R., Sengupta, S. S., Harris, T. E., Carmack, A. E., Kang, S. A., Balderas, E., Guertin, D. A., Madden, K. L., Carpenter, A. E., & Finck, B. N. (2011). mTOR complex 1 regulates lipin 1 localization to control the SREBP pathway. *Cell*, *146*(3), 408-420.

Prasad, S. S., Garg, A., & Agarwal, A. K. (2011). Enzymatic activities of the human AGPAT isoform 3 and isoform 5: localization of AGPAT5 to mitochondria [S]. *Journal of Lipid Research*, *52*(3), 451-462.

Puri, V., Konda, S., Ranjit, S., Aouadi, M., Chawla, A., Chouinard, M., Chakladar, A., & Czech, M. P. (2007). Fat-specific protein 27, a novel lipid droplet protein that enhances triglyceride storage. *Journal of Biological Chemistry*, *282*(47), 34213-34218.

Reshef, L., Olswang, Y., Cassuto, H., Blum, B., Croniger, C. M., Kalhan, S. C., Tilghman, S. M., & Hanson, R. W. (2003). Glyceroneogenesis and the triglyceride/fatty acid cycle. *Journal of Biological Chemistry*, *278*(33), 30413-30416.

Romanauska, A., & Köhler, A. (2018). The inner nuclear membrane is a metabolically active territory that generates nuclear lipid droplets. *Cell*, *174*(3), 700-715. e718.

Salo, V. T., Li, S., Vihinen, H., Holtta-Vuori, M., Szkalisity, A., Horvath, P., Belevich, I., Peranen, J., Thiele, C., Somerharju, P., Zhao, H., Santinho, A., Thiam, A. R., Jokitalo, E., & Ikonen, E. (2019). Seipin Facilitates Triglyceride Flow to Lipid Droplet and Counteracts Droplet Ripening via Endoplasmic Reticulum Contact. *Dev Cell*, *50*(4), 478-493 e479. https://doi.org/10.1016/j.devcel.2019.05.016

Santinho, A., Salo, V. T., Chorlay, A., Li, S., Zhou, X., Omrane, M., Ikonen, E., & Thiam, A. R. (2020). Membrane curvature catalyzes lipid droplet assembly. *Current Biology*, *30*(13), 2481-2494. e2486.

Sathyanarayan, A., Mashek, M. T., & Mashek, D. G. (2017). ATGL promotes autophagy/lipophagy via SIRT1 to control hepatic lipid droplet catabolism. *Cell reports*, *19*(1), 1-9.

Schuldiner, M., & Bohnert, M. (2017). A different kind of love–lipid droplet contact sites. *Biochimica et Biophysica Acta (BBA)-Molecular and Cell Biology of Lipids*, *1862*(10), 1188-1196.

Shimabukuro, M., Zhou, Y.-T., Levi, M., & Unger, R. H. (1998). Fatty acid-induced β cell apoptosis: a link between obesity and diabetes. *Proceedings of the National Academy of Sciences*, *95*(5), 2498-2502.

Shin, J.-Y., Hernandez-Ono, A., Fedotova, T., Östlund, C., Lee, M. J., Gibeley, S. B., Liang, C.-C., Dauer, W. T., Ginsberg, H. N., & Worman, H. J. (2019). Nuclear envelope–localized torsinA-LAP1 complex regulates hepatic VLDL secretion and steatosis. *The Journal of clinical investigation*, *129*(11), 4885-4900.

Sinclair, C. J., Chi, K. D., Subramanian, V., Ward, K. L., & Green, R. M. (2000). Functional expression of a high affinity mammalian hepatic choline/organic cation transporter 1. *Journal of Lipid Research*, *41*(11), 1841-1848.

Singh, R., Kaushik, S., Wang, Y., Xiang, Y., Novak, I., Komatsu, M., Tanaka, K., Cuervo, A. M., & Czaja, M. J. (2009). Autophagy regulates lipid metabolism. *Nature*, *458*(7242), 1131-1135. https://doi.org/10.1038/nature07976

Sołtysik, K., Ohsaki, Y., Tatematsu, T., Cheng, J., & Fujimoto, T. (2019). Nuclear lipid droplets derive from a lipoprotein precursor and regulate phosphatidylcholine synthesis. *Nature communications*, *10*(1), 1-12.

Sołtysik, K., Ohsaki, Y., Tatematsu, T., Cheng, J., Maeda, A., Morita, S.-y., & Fujimoto, T. (2021). Nuclear lipid droplets form in the inner nuclear membrane in a seipin-independent manner. *Journal of Cell Biology*, *220*(1).

Stadler, M., Chelbi-Alix, M. K., Koken, M., Venturini, L., Lee, C., Saib, A., Quignon, F., Pelicano, L., Guillemin, M.-C., & Schindler, C. (1995). Transcriptional induction of the PML growth suppressor gene by interferons is mediated through an ISRE and a GAS element. *Oncogene*, *11*(12), 2565-2573.

Tauchi-Sato, K., Ozeki, S., Houjou, T., Taguchi, R., & Fujimoto, T. (2002). The surface of lipid droplets is a phospholipid monolayer with a unique fatty acid composition. *Journal of Biological Chemistry*, *277*(46), 44507-44512.

Thiam, A. R., Farese, R. V., Jr., & Walther, T. C. (2013). The biophysics and cell biology of lipid droplets. *Nat Rev Mol Cell Biol*, *14*(12), 775-786. https://doi.org/10.1038/nrm3699

Thiam, A. R., & Ikonen, E. (2021). Lipid Droplet Nucleation. *Trends Cell Biol*, *31*(2), 108-118. https://doi.org/10.1016/j.tcb.2020.11.006

Truong, N., Love-Rutledge, S., Lydic, T., & Olson, L. K. (2019). Effect of interferon gamma on neutral lipid levels, lipid droplet formation, and antiviral responses in pancreatic islets and INS-1 β cells. *The FASEB Journal*, *33*(S1), 654.611-654.611.

Ueno, M., Shen, W.-J., Patel, S., Greenberg, A. S., Azhar, S., & Kraemer, F. B. (2013). Fat-specific protein 27 modulates nuclear factor of activated T cells 5 and the cellular response to stress [S]. *Journal of Lipid Research*, *54*(3), 734-743.

Ullman, A. J., & Hearing, P. (2008). Cellular proteins PML and Daxx mediate an innate antiviral defense antagonized by the adenovirus E4 ORF3 protein. *Journal of virology*, *82*(15), 7325-7335.

Van Der Veen, J. N., Lingrell, S., & Vance, D. E. (2012). The membrane lipid phosphatidylcholine is an unexpected source of triacylglycerol in the liver. *Journal of Biological Chemistry*, *287*(28), 23418-23426.

Vancura, A., & Haldar, D. (1994). Purification and characterization of glycerophosphate acyltransferase from rat liver mitochondria. *Journal of Biological Chemistry*, *269*(44), 27209-27215.

Vanhamme, L., Paturiaux-Hanocq, F., Poelvoorde, P., Nolan, D. P., Lins, L., Van Den Abbeele, J., Pays, A., Tebabi, P., Van Xong, H., & Jacquet, A. (2003). Apolipoprotein LI is the trypanosome lytic factor of human serum. *Nature*, *422*(6927), 83-87.

Vatner, D. F., Majumdar, S. K., Kumashiro, N., Petersen, M. C., Rahimi, Y., Gattu, A. K., Bears, M., Camporez, J.-P. G., Cline, G. W., & Jurczak, M. J. (2015). Insulin-independent regulation of hepatic triglyceride synthesis by fatty acids. *Proceedings of the National Academy of Sciences*, *112*(4), 1143-1148.

Vázquez-Vela, M. E. F., Torres, N., & Tovar, A. R. (2008). White adipose tissue as endocrine organ and its role in obesity. *Archives of medical research*, *39*(8), 715-728.

Velázquez, A. P., Tatsuta, T., Ghillebert, R., Drescher, I., & Graef, M. (2016). Lipid droplet–mediated ER homeostasis regulates autophagy and cell survival during starvation. *Journal of Cell Biology*, *212*(6), 621-631.

Wang, H., Becuwe, M., Housden, B. E., Chitraju, C., Porras, A. J., Graham, M. M., Liu, X. N., Thiam, A. R., Savage, D. B., Agarwal, A. K., Garg, A., Olarte, M. J., Lin, Q., Frohlich, F., Hannibal-Bach, H. K., Upadhyayula, S., Perrimon, N., Kirchhausen, T., Ejsing, C. S., . . . Farese, R. V. (2016). Seipin is required for converting nascent to mature lipid droplets. *Elife*, *5*. https://doi.org/10.7554/eLife.16582

Wang, M., Wang, L., Qian, M., Tang, X., Liu, Z., Lai, Y., Ao, Y., Huang, Y., Meng, Y., & Shi, L. (2020). PML2-mediated thread-like nuclear bodies mark late senescence in Hutchinson–Gilford progeria syndrome. *Aging cell*, *19*(6), e13147.

Wang, S., Idrissi, F.-Z., Hermansson, M., Grippa, A., Ejsing, C. S., & Carvalho, P. (2018). Seipin and the membrane-shaping protein Pex30 cooperate in organelle budding from the endoplasmic reticulum. *Nature communications*, *9*(1), 1-12.

Wang, Y., & Kent, C. (1995). Effects of altered phosphorylation sites on the properties of CTP: phosphocholine cytidylyltransferase. *Journal of Biological Chemistry*, *270*(30), 17843-17849.

Wang, Y., MacDonald, J., & Kent, C. (1993). Regulation of CTP: phosphocholine cytidylyltransferase in HeLa cells. Effect of oleate on phosphorylation and intracellular localization. *Journal of Biological Chemistry*, *268*(8), 5512-5518.

Weiss, S. B., Kennedy, E. P., & Kiyasu, J. Y. (1960). The enzymatic synthesis of triglycerides. *Journal of Biological Chemistry*, *235*(1), 40-44.

Welte, M. A., & Gould, A. P. (2017). Lipid droplet functions beyond energy storage. *Biochimica et Biophysica Acta (BBA)-Molecular and Cell Biology of Lipids*, *1862*(10), 1260-1272.

Wilfling, F., Haas, J. T., Walther, T. C., & Farese Jr, R. V. (2014). Lipid droplet biogenesis. *Current opinion in cell biology*, *29*, 39-45.

Wilfling, F., Wang, H., Haas, J. T., Krahmer, N., Gould, T. J., Uchida, A., Cheng, J. X., Graham, M., Christiano, R., Fröhlich, F., Liu, X., Buhman, K. K., Coleman, R. A., Bewersdorf, J., Farese, R. V., Jr., & Walther, T. C. (2013). Triacylglycerol synthesis enzymes mediate lipid droplet growth by relocalizing from the ER to lipid droplets. *Dev Cell*, *24*(4), 384-399. https://doi.org/10.1016/j.devcel.2013.01.013

Wu, L., Xu, D., Zhou, L., Xie, B., Yu, L., Yang, H., Huang, L., Ye, J., Deng, H., & Yuan, Y. A. (2014). Rab8a-AS160-MSS4 regulatory circuit controls lipid droplet fusion and growth. *Developmental Cell*, *30*(4), 378-393.

Yamaguchi, T., Fujikawa, N., Nimura, S., Tokuoka, Y., Tsuda, S., Aiuchi, T., Kato, R., Obama, T., & Itabe, H. (2015). Characterization of lipid droplets in steroidogenic MLTC-1 Leydig cells: Protein profiles and the morphological change induced by hormone stimulation. *Biochimica et Biophysica Acta (BBA)-Molecular and Cell Biology of Lipids*, *1851*(10), 1285-1295.

Yao, Z., & Vance, D. E. (1988). The active synthesis of phosphatidylcholine is required for very low density lipoprotein secretion from rat hepatocytes. *Journal of Biological Chemistry*, *263*(6), 2998-3004.

Yue, L., McPhee, M. J., Gonzalez, K., Charman, M., Lee, J., Thompson, J., Winkler, D. F., Cornell, R. B., Pelech, S., & Ridgway, N. D. (2020). Differential dephosphorylation of CTP: phosphocholine cytidylyltransferase upon translocation to nuclear membranes and lipid droplets. *Molecular biology of the cell*, *31*(10), 1047-1059.

Yun, H. J., Yoon, J. H., Lee, J. K., Noh, K. T., Yoon, K. W., Oh, S. P., Oh, H. J., Chae, J. S., Hwang, S. G., & Kim, E. H. (2011). Daxx mediates activation-induced cell death in microglia by triggering MST1 signalling. *The EMBO journal*, *30*(12), 2465-2476.

Zanghellini, J., Wodlei, F., & von Grunberg, H. H. (2010). Phospholipid demixing and the birth of a lipid droplet. *J Theor Biol*, *264*(3), 952-961. https://doi.org/10.1016/j.jtbi.2010.02.025

Zhao, B., Song, J., Clair, R. W. S., & Ghosh, S. (2007). Stable overexpression of human macrophage cholesteryl ester hydrolase results in enhanced free cholesterol efflux from human THP1 macrophages. *American Journal of Physiology-Cell Physiology*, *292*(1), C405-C412. https://doi.org/10.1152/ajpcell.00306.2006

Zhaorigetu, S., Yang, Z., Toma, I., McCaffrey, T. A., & Hu, C.-A. A. (2011). Apolipoprotein L6, induced in atherosclerotic lesions, promotes apoptosis and blocks Beclin 1-dependent autophagy in atherosclerotic cells. *Journal of Biological Chemistry*, *286*(31), 27389-27398.

Zhou, Y., & Grill, V. (1995). Long term exposure to fatty acids and ketones inhibits B-cell functions in human pancreatic islets of Langerhans. *The Journal of Clinical Endocrinology & Metabolism*, *80*(5), 1584-1590.

Zoumi, A., Datta, S., Liaw, L.-H. L., Wu, C. J., Manthripragada, G., Osborne, T. F., & LaMorte, V. J. (2005). Spatial distribution and function of sterol regulatory element-binding protein 1a and 2 homo-and heterodimers by in vivo two-photon imaging and spectroscopy fluorescence resonance energy transfer. *Molecular and cellular biology*, *25*(8), 2946-2956.